Ozone in Southern Europe

–

Assessment and effectiveness of measures

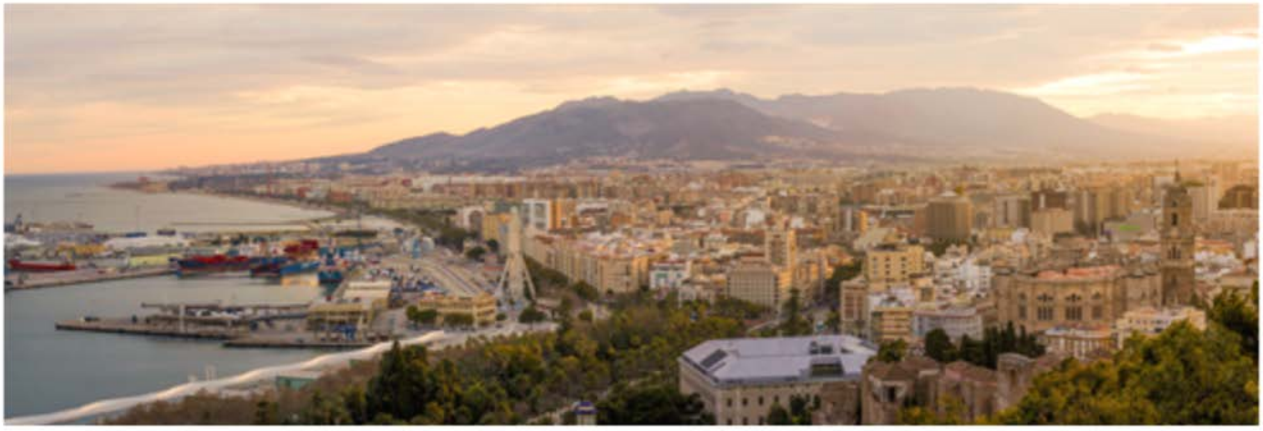

ETC/ACM Technical Paper 2017/3
April 2018

Mar Viana, Marc Padrosa, Xavier Querol, Andrés Alastuey,
Nina Benesova, Blanka Krejčí, Vladimíra Volná, Elsa Real,
Augustin Colette, Frank de Leeuw, Alberto González Ortiz

European Topic Centre on Air Pollution and Climate Change Mitigation

The European Topic Centre on Air Pollution and Climate Change Mitigation (ETC/ACM)
is a consortium of European institutes under contract of the European Environment Agency
RIVM Aether CHMI CSIC EMISIA INERIS NILU ÖKO-Institut ÖKO-Recherche PBL UAB UBA-V VITO 4Sfera

Front page picture:
Courtesy of Pexels.com, CC0 License Adrianna Calvo (photo 58737).

Author affiliation:
Mar Viana, Marc Padrosa, Xavier Querol, Andrés Alastuey: IDAEA-CSIC, Spain.
Nina Benesova, Blanka Krejčí, Vladimíra Volná: CHMI, Czech Republic.
Elsa Real, Augustin Colette: INERIS, France.
Frank de Leeuw: RIVM, The Netherlands.
Alberto González Ortíz: EEA, Denmark.

DISCLAIMER

This ETC/ACM Technical Paper has not been subjected to European Environment Agency (EEA) member country review. It does not represent the formal views of the EEA.

ETC/ACM Technical Paper 2017/3
European Topic Centre on Air Pollution and Climate Change Mitigation
PO Box 1
3720 BA Bilthoven
The Netherlands
Phone +31 30 2748562
Fax +31 30 2744433
Email etcacm@rivm.nl
Website http://acm.eionet.europa.eu/

Contents

1. Ozone episodes in Southern Europe

Tropospheric (ground-level) ozone (O_3) is a secondary pollutant which is not directly emitted into the atmosphere, and is instead formed from chemical reactions in the presence of sunlight and following emissions of precursor gases of both natural and anthropogenic origin. Owing to its chemical properties, O_3 is a dangerous pollutant in the lower troposphere, causing harm to human health (WHO, 2008) and ecosystems (e.g., Nali et al., 2002; Paoletti, 2006; Scebba et al., 2006). This is why both the World Health Organization (WHO, 2006) and the European Union (EU, 2008) have set thresholds for O_3, as follows.

- A human health EU target value (TV) fixed at 120 $\mu g/m^3$, for the maximum daily eight-hour mean that should not be exceeded more than 25 days/year as a mean over three years. The WHO guideline is set at 100 $\mu g/m^3$, also for the daily maximum eight-hour mean, with no exceedances allowed.
- An EU population information hourly threshold of 180 $\mu g/m^3$.
- An EU population alert hourly threshold of 240 $\mu g/m^3$.
- An EU long-term objective (LTO) for the protection of human health (maximum daily eight-hour mean concentration) of 120 $\mu g/m^3$.
- A vegetation protection EU TV: AOT40 ([1]) from May to July should not exceed 18 000 $\mu g/m^3 \cdot h$, as a mean over 5 years. And an EU LTO, where AOT40 May to July should not exceed 6 000 $\mu g/m^3 \cdot h$.

The number and variety of thresholds shown above reflect the complexity linked to the quantification and regulation of this atmospheric pollutant.

Regarding the attainment of those regulated thresholds, for instance and according to EEA (2016), in 2014 conformity with the WHO air quality guideline was observed in fewer than 4 % of all stations and in only 5 of 503 rural background stations. Also 16 countries of the EU-28 registered concentrations above the LTO more than 25 times (Figure 1.1).

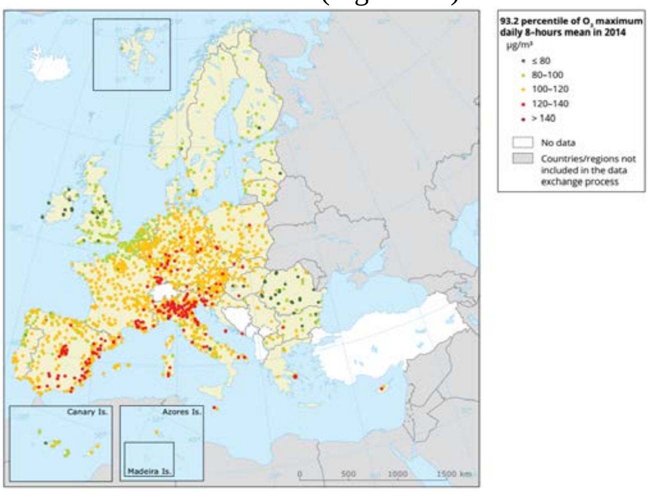

Figure 1.1. O_3 concentrations (93.15 percentile of O_3 maximum daily 8-hours mean) monitored in 2014. Source: EEA (2016).

([1]) AOT40 (expressed as $\mu g/m^3$ per hour) is the sum of the difference between hourly concentrations greater than 80 $\mu g/m^3$ (= 40 parts per billion) and 80 $\mu g/m^3$ over a given period using only the one-hour values measured between 8:00 and 20:00 Central European Time each day.

The *Air Quality in Europe - 2016 Report* (EEA, 2016) evidenced that O_3 concentrations are decreasing at rural sites, reflecting the decline in precursor emissions. The largest decrease is observed for metrics based on the highest O_3 concentrations, for which the reduction in photochemical production at the European level is more important than changes in the tropospheric background. On the other hand, the trend in the O_3 mean is small and frequently not statistically significant. Conversely, at traffic stations, where the local titration effect dominates (O_3 removal by reaction with NO to form NO_2, Mészáros, 1999, among others), there is an upward trend in the annual averaged concentrations. The behaviour at urban and suburban stations falls between the traffic and rural situations (EEA, 2016). Studies predict that O_3 will continue to be an issue of concern regarding air pollution and population exposure in the near future, and that modelling tools will be key to achieve high-quality O_3 data (e.g., Figure 1.2; Monks et al., 2015; EEA, 2015).

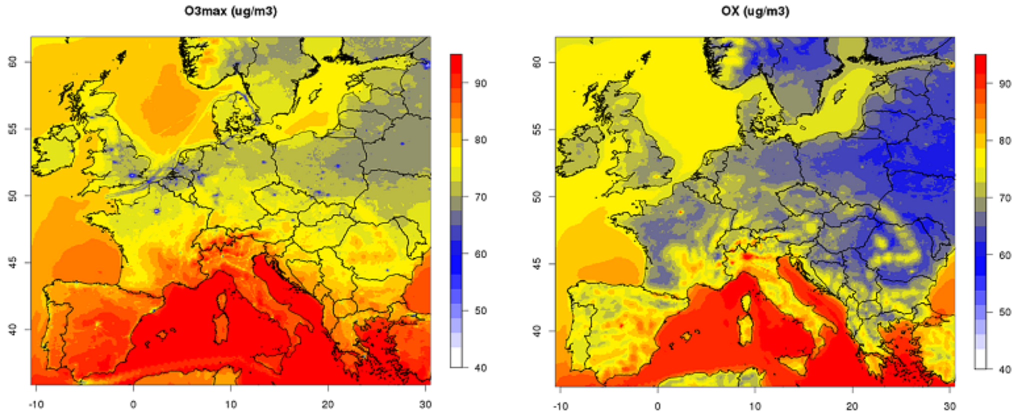

Figure 1.2. In a continental chemistry transport simulation with the CHIMERE model at a resolution of 8 km, major urban centres in northern and central Europe highlight the NO_x titration process (left: summertime average of daily maximum O_3), while the total oxidant level (right: Ox as NO_2+O_3, annual mean) is high in most European cities. Source: Monks et al. (2015).

When compared to other air pollutants such as particulate matter (PM) or NOx, it seems that O_3 may have received less attention from the public and policy-makers, which could be due to different reasons:

- Whereas for PM and NO_2 the EU has set limit values, for ozone target values have been set. While compliance with limit value is legally binding, a target should be attained where possible not entailing disproportionate costs.
- A total of 16 000 premature deaths are attributed to exposure to O_3 in EU-28 in 2013, in contrast with 436 000 attributed to $PM_{2.5}$ or 68 000 attributed to NO_2 (EEA, 2016).
- The impact on the gross domestic product (GDP) of the costs associated with PM-attributable health effects is estimated to be 5%, whereas it is 0.2% for O_3 (World Bank, 2016).
- O_3 in Europe is an environmental issue affecting mainly the Southern regions, and therefore the political and environmental pressure for action is lower than for other, more widespread pollutants. High O_3 episodes are however also recorded in central Europe (e.g., in summer 2003).
- O_3 episodes have stronger impacts on rural than urban areas, where less population is exposed. In contrast, the impact of this pollutant on crops and vegetation, especially significant in rural areas, can be serious.
- O_3 phenomenology involves a higher degree of complexity than that of other air pollutants, and this is a limiting factor for the efficiency of potential action plans (Millan et al., 2002; Querol et al., 2017)

Strategies to mitigate O_3 pollution also differ with regard to other atmospheric pollutants, mainly due to its secondary nature which implies that precursor species (VOCs, NOx) must be targeted instead. Short- and long-term measures available to tackle this pollutant, as well as their effectiveness, are discussed in section 3.

1.1. O_3 formation and transport mechanisms

Tropospheric O_3 is a secondary pollutant characterised by complex formation mechanisms based on the photo oxidation of volatile organic compounds (VOCs) in the presence of nitrogen oxides (NO_X=NO+NO_2). O_3 precursor gases such as NO_X and non-methane VOCs (NMVOCs) may have both natural (biogenic) and anthropogenic origin. It is essential to consider that the O_3 formation pathways are not linear (Monks et al., 2015; Pusede et al., 2015; among others), as NO_X are also involved in O_3 removal in the titration reaction with NO to form NO_2 (Mészáros, 1999). At the continental scale, CH_4 and CO also play a role in O_3 formation. O_3 formation processes are intensified with high insolation in summer (Monks et al., 2015), resulting in characteristic O_3 episodes especially in Southern European regions (Millán et al., 1991, 1997; Kassomenos et al., 1995; Gangoiti et al., 2001; Gerasopoulos et al., 2006; Cristofanelli and Bonasoni, 2009; Kallos et al., 2014; Myriokefalitakis et al., 2016; Querol et al., 2016, 2017; among others).

O_3 formation has a relevant spatial component, given that it involves not only local and regional air masses but also regional, long-range or hemispheric transport of the previously-described gaseous precursors. Large agglomerations generate high emissions of gaseous precursors of O_3, which originate mainly from traffic, industry, airports or shipping activities, and biomass combustion plants, among others. Through atmospheric transport, precursor gases emissions in a given region result in O_3 impacts in distant areas, in such a way that establishing a link between the emitters of precursor gases and the populations exposed to high O_3 concentrations is not always straightforward. Examples of this may be found at different spatial scales, e.g. Asian emissions impacting O_3 concentrations in North America (Lin et al., 2017), precursor emissions from Italy and France impacting O_3 concentrations in Spain (Millán et al., 1997, 2000; Gangoiti et al., 2001), long-range transport of O_3 and its precursors influencing the background O_3 concentrations in Europe (UNECE, 2010; Doherty et al., 2013), or urban emissions resulting in O_3 episodes in surrounding rural areas (within a <200 km radius; Querol et al., 2016, 2017).

Specifically, the Mediterranean is among the most climatically sensitive regions of Europe, often exposed to multiple stresses, such as simultaneous water shortage and air pollution exposure (IPCC, 2013). It is a characteristic region of a strongly coupled atmosphere-ocean system, composed by two basins that differ in air circulation patterns (Millán et al., 2005; Kallos et al., 2007): the Eastern and the Western regions. With regard to O_3 pollution, the Mediterranean basin is characterised by a large variety of VOCs and NOx emissions influencing O_3 formation and destruction (Whalley et al., 2014; Sahu and Saxena, 2015; Sahu et al., 2016), as well as by high insolation and atmospheric recirculation patterns which favour O_3 formation, accumulation, and continuous vertical recirculation (Millán et al., 1997, 2000; Gangoiti et al., 2001; Gonçalves et al., 2009; Dieguez et al., 2009). These factors account for a complex scenario and a high frequency of tropospheric O_3 episodes which have been studied in depth, as evidenced by the ample literature available (e.g., Millán et al., 2002; Pilinis et al., 1993; Kassomenos et al., 1995; Peleg et al., 1997; Varinou et al., 2000; Millán and Sanz, 1999; Mantilla et al., 1997; Salvador et al., 1999; Gangoiti et al., 2001; Stein et al., 2005; Astitha et al., 2008; Kalabokas et al., 2008; Cristofanelli and Bonasoni, 2009; Asaf et al., 2011; Doval et al., 2012; Castell et al. 2012; Escudero et al., 2014; Querol et al., 2016, 2017; among others). These studies describe different patterns of O_3 formation and transport episodes in the West and East of the Mediterranean basin which are described below.

1.1.1. *Western Mediterranean basin*

The Western Mediterranean is characterised by the absence of strong Atlantic wind advections, which result in dominant winds in the form of breezes originated by atmospheric pressure changes between the coastal and inland regions. Sea breezes thus transport air masses from the coast towards inland during the day, transferring precursor gases from coastal urban agglomerations towards inland suburban and rural areas (Millán, et al., 2000; Querol et al., 2016). In addition to this, the Mediterranean coastal orography, with mountain ranges surrounding the basin, also plays a major role in the air mass transport mechanisms, mainly through channelling of air masses along valleys originating from the coast. The vertical stratification of air masses and recirculation of pollutants, and their impact on O_3 concentrations, is a well-studied trait of the Western Mediterranean basin (Millán et al., 1996, 2000; Castell et al., 2008). Finally, emissions of gaseous precursors NOx and VOCs are high in this region as a consequence of the dense population (with major urban areas such as Barcelona, Marseille or Valencia) and the presence of Mediterranean forest landscape areas (Varinou et al., 1999; Toll and Baldasano 2000; Barros et al., 2003; Poupkou et al., 2008; Gonçalves et al., 2009; Seco et al., 2013; Valverde et al., 2016).

A review of classical O_3 literature and recent studies in the Western Mediterranean, specifically in North-eastern Spain, points to 3 main mechanisms leading to the occurrence of high O_3 episodes (Millán et al., 2000; Gangoiti et al., 2001): (i) the surface fumigation from high O_3 reservoir layers located at 1500-3000 m a.g.l. originating from the injection of polluted air masses at high altitude during previous day(s); (ii) local/regional photochemical production and transport (at lower heights) from the Barcelona metropolitan area and the surrounding coastal settlements, into the inland valleys); and (iii) external (to the study area) contributions of both O_3 and its gaseous precursors. In this framework, and focusing specifically on the Barcelona region in July 2015 as a case study representative of the Western Mediterranean, 2 types of O_3 episodes have been identified (Millán et al., 2000; Gangoiti et al., 2001; Querol et al., 2017):

- Type A: characterised by major local/regional O_3 recirculation and including fumigation of O_3 from high atmospheric layers (1500–3000 m a.g.l.) where air masses are transported towards the sea. These O_3 concentrations are superimposed on the typical regional/long-range O_3 transport mechanisms. The episodes produced in this way are characterised by major exceedances of the O_3 information threshold, as they are triggered by the overlap between direct surface transport of O_3 formed from local/regional polluted air masses and vertical fumigation of O_3 from higher atmospheric layers. This atmospheric scenario is governed by poor ventilation, local breeze circulations, and vertical recirculation of air masses over the study area. Spatially, this type of episodes affects mainly rural areas downwind of major urban agglomerations, possibly within 100-200 km.
- Type B: characterised by larger-scale, regionally transported O_3 contributions governed by the arrival of aged air masses (in the case of the Western Mediterranean, from the East/Northeast). Transport from the coastal urban agglomerations (e.g., Barcelona) to inland or vertical recirculation of air masses are not determining factors during this type of O_3 episode. The spatial impact of this kind of episode, when compared to the previous one, is generally much larger.

Thus, the major difference between the two types of O_3 episodes lies in their origin: while type A episodes depend largely on meso-scale meteorology and air mass transport patterns, in type B meso-scale meteorology is not as relevant as orography and larger-scale air mass dynamics. In sum, surface O_3 concentrations may be considered the addition of locally-produced O_3 and background contributions resulting from a combination of (a) hemispheric background concentrations, (b) the exchange between the free troposphere and the boundary layer, and (c) stratospheric inputs (Chevalier et al., 2007; Lefohn et al., 2012; Parrish et al., 2012, Kalabokas et al., 2017; Zanis et al., 2014; Akritidis et al., 2016; Sicard et al., 2017). Local O_3 contributions may be VOC- or NOx-driven (Sillman, 1999; Chang et al., 2016). As described in the literature (Chang et al., 2016), reductions in NOx emissions from local and/or upwind sources will decrease ambient O_3 formation (and ground-level ozone concentrations) in NOx-limited (VOC-driven) areas but increase O_3 formation in VOC-

limited (NOx-driven) areas, and vice-versa for VOC-limited regimes. Reductions in NOx and VOC emissions should decrease ozone formation in the transition regime.

Type A episodes may be tracked by regional air quality monitoring networks, as shown in Figure 1.3. In this example from the Catalonian air quality monitoring network (http://dtes.gencat.cat/icqa/), the evolution of pollutant concentrations throughout the day is shown for 4 stations located at increasing distances to the coast (from Barcelona, at the coast, to Bellver de Cerdanya, at approximately 150 km from the coast; Figure 1.3, top). Results evidence transport of gaseous precursors (NOx) from the coast towards inland, with decreasing concentrations due to increasing O_3 formation. In parallel, O_3 concentrations increased between 12h and 20h (solar time) with increasing distance to the coast. As shown in Figure 1.3, bottom, the hourly O_3 concentrations peaked at different times of the day as air masses were transported by sea breeze circulations from the coast (Barcelona, where the main precursor gas emissions are generated) to the inland locations (Vic, Bellver de Cerdanya). As described by Querol et al. (2016), this regional-local O_3 production decisively contributes to the exceedances of the O_3 information threshold in the proximity of densely populated urban/industrial areas in Spain.

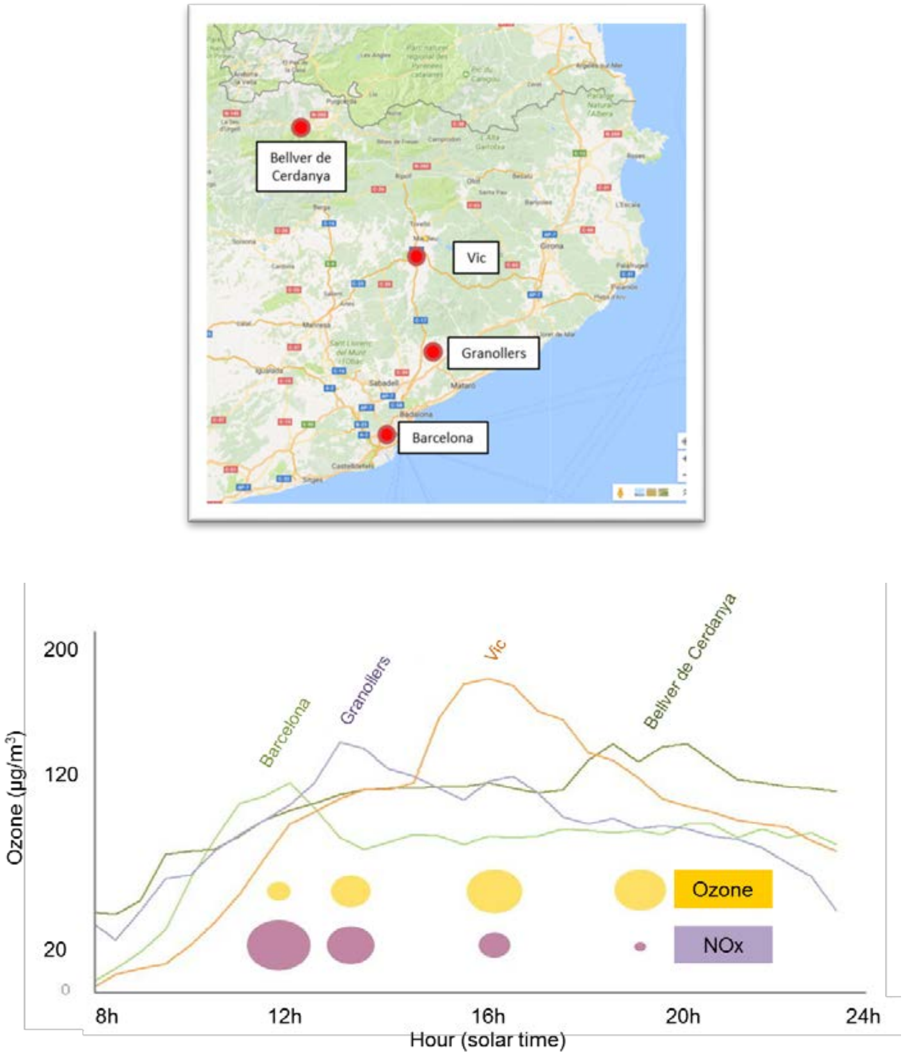

Figure 1.3. Example of the hourly evolution of O_3 concentrations throughout one day in the Osona region in Catalonia, NE Spain, in summer 2016. Source: Department of Sustainability, Catalonia Regional Government.

1.1.2. Eastern Mediterranean basin

O_3 episodes have also been studied by numerous authors in the Eastern Mediterranean basin (Pilinis et al., 1993; Kassomenos et al., 1995; Peleg et al., 1997; Varinou et al., 1999; Gerasoppoulos et al., 2006; Astitha et al., 2008; Kalabokas et al., 2008; Cristofanelli and Bonasoni, 2009; Asaf et al., 2011; Kallos et al., 2014; Myriokefalitakis et al., 2016). As in the case of the Western region, the Eastern Mediterranean is characterised by enhanced O_3 levels, especially during the summer months, due to a combination of factors and sources. This region is affected by pollutant emissions from several large agglomerations, including two megacities (Istanbul and Cairo) and one major agglomeration (Athens) (Myriokefalitakis et al., 2016). Air masses from upwind locations carrying anthropogenic emissions, mainly from Europe, the Balkans and the Black Sea, meet with biomass burning of agricultural waste and forest fires (Sciare et al., 2008), biogenic (Liakakou et al., 2009) and other natural emissions (Gerasopoulos et al., 2011) from surrounding regions under sunny and warm conditions that enhance photochemical build-up of pollutants (Lelieveld et al., 2002; Kanakidou et al., 2011).

During summer, the dispersion conditions in the Eastern Mediterranean depend on the relative strength of the high pressure system covering the Eastern Mediterranean and Balkan area and the balance between this system and the thermal low over the Anatolian Plateau (Figure 1.4, top; Kassomenos et al., 1995; Kalabokas et al., 2008; among others). When the pressure gradient is strong, northerly winds (stronger during the day and weaker during the night) dominate, creating good ventilation in the Athens Basin. This wind pattern consists of a regional-scale phenomenon called Etesians (Figure 1.5; Carapiperis, 1977; Kallos et al., 2014), and gives rise to O_3 episodes such as described in type B in 2.1, with O_3 transport from other regions. This type of transport originates pollution episodes for O_3 as well as for other air pollutants (Lazaridis et al., 2006).

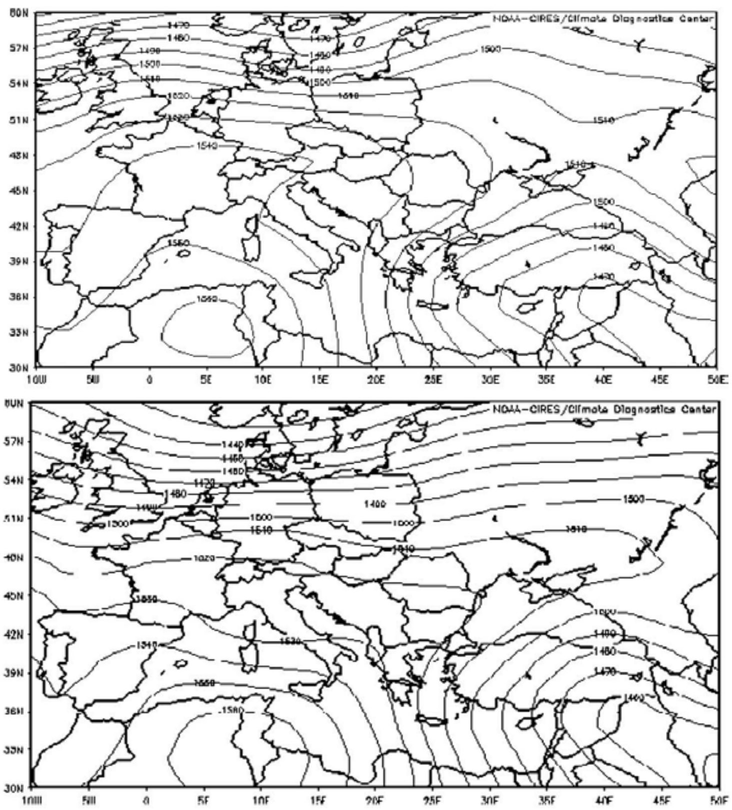

Figure 1.4. Examples of composite weather maps of geopotential heights at 850 hPa showing the characteristic synoptic scenarios giving rise to long-range transport of O_3 (Etesians, top) and local photochemical O_3 events (bottom). Source: Kalabokas et al. (2008).

On the contrary, when the pressure gradient is weak, the synoptic circulation is weak from the North and the local circulations define the dispersion conditions, giving rise to local-regional O_3 events (Figure 1.4, bottom). O_3 episodes of the type A described in 2.1 are developed under this kind of scenario in the Greater Athens Area, as an example (Kassomenos et al., 1995). In Greece, fumigation from higher altitude layers also occurs during these episodes and contributes to the average surface O_3 levels, with ozone concentrations in the free troposphere and the boundary layer during summer regularly exceeding 60 ppb (Kalabokas et al., 2000; Kourtidis et al., 2002; Lelieveld et al., 2002; Kalabokas and Repapis, 2004; Gerasopoulos et al., 2005). Stratospheric O_3 contributions have also been reported to increase surface O_3 concentrations during specific meteorological scenarios in the region (Kalabokas et al., 2013, 2015; Parrish et al., 2012; Lefohn et al., 2012; Zanis et al., 2014; Akritidis et al., 2016, Querol et al., 2018, among others). The effect of mesoscale circulations in the Greater Athens Area on the formation of air pollution episodes has been the subject of several studies (Pilinis et al., 1993, and references therein), emphasising the role of persistent stationary anticyclonic conditions as well as of the sea/land breeze mechanisms (Kassomenos et al., 1995; Kallos et al., 1993, 2007). However, other studies (Gerasopoulos et al., 2006, 2007) suggest that, on average throughout the year, the role of local photochemistry is limited as it contributed with less than 4% to the observed O_3 levels. Particularly in summer, transport from the main European continent is the dominant mechanism responsible for the elevated O_3 (Gerasopoulos et al., 2005, 2006). It is also proposed (by observations and modelling results) that local photochemistry actually acts as a sink for O_3 (Gerasopoulos et al., 2006).

As a result, the existing literature seems to conclude that, even though type A episodes are recorded across the Mediterranean basin, it is type B episodes which are dominant in the Eastern Mediterranean. Additional research applying a consistent methodology in the Eastern and Western Mediterranean regions, as done in the present study, will allow for a statistically robust confirmation of this assessment.

Figure 1.5. Etesian winds, strong, dry north winds of the Aegean Sea, which blow from about mid-May to mid-September. Source: Hogan C.M. (2011).

1.2. Methodological approach

The studies reviewed in this work suggest that the assessment of O_3 episodes in the Mediterranean region is best accomplished though the combination of experimental and modelling tools. Because of the major spatial component of this pollutant, strongly influenced by local, regional and long-range transport, the availability of sufficiently-resolved spatial and temporal data is paramount for this kind of assessment. While modelling approaches seem more necessary for the assessment of long-range transport O_3 episodes (type B), experimental data might be a more effective tool (possibly, in

combination with modelling tools) for local/regional episodes of the type A. Data and potential tools available for the assessment and quantification of O_3 episodes across the Mediterranean basin are:

- Online measurement of gaseous pollutants: available from local or regional air quality monitoring networks, online measurements are necessary to understand the O_3 formation and transport mechanisms. Continuous monitoring of O_3 and related variables (e.g., NOx) in background conditions represents a fundamental activity for understanding the processes influencing the tropospheric O_3 budget (Cristofanelli and Bonasoni, 2009).
- Ox concentrations: Ox concentrations (defined as the sum of NO_2+O_3) may be calculated to complement the interpretation of O_3 concentrations. The concept of Ox (de Leeuw et al., 1990; Kley and Geiss, 1994; van Loon et al., 2007) was proposed to analyse the O_3 spatial and temporal variability by diminishing the effect of titration of O_3 by NO ($NO+O_3 \rightarrow NO_2+O_2$, with the subsequent consumption of O_3) in highly polluted areas with high NO concentrations. The use of Ox data from strategically selected monitoring is considered a useful tool to assess the different regimes leading to high O_3 concentrations, and to differentiate between type A and type B episodes, with important implications in the design of potential abatement strategies (Querol et al., 2017). According to these authors, during type A episodes Ox concentrations follow a positive and marked gradient towards inland, which is not the case during type B episodes (see section 2.5 for more information).
- Modelling results: numerous chemical transport models have been applied to simulate O_3 concentrations in the Mediterranean region. As an example, the O_3-forecasting system applied to the Mediterranean Region has operated since July 2004 for the Athens Olympics (http://forecast.uoa.gr). The operational use of atmospheric and air quality models provides the opportunity to study photochemical activity and particle formation and transport in various scales, from mesoscale to regional (Asthita et al., 2008). Modelling should be improved, especially with regard to forecasting the occurrence of vertical recirculation episodes.
- Meteorological parameters: wind direction and speed, temperature, relative humidity, etc. are also necessary inputs for the modelling and experimental approaches to characterise O_3 episodes.
- Additionally, a robust network of O_3 VOC precursors would be essential to understand the complex phenomenology of O_3 episodes, though it is in general currently not available across Europe.

Aside from those, passive dosimeters provide data with a lower time resolution (e.g., 1 week in the case of O_3) but due to its relatively low analytical cost they may be useful to obtain high spatially-resolved O_3 concentration maps for specific study areas. When using passive dosimetres it is essential to take into account the need for replicate measurements and a potentially low data availability (on average, 20% of the dosimeters may be lost). Because of their coarse temporal resolution, dosimeters are not suitable to study O_3 episodes and should therefore be used for different approaches, e.g., temporal or spatial trends.

Two main limitations or gaps have been identified by means of this review:

a) Selection of O_3 indicators: the assessment of different metrics for O_3 monitoring has a significant impact on the conclusions and interpretations which may be extracted. As shown in Figure 1.6 (Querol et al., 2016), different regions are highlighted as reporting high O_3 concentrations as a function of the metric used (annual mean concentrations, 93.15 percentile of the maximum daily 8-h mean, total number of hourly accumulated exceedances of the O_3 information threshold, and AOT40 values). Annual mean O_3 concentrations (Figure 1.6a) show a larger variability than the percentile 93.15 (Figure 1.6b), which is more homogeneous across the Iberian Peninsula (with the exception of the North-western coast) and which highlights higher concentrations. Conversely, the AOT40 (protection of vegetation, Figure 1.6c) clearly highlights the Mediterranean coastline and the Madrid region as the regions with the highest concentrations. Finally, the number of exceedances of the information threshold (Figure 1.6d) points to the major cities in Spain (Madrid and Barcelona).

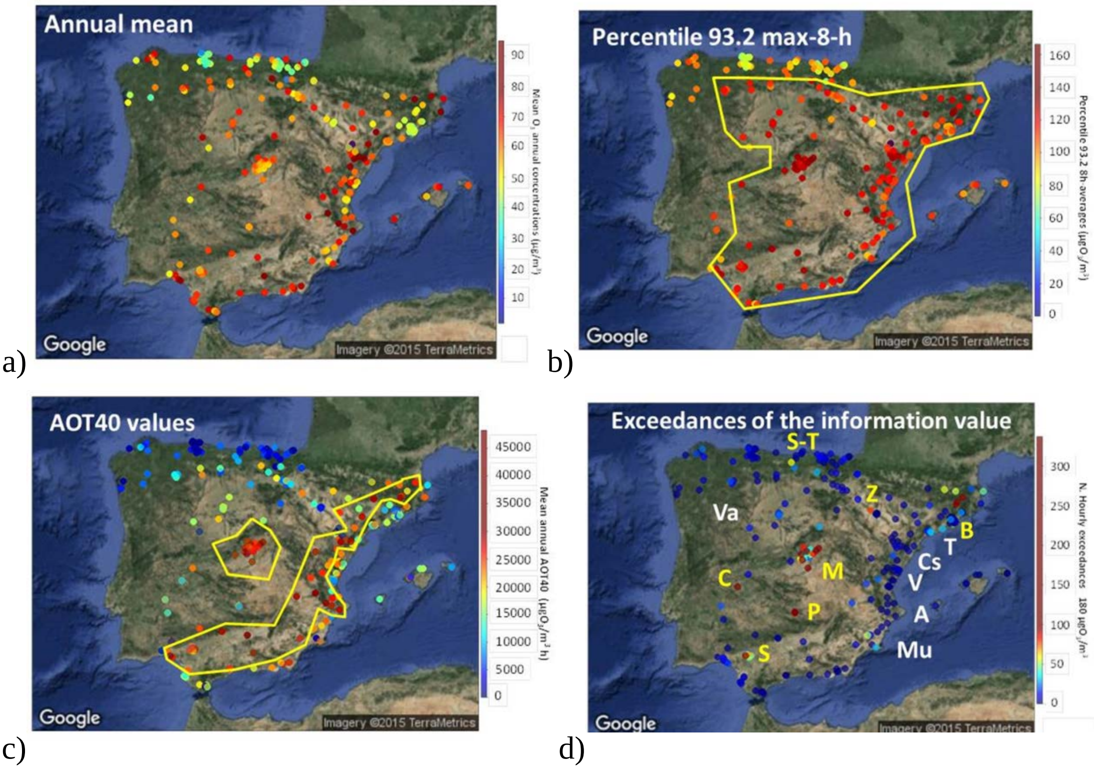

Figure 1.6. **Spatial variability of 2000–2015 mean O_3 concentrations, mean 93.15 percentile of the 8 h averaged O_3 concentrations, total number of hourly accumulated exceedances of the O_3 information threshold, and mean AOT40 values. Source: Querol et al. (2016).**

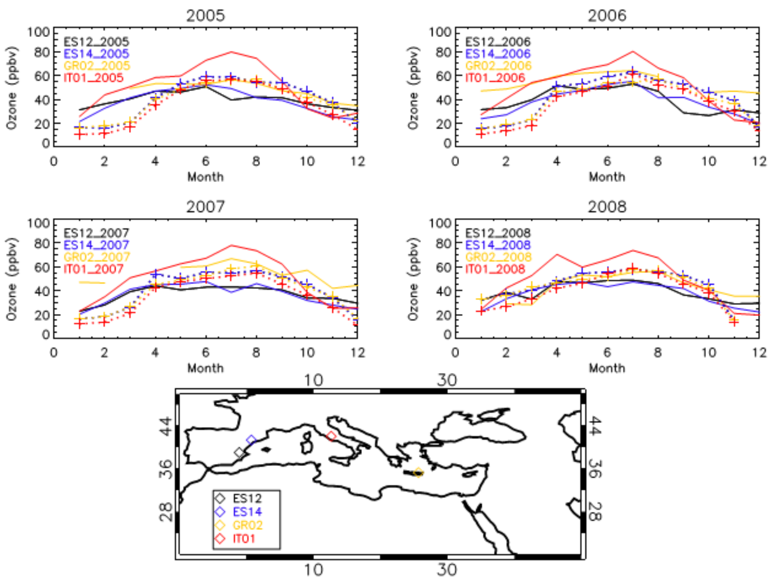

Figure 1.7. **Comparison of the results from models TOMCAT (dotted lines/symbols) and EMEP (solid lines) for the monthly mean surface O_3 (ppbv) for the years 2005-2008. The different colours represent the different stations as depicted on the map in the lower panel, where ES12 = Zarra, ES14 =Els Torms, GRO2 = Finokalia and IT01 = Montelibretti. Source: Richards et al. (2013).**

b) Assessment of the magnitude of O_3 events across the Mediterranean basin: the magnitude of O_3 episodes has not received as much attention as their formation processes, based on this literature review. While several case studies are available for specific episodes, a systematic review seems to be lacking. The results available so far suggest that, when assessing mean concentrations (e.g., monthly), the intensity of O_3 events is comparable between the Eastern and Western Mediterranean (Figure 1.7; Richards et al., 2013). Further research would be necessary to quantify the maximum concentrations reached and the frequency of the different types of O_3 episodes (e.g., see Figure 1.7) in each of the Mediterranean regions. An example of this kind of assessment for different types of stations, as well as of how different metrics offer different conclusions, is shown for Spain in Figure 1.8 (Querol et al., 2016).

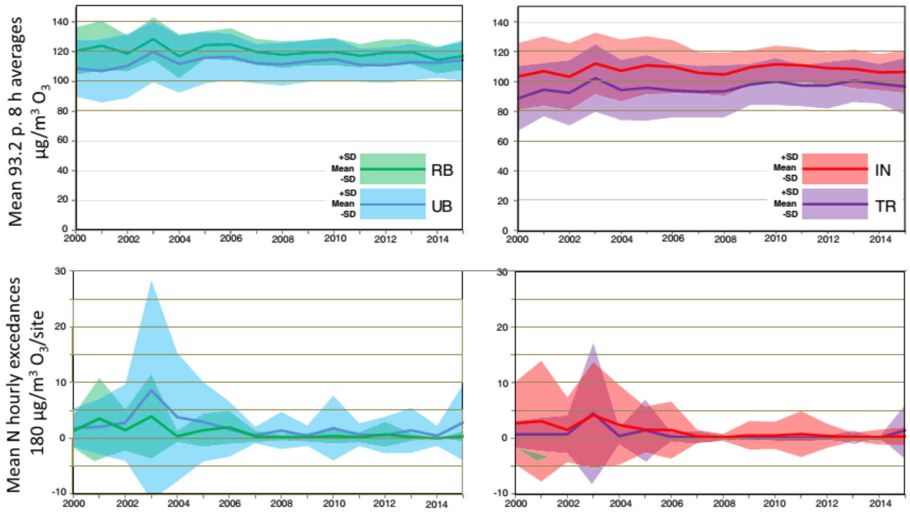

Figure 1.8. Top: 2000–2015 evolution of annual mean values (and ±standard deviations, SD) recorded for the 93.15 percentile of the max daily 8 h mean for the 4 types of sites in Spain: RB (regional background), UB (urban background), IN (industrial) and TR (traffic). Bottom: 2000–2015 evolution of aggregated annual number of hourly exceedances (and ± standard deviations, SD) of the O_3 information threshold of 180 µg/m3 for each type of site normalised by the number of existing stations. Source: Querol et al. (2016).

1.3. Concluding remarks

Current studies show that major agglomerations are sources of O_3 episodes in rural areas, therefore implying that actions could be taken to reduce these impacts. However, trend analysis shows that despite the general decrease in NO_2 concentrations, O_3 concentrations do not show a clear pattern in urban and suburban stations (EEA, 2016). Even if NO_2 and O_3 concentrations are not linearly linked, a certain decrease in O_3 concentrations may have been expected. This suggests that there is relatively little room for improvement if only NO_2 emissions are targeted. In addition, O_3 episodes seem to be strongly dependent on heat waves. These results indicate the need for further research to understand the specific complexity of O_3 formation in the Mediterranean basin, especially linked to vertical transport, and to develop methodologies and interpretations tailored to this environmentally sensitive region. The ultimate goal of this research should be the design and implementation of effective mitigation plans and programs for this air pollutant.

With the aim to partially fill these research gaps, in the following section O_3 concentrations in six regions across the Mediterranean basin are assessed. This assessment intends to understand the mechanisms controlling O_3 episodes in the vicinity of major urban agglomerations, the different patterns observed in the eastern and western Mediterranean regions, and their potential impact on the design of effective mitigation strategies. The availability and effectiveness of mitigation strategies is discussed in section 3.

2. O_3 concentrations across the Mediterranean basin: time series analysis

2.1. Selection of study regions and stations

The variability of O_3 concentrations across the Mediterranean basin between 2011-2015 was assessed based on time series analysis for a selected number of stations in 6 coastal regions under the influence of major urban areas: Valencia (Spain), Barcelona (Spain), Marseille (France), Rome (Italy), Brindisi and Taranto (Italy), and Athens (Greece) (Figure 2.1). The aim of this work was to understand O_3 formation and transport mechanisms at different spatial scales (urban and regional), the magnitude and impact of episodes on population exposure across the basin, and the differences between episodes in the Eastern and Western regions. To this end, urban stations were selected in each region to represent the source of urban pollutants, as well as suburban and rural stations to represent areas which receive pollution (in this case, O_3) from the main urban area.

Figure 2.1. Location of the study regions across the Mediterranean basin.

Within each of the 6 study regions, an initial assessment of the type of stations available per region and of data availability for the period 2011-2015 was carried out to ensure sufficient spatial and temporal data coverage. Stations were selected based on their location (distance to the coastline and to the urban area), type (urban, suburban, rural), and data availability for the period 2011-2015. The main objective of this selection was to obtain a good representation of different types of stations per region, which in addition would be representative of O_3 formation and transport (or its absence) from the urban areas towards the inland rural areas. As discussed in section 1, air mass transport from the coast towards inland, frequently channeled through coastal valleys, is a major source of O_3 episodes in Southern Europe.

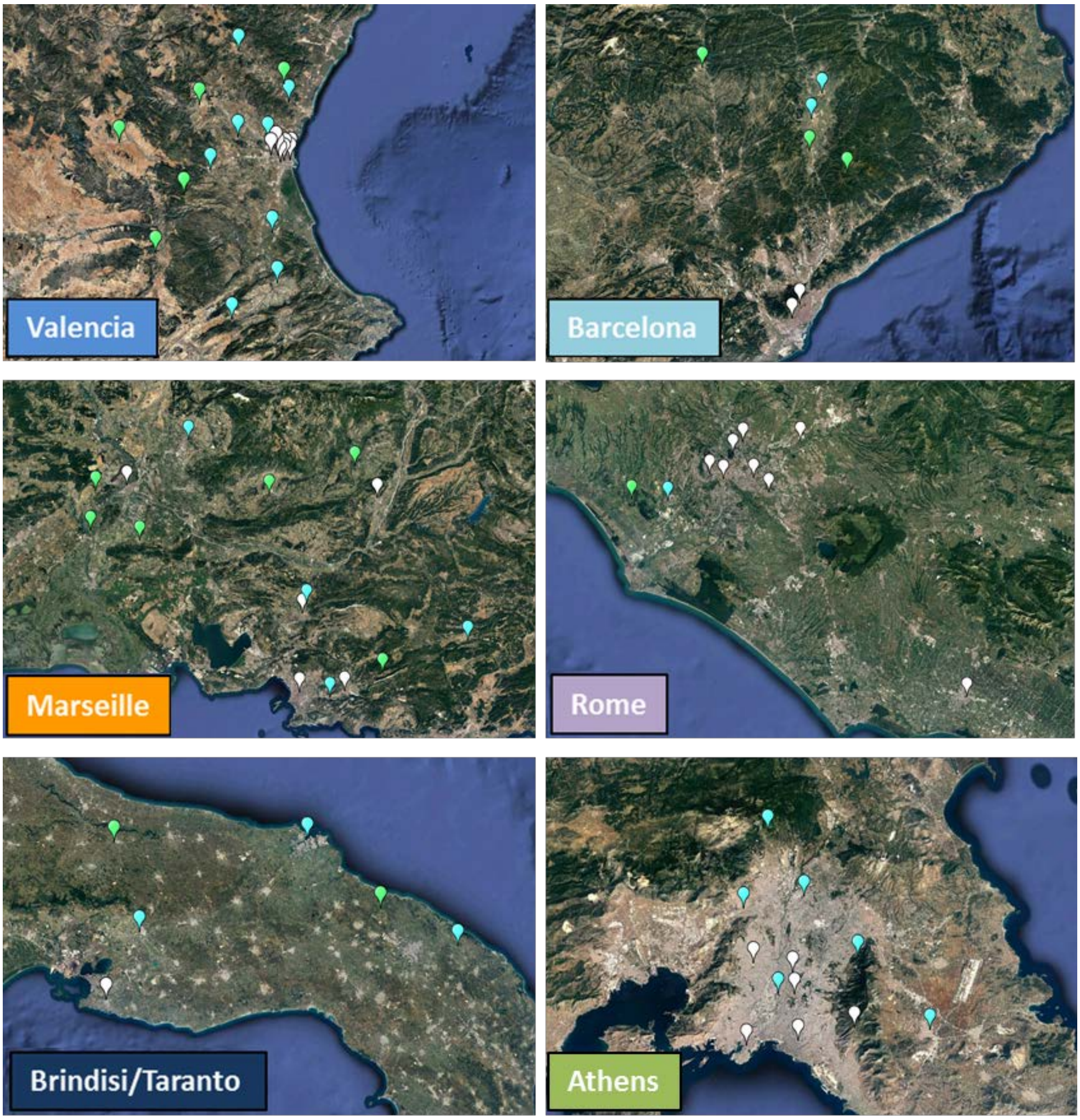

Figure 2.2. Location of air quality monitoring stations selected in each of the study regions. Green: rural stations. Blue: suburban stations. White: urban stations.

Table 2.1 summarises the number and type of air quality monitoring stations selected in each region. The total number of stations evaluated was 71 (Figure 2.2 and Table 2.1), the majority of which are located in the Valencia (21 stations) and Marseille (15 stations) regions, with the lowest station coverage evidenced for Brindisi/Taranto and Barcelona. The main limitation found in this assessment was the absence in the Athens region of rural stations, with only urban and suburban stations being available (Table 2.1). The stations evaluated were located within a 60 - 80 km radius from the main urban area (Figure 2.3), which was frequently (although not always) located along the coastline.

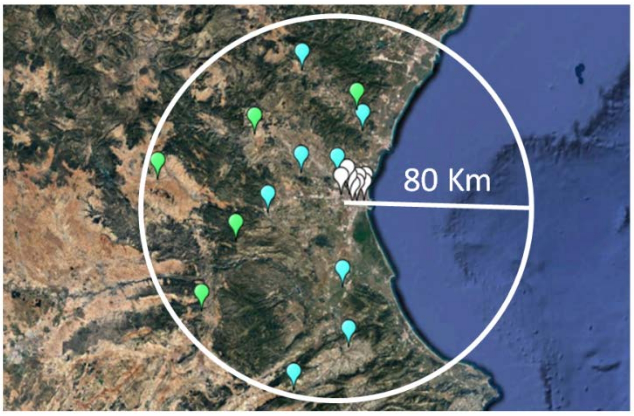

Figure 2.3. Graphical representation of the strategy followed for station selection.

Table 2.1. Number and type of stations selected in each of the 6 study regions.

City	City geolocation		Station type			Nr. stations	Max. dist.* (Km)
	Latitude	Longitude	Rural	Suburban	Urban		
Valencia	39,46899° N	-0,3769°E	5	8	8	21	80
Barcelona	41.390205ºN	2,1540ºE	3	2	2	7	80
Marseille	43,29337° N	5,3713°E	6	4	5	15	80
Roma	41,90322° N	12,4956°E	1	1	8	10	60
Brindisi/Taranto	40,63325° N	17,9396°E	2	3	1	6	80
Athens	37,97693° N	23,7259°E	0	6	6	12	60

*: maximum radius (km) of the circumference inside which the stations were located, with the urban area at the centre of the circumference, see Figure 2.3.

As concluded in section 1, analysis of O_3 concentrations is complex due to the variety of statistics available (8-hr mean concentrations, P93.15 of the maximum daily 8-hour mean (MDA), number of exceedances of the information or alert thresholds, etc.), which target different aspects of O_3 pollution such as the highest concentrations, mean concentrations, or concentrations triggering alerts. Even though all of the statistics available can be calculated for each of the analyses below (see Annex 1), a selection of the most relevant ones in each case was chosen with the aim to facilitate reading of the text below.

2.2. Temporal variability and main statistics across 2011-2015

As an initial step, the representativeness of calculating mean values over the period 2011-2015, for any of the O_3 statistics shown in this work, was assessed. The idea was to understand whether any of the study years showed an unusual behaviour with regard to the rest, or whether (on the contrary) averaging values across 2011-2015 is statistically representative. The aim was thus to evaluate the inter-annual variability of different O_3 metrics, and for this exercise the P93.15 was selected as an example (other statistics might have been used instead). Thus, the temporal variability of the 93.15 percentile of the maximum daily 8-hour mean (MDA8) concentrations (P93.15) across the study period (April to September) is described in Figure 2.4. The P93.15 is used to characterise the situation in relation to the EU target value in each region. According to these results, the P93.15 did not vary significantly across the different years in the different study regions. Slightly higher P93.15 values were only recorded in 2015, a trend that was consistent across the Mediterranean basin and across all station types. The year 2015 was in Europe as a whole the second warmest since instrumental records

began (EEA, 2017a). The year 2013 also showed relatively higher values around Marseille, but this was not detected simultaneously in other regions. Thus, over all, it may be concluded that P93.15 values did not vary largely throughout the study years (2011-2015), and it is therefore statistically representative to carry out the assessments below on the basis of mean values for the 2011-2015 period. For the purpose of this work, it is assumed that the same will be true for other O_3 statistics used (e.g., mean concentrations, number of exceedances, etc.).

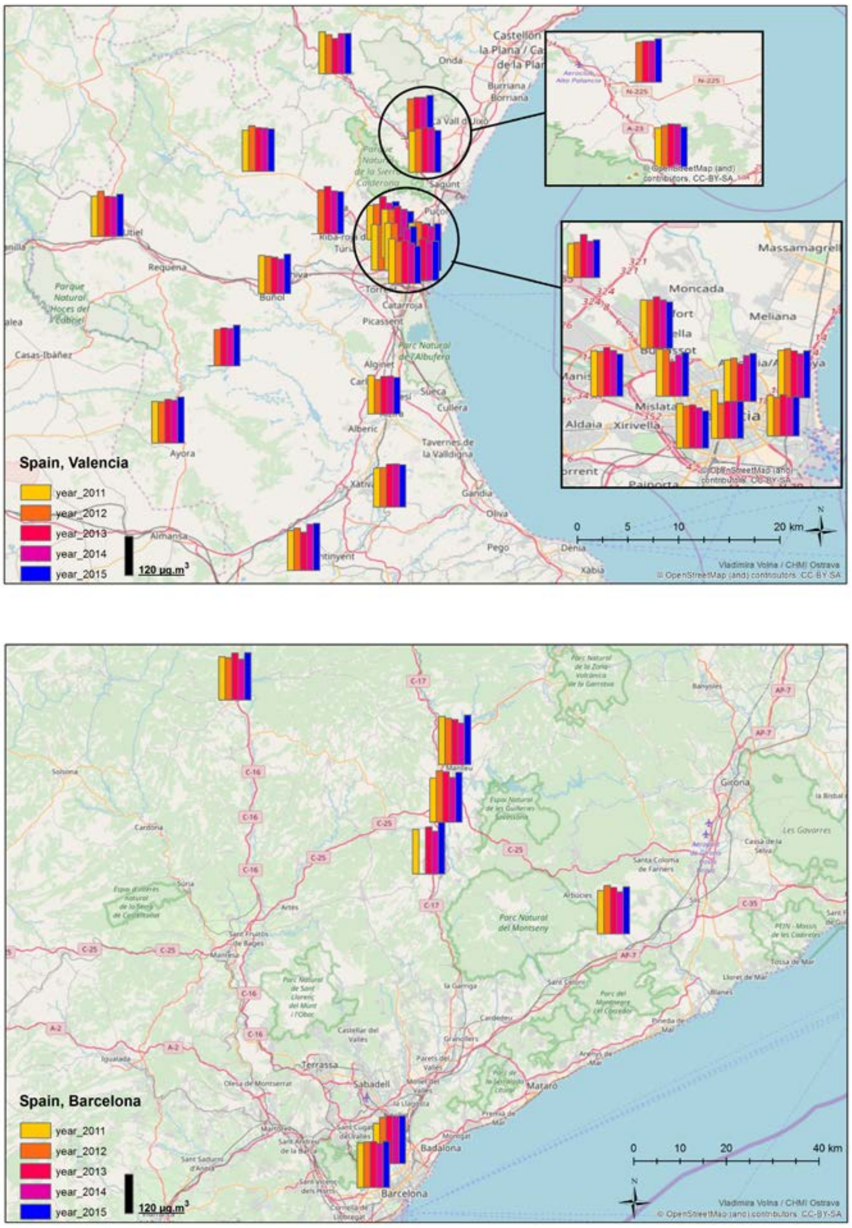

Figure 2.4. Annual evolution of the P93.15 percentile of the maximum daily 8-hr mean concentrations (MDA8) between 2011-2015 in each of the study regions. The black bar (bottom, left) indicates the concentration scale, for comparison with the coloured bars in the graph. The figure continues on the two following pages.

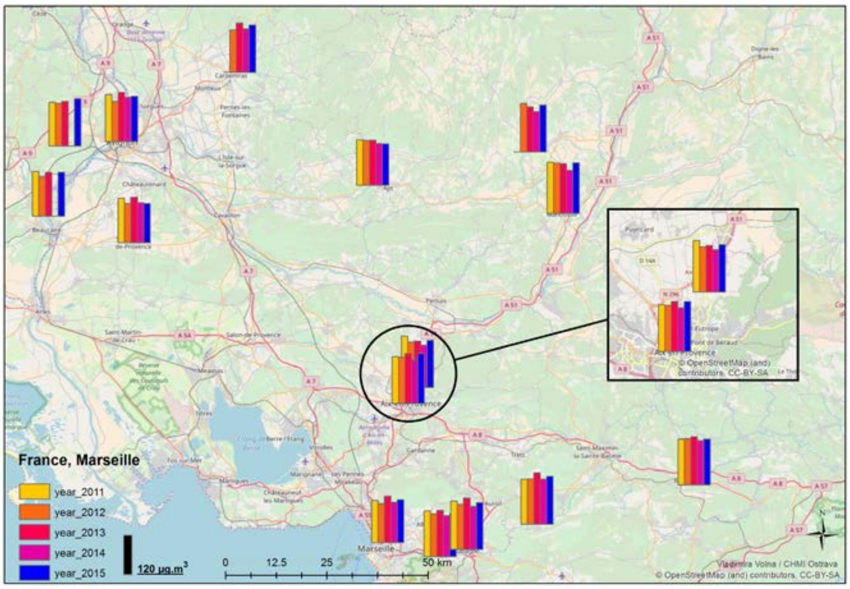

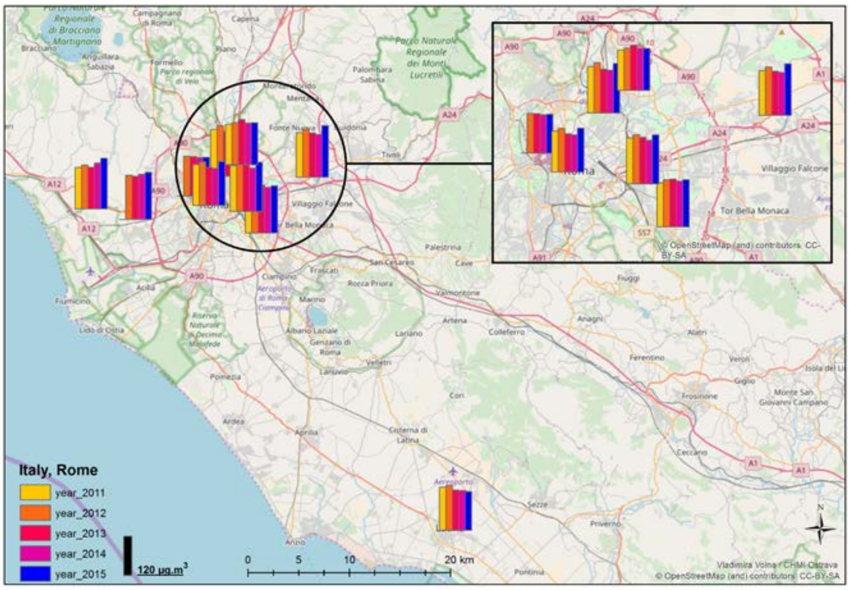

Figure 2.4. **Continued. Annual evolution of the P93.15 percentile of the maximum daily 8-hr mean concentrations (MDA8) between 2011-2015 in each of the study regions. black bar (bottom, left) indicates the concentration scale, for comparison with the coloured bars in the graph. The figure continues on the two following page.**

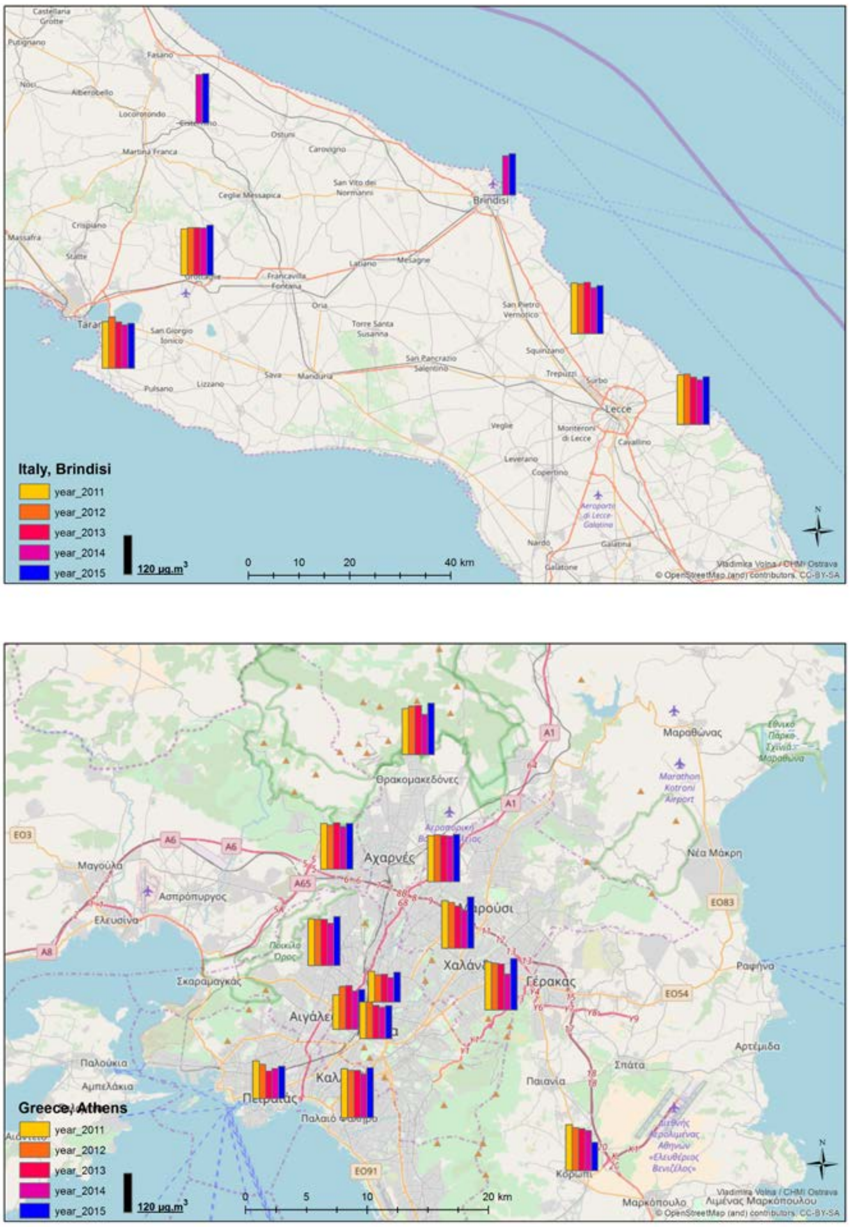

Figure 2.4. Continued. Annual evolution of the P93.15 percentile of the maximum daily 8-hr mean concentrations (MDA8) between 2011-2015 in each of the study regions. The black bar (bottom, left) indicates the concentration scale, for comparison with the coloured bars in the graph.

An assessment of average O_3 statistics across 2011-2015 (between April and September, both months included) is presented in Figures 2.5, as a function of station type. The metrics presented are: (a) the average of the P93.15 of the maximum daily 8-hr mean concentrations; (b) the average of the P99 of the maximum daily 8-hr mean concentrations; (c) the maximum hourly concentrations (maximum 1hr concentrations reached across the 5 years); (d) the mean of all hourly concentrations and (e) the total number of exceedances of 120 µg/m^3 between 2011-2015, calculated using 8-hr running means.

As expected, results show a clear concentration gradient when assessing P93.15 (Figure 2.5a) from rural to urban stations (113-150 µg/m^3 at rural sites; 82-140 µg/m^3 at urban sites), supporting the evidence found in the literature of (a) consumption of O_3 in urban areas due to NOx titration ($NO+O_3 = NO_2+O_2$), and (b) the influence of urban precursor gaseous emissions on O_3 formation in nearby

suburban and rural areas. As discussed above, rural sites receive O_3 from: (1) hemispheric transport, (2) regional transport (<500 km) of O_3 and gaseous precursors from surrounding regions, (3) urban areas close to the site by (a) vertical re-circulation and fumigation from reservoir layers and (b) surface plume transport of O_3 precursors, and (4) in situ photochemical formation (Gangoiti et al., 2001; Millán et al., 2000, 2002; Zaniz et al., 2014; Kalabokaset al., 2017; Querol et al., 2017). Decreasing concentrations from rural to urban sites were detected in general across the Mediterranean basin, irrespective of the size or population of the urban area (e.g., Rome, 2863000 inhabitants; Barcelona, 1602000 inhabitants; Marseille, 1049000 inhabitants; Taranto, 203000 inhabitants; source: Eurostat, 2014) or the type of anthropogenic emissions present (e.g., Rome, mostly traffic; Valencia, traffic, industry; Marseille, industry). Another influencing parameter may be the altitude, as the rural stations in the study areas are frequently located at higher altitudes than the urban sites (usually, at sea level). This is common for most of the 6 regions (except for Brindisi/Taranto and Rome). Thus, based on these results, NOx titration and air mass transport from urban to rural areas may be considered relevant variables influencing O_3 trends in Southern Europe. Other factors are also relevant: according to Otero et al. (2016), a key determinant of O_3 extreme events in Southern Europe is the previous day concentration (lag-24, lag-48) at a given station, indicating that such events are determined by air mass re-circulation processes as described by Millán et al. (1997) and subsequent articles (e.g., Zanis et al., 2014; Kalabokas et al., 2017). Conversely, ambient temperature is the dominant parameter in central and Northern Europe (Otero et al., 2016).

When compared to the rest of the metrics assessed in Figure 2.5, the results from the P93.15 seem to suggest that this metric is useful to describe the impact of O_3 sinks (NOx titration) and sources (formation during air mass transport) but that it does not provide sufficient information regarding the magnitude or the spatial distribution of O_3 episodes across the Mediterranean basin. This kind of information seems to appear more clearly when assessing other metrics such as P99 (Figure 2.5b) which is a better representation of the magnitude of the O_3 episodes, or the maximum hourly concentrations (Figure 2.5c; 1 hour across the 5 study years), which is however very sensitive to monitoring errors and/or local influences. In this way, the evaluation of the P99 (Figure 2.5b) and the maximum hourly concentrations (1 hour across the 5 study years) shows that the highest values were obtained for suburban stations in Greece (with maximum hourly concentrations of 233-256 $\mu g/m^3$), followed by stations in France (up to 222 $\mu g/m^3$; Figure 2.5). In addition, the increasing gradient from urban to rural stations described above is not so evident anymore when assessing these parameters, suggesting that O_3 formation during air mass transport from urban to rural sites was not the dominant mechanism generating maximum 1-hr O_3 concentrations across the entire Mediterranean basin. Alternatively, regional-scale O_3 transport could be the main source of O_3 in these cases (Kallos et al., 1993, 2007; Millán et al., 1997, 2002), which would be supported by the fact that the highest concentrations were recorded in Greece, where this type of episodes has been reported to dominate (Gerasopoulos et al., 2006). Finally, similar results were obtained for the total number of exceedances of the 120 $\mu g/m^3$ threshold, which were highest for Greek and Spanish suburban stations and one French rural station (336-383 exceedances/station in 5 years; Figure 2.5e).

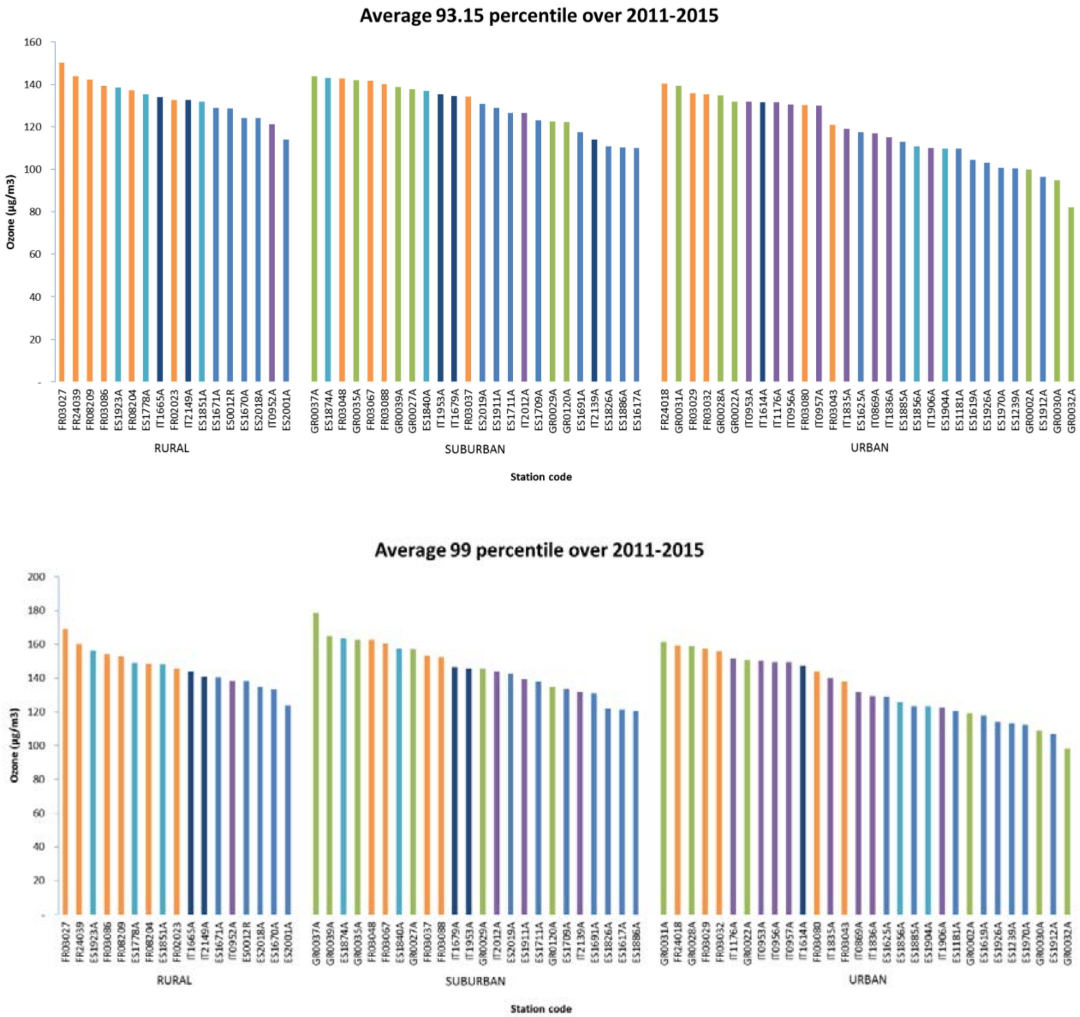

(a)

(b)

Figure 2.5. Average of the P93.15 (a) and P99 (b) of the maximum daily 8-hr mean concentrations, for 2011-2015 (April to Sept.), as a function of station type.

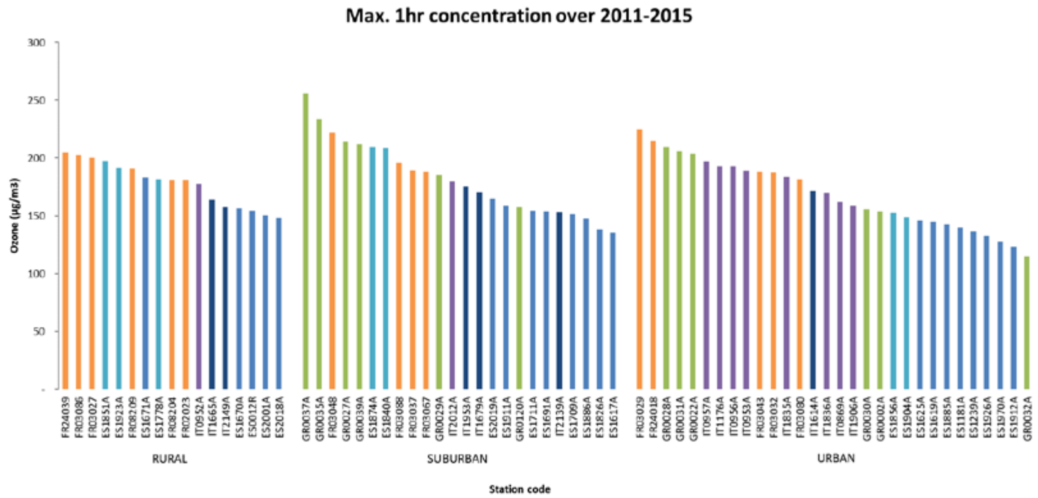

(c)

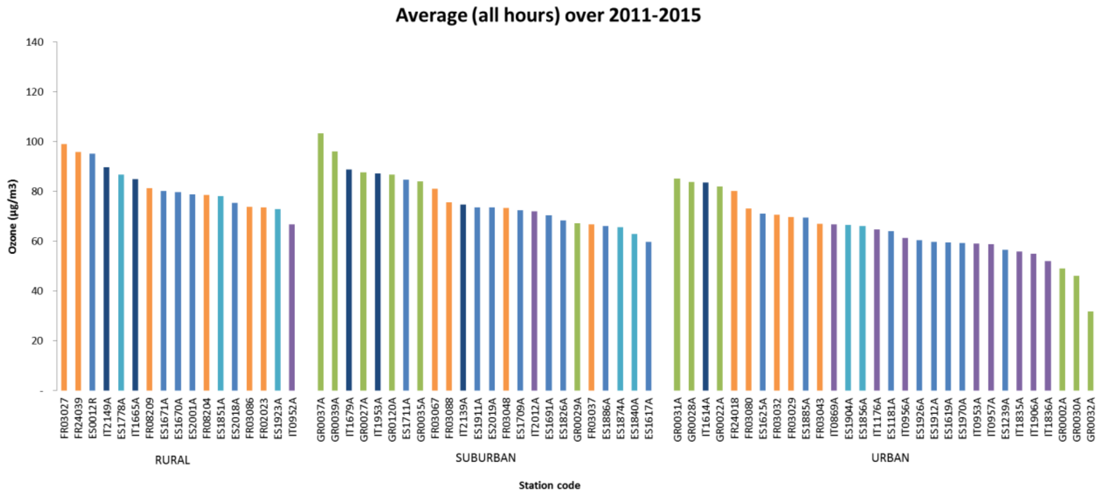

(d)

Figure 2.5. Continued. Maximum 1-hr concentrations (1 hour across the 5 study years) (c) and mean of all hourly concentrations (d), for April-September 2011-2015, as a function of station type.

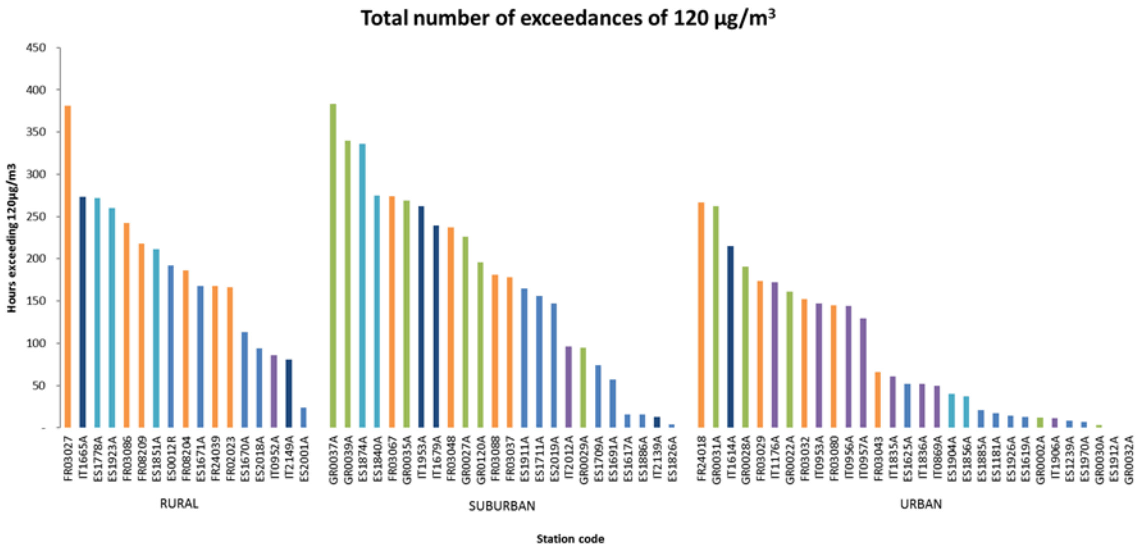

(e)

Figure 2.5. Continued. Sum of the total number of exceedances (maximum daily 8-hr mean concentrations) of 120 µg/m³ for 2011-2015 (April to September), as a function of station type.

As mentioned above and evidenced by the analysis of Figure 2.5, the use of the different O_3 statistics available results in different interpretations and provides information on different aspects of this environmental pollutant.

2.3. O_3 concentrations in the study regions

O_3 concentrations in each of the different study regions are summarised in Table 2.2 as a function of the P93.15, the P99 (both as an average across 2011-2015), the total number of exceedances of 120 µg/m^3, and the maximum 1-hour concentration (both for the whole period 2011-2015), for all station types. On average, the highest O_3 concentrations were recorded during the study period in the Marseille region (maximum P93.15 reaching 134 µg/m^3, with up to 381 exceedances of 120 µg/m^3 between 2011 and 2015) and in Athens (also with a maximum P93.15 of 134 µg/m^3). The highest peak concentrations as indicated by the maximum 1-hr concentrations were recorded in Athens (343 µg/m^3), which contrasts with the relatively low concentrations which may be recorded in this region (for instance, minimum P93.5 = 70 µg/m^3). The lowest minima could be due to the fact that the Athens stations were urban and suburban, and the highest maxima could suggest that O_3 concentrations in the Athens region were especially high during the summer months and also may have been affected by high short-term peak episodes. However, it should be noted that such high concentrations (343 µg/m^3) are rare and could be linked to instrumental issues. A more stable situation was observed for Brindisi/Taranto, where P93.15 concentrations (95-125 µg/m^3) were relatively similar to other regions (Rome, Barcelona) and the number of exceedances of 120 µg/m^3 (13-273) and the maximum 1-hr averages (158-196 µg/m^3) were in the average of the six regions. Finally, the Barcelona region showed a mixed pattern, similar to Brindisi/Taranto with respect to the number exceedances of 120 µg/m^3 (37-336), and to Rome in the maximum 1-hr concentrations (164-227 µg/m^3). Valencia showed relatively low concentrations for all of the parameters assessed (e.g., P93.15 between 82 and 118 µg/m^3), and Rome showed similar results as Brindisi/Taranto (P93.15 between 92 and 110 µg/m^3) although with higher peak concentrations (maximum 1-hr between 176 and 227 µg/m^3).

Table 2.2. Minimum and maximum values for all station types for the percentile 93.15 (P93.15) and the percentile 99 (P99) of the maximum daily 8-hr mean concentrations, the total number of exceedances of 120 µg/m^3 in 2011-2015, and the maximum 1-hr concentration in each of the study regions.

All station types	P93.15 (µg/m^3) Min-Max	P99 (µg/m^3) Min-Max	Exceedances>120 (Nr.) Min-Max	Max 1-hr (µg/m^3) Min-Max
Valencia	82-118	107-143	0-192	127-199
Barcelona	95-121	123-163	37-336	164-227
Marseille	102-134	138-169	66-381	190-282
Rome	92-110	122-152	11-172	176-227
Brindisi/Taranto	95-125	132-147	13-273	158-196
Athens	70-134	98-178	0-383	123-343

When comparing O_3 concentrations (P93.15, P99) as a function of station type (Figure 2.6a and b), similar results are found for both statistics and a high variability for certain regions:

- Rural sites: the highest P93.15 and P99 values (with also the highest variability) were recorded in Marseille, and the lowest in Rome and Valencia. It should be noted that the rural stations in Rome are located in close proximity to the urban area, and between the urban area and the coast. No data were available for Athens.

- Suburban sites: the variability in O_3 concentrations between stations in suburban areas was relatively high when compared to rural areas. Mean P93.15 suburban values were similar in Athens, Barcelona, Brindisi/Taranto and Marseille, and lower in Rome and Valencia (lowest).
- Urban sites: the highest P93.15 values were recorded in Marseille, followed closely by Brindisi/Taranto. The highest variability was observed in Athens. As discussed above, no clear relationship was observed between urban O_3 concentrations and population in each city (as a proxy for size and, potentially, anthropogenic emissions).

Over all, it is relevant to highlight that this analysis is strongly influenced by factors such as the specific location of each station, the compactness of the station network (e.g., Rome or Athens), or the presence of more than one urban nucleus (e.g., Marseille). This results in the added complexity in O_3 data interpretation.

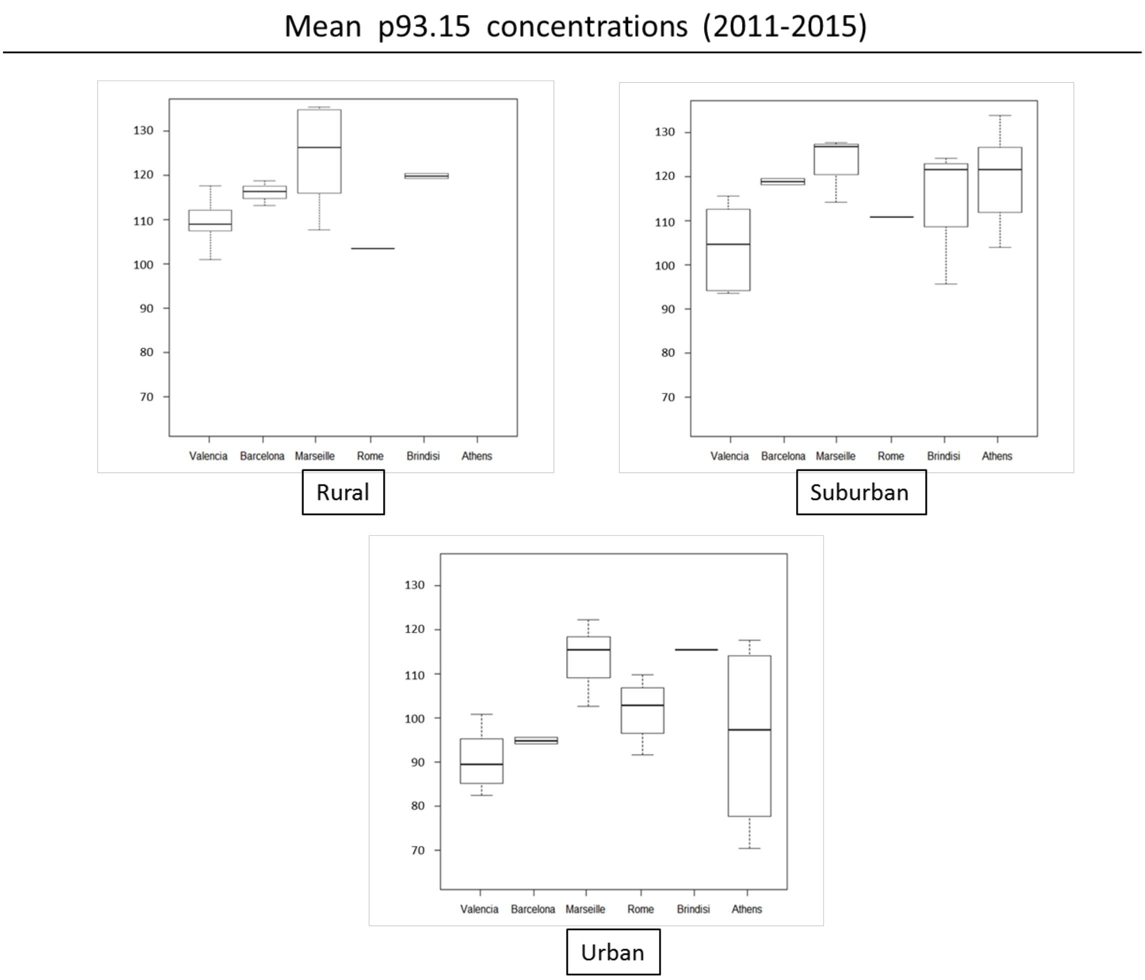

Figure 2.6a. Mean P93.15 concentrations (µg/m^3) (2011-2015) at rural, suburban and urban stations in each of the study regions. Box and whiskers plot indicating the statistical distribution of the concentrations (mean, and percentiles 5, 25, 75, and 95).

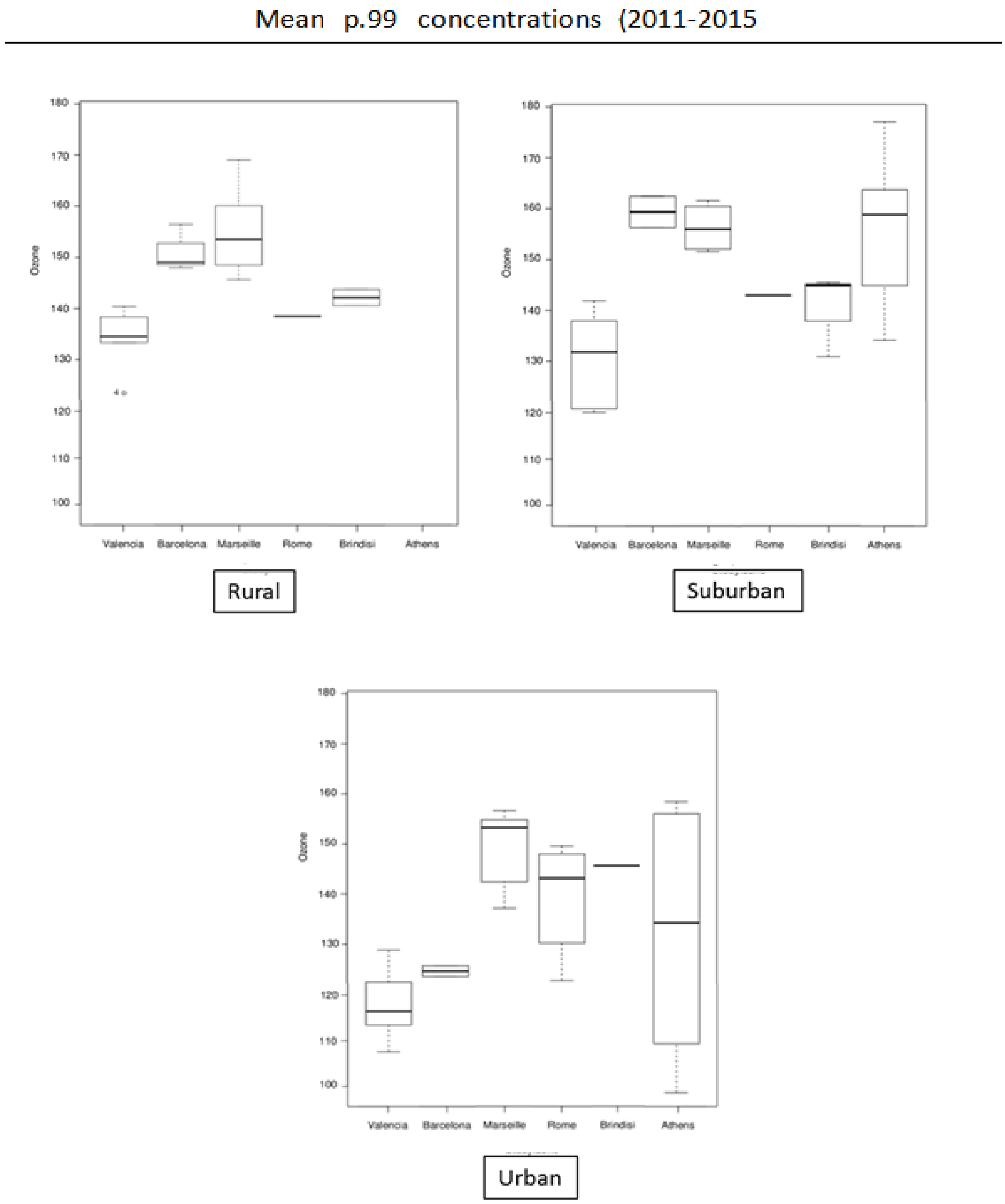

Figure 2.6b. Mean P99 concentrations (µg/m^3) (2011-2015) at rural, suburban and urban stations in each of the study regions. Box and whiskers plot indicating the statistical distribution of the concentrations (mean, and percentiles 5, 25, 75, and 95).

2.4. O_3 spatial trends and formation mechanisms across the study regions

The mean P99 and total number of exceedances of 120 µg/m^3 for the period 2011-2015 were plotted for each station in Figure 2.7, and are presented grouped by station type. The number of exceedances of 120 µg/m^3 and P99 in the different study regions seemed to follow a decreasing gradient from rural to urban stations, although the trend was not equally evident in each of them. This is partly linked to station location and classification, which raises the question of the optimisation of the design of air quality monitoring networks to obtain comparable data regarding ambient concentrations and population exposure. In addition, the absence or presence of such gradient may be considered an indicator of the dominant O_3 formation processes in each region. The Valencia, Marseille and Athens regions are examples of decreasing O_3 concentrations from rural to urban sites, which is mostly

consistent across a large number of stations (21, 15 and 12, respectively) on average across the study period. In Barcelona, P99 concentrations were similar in suburban and rural sites, and even slightly higher at suburban sites, which was linked to their location along the valley where the emissions from the urban area are channelled. As a result, O_3 formation and transport along the valley increased background concentrations in the suburban sites near Barcelona (Figure 2.7). This is the cause behind the apparent absence of gradient observed in the Barcelona region, despite the fact that regional re-circulation (type A episodes, see section 1) is the main source of O_3 episodes in the area. With regard to Athens, it should be noted that rural stations were not available in the vicinity of city for this study, and therefore it is only possible to conclude on differences between urban and suburban sites.

In Rome, on the other hand, the absence of suburban and rural sites (only 1 station of each type available) and the proximity of the stations selected limited the comparability between station types. Also, the fact that the rural station is located close to the coast, between the sea and the urban area (thus upwind of the urban area) should be considered. Mean P99 concentrations at the urban sites ranged from lower to slightly higher than at the rural station. Finally, no clear gradient was observed in the Brindisi/Taranto region. This area is characterised by high atmospheric ventilation and a prevalence of Easterly winds, transporting air masses from Brindisi (rural sites) to Taranto (urban sites). As a result, it may be concluded that regional/long-range transport (type B episodes, see section 1) is a likely source of O_3 episodes in this region.

The assessment of the total number of exceedances of 120 µg/m^3 (between April and September; Figure 2.7) provided similar interpretations. Larger numbers of exceedances were more prevalent in rural areas in Valencia and Marseille (up to 180 exceedances in Valencia and 350 in Marseille), and also in Barcelona if the similarity between suburban and rural stations is taken into account (up to 350 exceedances in Barcelona suburban sites). However, Rome and Brindisi/Taranto showed high numbers of exceedances of 120 µg/m^3 at different types of stations, following no clear pattern.

This assessment seems to suggest that different spatial patterns may be evident in different regions across the Mediterranean: while regional-scale re-circulation of atmospheric pollutants results in O_3 episodes in rural areas downwind of major cities in the Western Mediterranean (Valencia, Barcelona, even Marseille), in the Eastern Mediterranean (Brindisi/Taranto) this transport mechanism doesn’t seem to be a major source of O_3 episodes. The cases of Athens and Rome are complex: the absence of representative rural stations is confirmed as a strong limitation for this assessment.

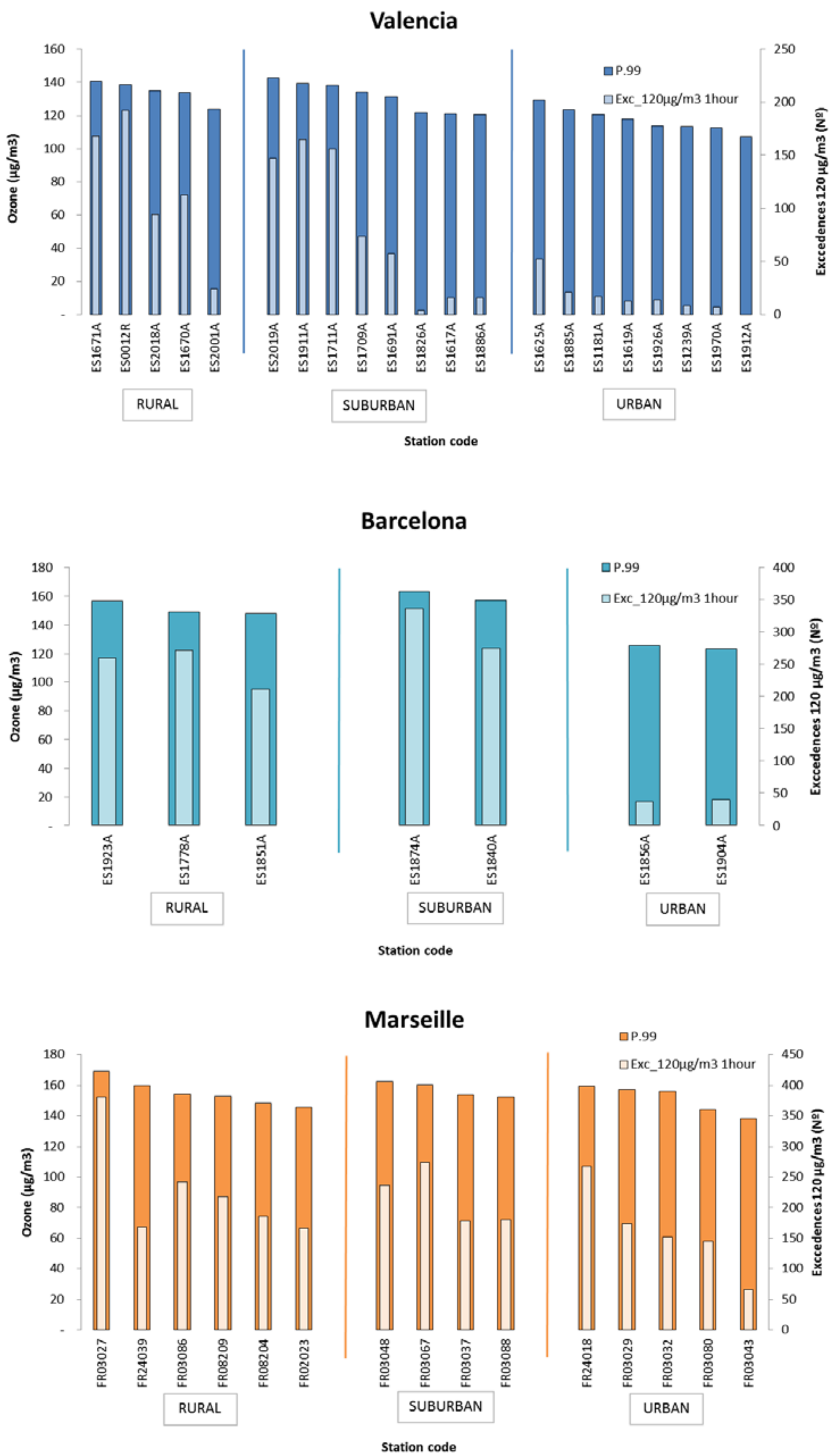

Figure 2.7. **Mean P99 in 2011-2015 and total number of exceedances of 120 µg/m^3 for the period 2011-2015, per region and station, grouped by type (rural, suburban, urban).**

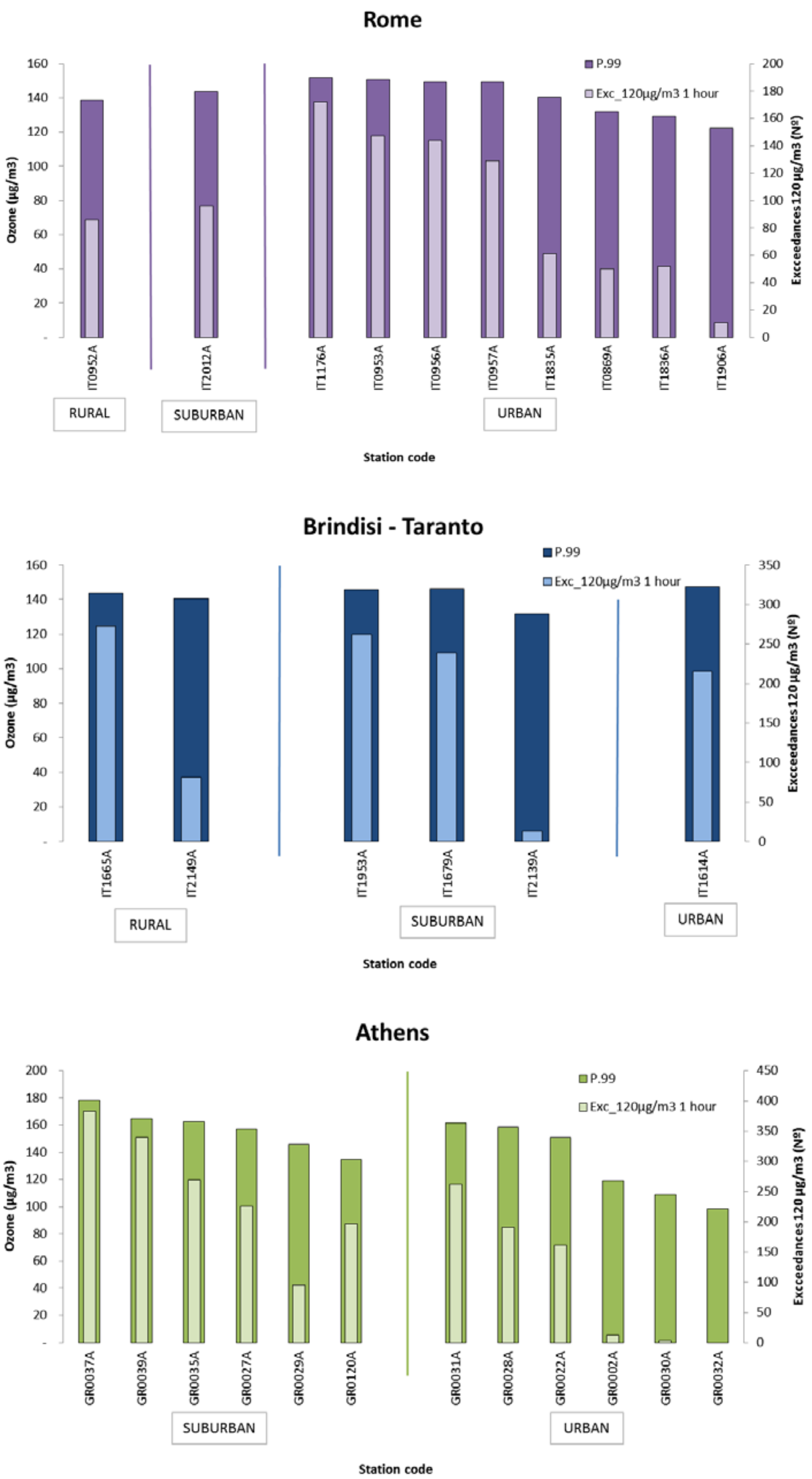

Figure 2.7. **Continued. Mean P99 in 2011-2015 and total number of exceedances of 120 µg/m^3 for the period 2011-2015, per region and station, grouped by station type (rural, suburban, urban).**

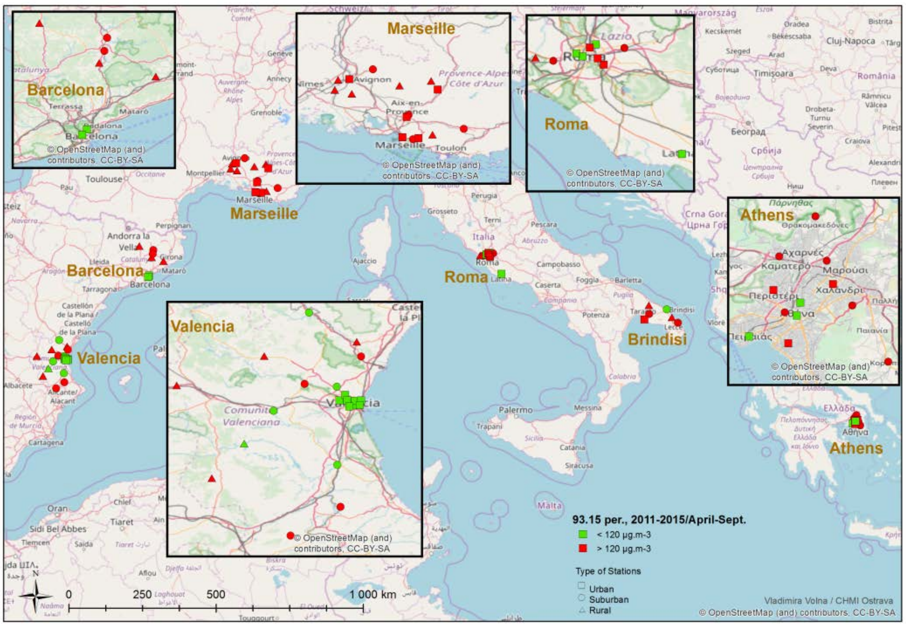

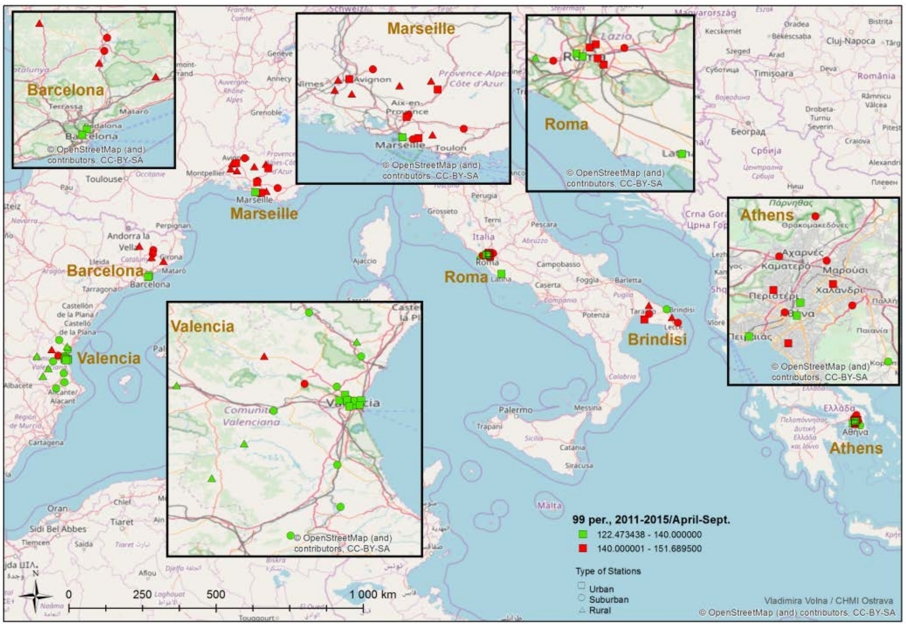

Figure 2.8. **P93.15, P99, number of exceedances of 120 µg/m^3, as average values for the years 2011-2015, and maximum 1-hr concentrations, at urban, suburban and rural sites in each study region. Data from April to September.**

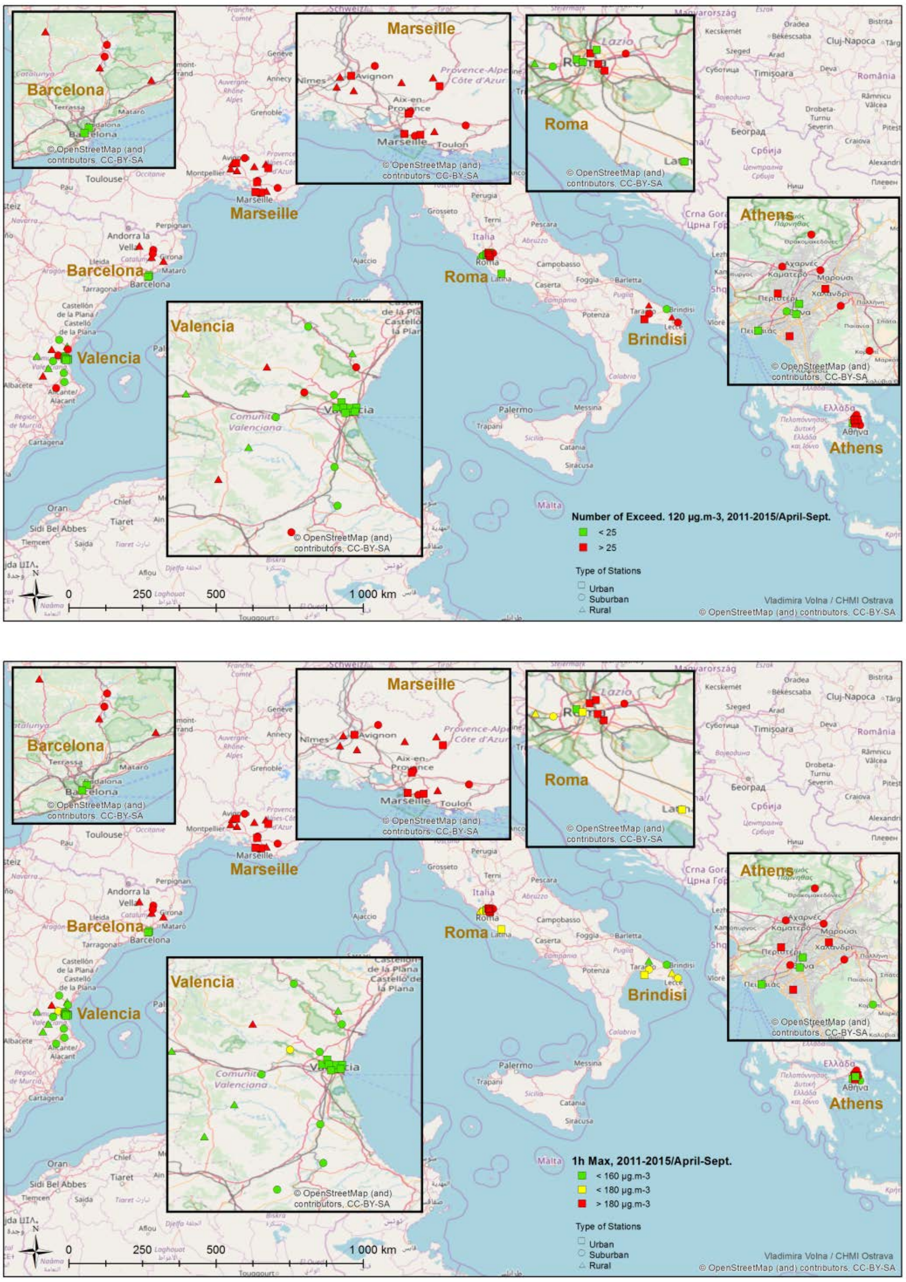

Figure 2.8. Continued. P93.15, P99, number of exceedances of 120 µg/m³, as average values for the years 2011-2015, and maximum 1-hr concentrations, at urban, suburban and rural sites in each study region. Data from April to September.

The variability of P93.15, P99, number of exceedances of 120 µg/m³ and maximum hourly concentrations within each study region are presented in Figure 2.8. The aim of this analysis was to identify specific intra-regional patterns which may aid in the interpretation of the processes governing O_3 concentrations and episodes. For the P93.15 assessment a threshold of 120 µg/m³ was selected, which was 140 µg/m³ for P99. Based on the P93.15 and P99 values, two clearly different patterns were observed: regions where the urban stations reported mean P93.15 and P99 values <threshold (120 µg/m³ and 140 µg/m³, respectively; marked in green) and suburban and rural stations >threshold (marked in red) (Barcelona and Valencia), and regions where urban stations recorded P93.15 and P99 values >threshold, similar to those in suburban and rural stations (all of them marked in red; Marseille, Athens, Brindisi/Taranto). Rome presents a mixed pattern (Figure 2.8) due to the compact distribution of the stations within the city and the lack of representative rural stations. The first pattern

(Barcelona and Valencia) would imply significantly lower O_3 concentrations in urban when compared to the rest of sites, which would suggest strong O_3 sinks in these two cities. This is probably related to high NO emissions and titration in both cities and the fact that the urban sites are concentrated in one single urban area in each region (as opposed to e.g. Marseille, where other towns as Avignon are also included). In addition, O_3 formation between the urban and rural areas results in high O_3 concentrations in the latter (type A episodes). This would have implications regarding potential mitigation strategies to achieve O_3 reductions in the suburban and rural areas.

On the other hand, in Marseille, Athens, and Brindisi/Taranto (second pattern), P93.15 and P99 values (between April and September) were on average >120 µg/m^3 at all sites. O_3 production in the Marseille region probably resulted in elevated O_3 background concentrations when air masses reached urban sites in Avignon or Aix en Provence, resulting in >120 µg/m^3 concentrations in those urban areas. Conversely, NO titration in Marseille city did not seem to constitute a sink sufficiently strong to reduce local O_3 concentrations below 120 µg/m^3. As stated above, this might be due to the less compact structure of the Marseille urban area (including other smaller urban areas). From the point of view of emissions and the generation of O_3 episodes downwind of the city, the case of Marseille would have similar policy implications to those of Barcelona and Valencia (above). However, from the point of view of NOx and O_3 emissions within the city, the patterns (and thus the policy implications) in Marseille are different to those in Barcelona and Valencia.

The situation is potentially different in Athens and Brindisi/Taranto: mean P93.15 and P99 values were relatively homogeneous across stations, which could suggest the influence on long-range transported O_3 concentrations. Under this scenario, despite O_3 consumption sinks in major cities, e.g., Athens or Taranto, P93.15 and P99 values would not decrease below the thresholds (120 µg/m^3 and 140 µg/m^3, respectively), while in suburban and rural areas they would remain high. The same conclusions may be extracted when assessing the 1-hr maximum concentrations over the 2011-2015 period, also shown in Figure 2.8. In these two regions policy actions to reduce O_3 impacts should not be addressed only at reducing local urban emissions, as in the pattern described above. It should be noted that these conclusions are limited by the fact that no representative rural stations were available for the Athens region, and that only one urban station was available for Brindisi/Taranto.

Finally, analysing the average number of exceedances of the 120 µg/m^3 threshold (Figure 2.8) allows to identify the stations which were most influenced by NOx urban emissions and which acted as O_3 sinks due to titration, as they resulted in the lowest numbers of exceedances. As shown in Figure 2.8, the lowest numbers of exceedances were recorded in the city centres of Valencia, Barcelona, Athens and Rome. Higher number of exceedances (>25 on average per year) were recorded in Brindisi/Taranto, which probably confirms that regional/long-range transport was the dominant mechanism in this area, as well as the absence of major urban areas (O_3 sinks due to the titration reaction). O_3 concentrations in this region were relatively constant and relatively high (P93.15 = 95-125 µg/m^3, all station types; Table 2.2) throughout the study period. The higher number of exceedances also found in Marseille could be explained by the less compact structure of the urban area, resulting in a weaker ozone sink, as described above.

2.5. Assessment of Ox concentrations

The interpretation of the variability of O_3 concentrations alone, not in combination with NOx, may be misleading because a given output (e.g., a decrease in O_3 concentrations) may originate from different atmospheric processes (e.g., titration by NO, or air mass renovation). To overcome this issue, the assessment of Ox concentrations, defined as the sum of O_3 and NO_2 concentrations ($Ox=O_3+NO_2$), is proposed (Kley and Geiss, 1994; van Loon et al., 2007). Thus, assessing Ox concentrations (as opposed to O_3 or NOx separately) may provide insights into the mechanisms governing O_3 concentrations and the relative differences between rural, urban and suburban stations. In this framework, Ox concentrations were calculated for the years 2011-2015 for two regions representative of Eastern and Western Mediterranean conditions: Valencia and Brindisi/Taranto. Ox concentrations were calculated as the sum of O_3 + NO_2 concentrations for each hour in the Valencia and

Brindisi/Taranto time series, respectively. Whenever gaps in the input series (O_3 or NO_2) were detected, the corresponding Ox datapoint was removed (for that specific hour). Once the hourly Ox concentrations were calculated, they were averaged over 24-hr periods to obtain the mean daily Ox concentration.

The aim of this analysis was to assess the relative differences between Ox concentrations in urban and rural sites, in order to estimate the relative prevalence of type A (dominated by local/regional scale transport between urban and rural areas) vs. type B situations (dominated by regional/long range transport) in each region. The initial hypotheses were that (Figure 2.9):

- During type A situations:
    - urban O_3 concentrations decrease due to titration, but NO_2 concentrations increase, so the sum (that is, Ox concentrations) remain mostly constant and
    - rural O_3 concentrations increase due to O_3 formation and transport, so Ox concentrations increase
    - As a result, Ox concentrations in rural areas should be higher than in urban areas. The ratio between Ox concentrations at urban and rural sites (Urban/Rural) should be lower than 1.

- During type B situations:
    - urban O_3 concentrations decrease due to titration, but NO_2 concentrations increase, so the sum (that is, Ox concentrations) remain mostly constant and
    - rural O_3 concentrations do not increase with respect to those in urban areas (before titration) due to the fact that O_3 originates from long-range transport, and therefore similar concentrations would be registered at urban and rural sites in absence of titration, so Ox concentrations do not increase.
    - As a result, Ox concentrations in rural areas should be relatively similar to those in urban areas (where concentrations would be only slightly lower). The ratio between Ox concentrations at urban and rural sites (Urban/Rural) should be close to 1.

As a result, in regions dominated by type A situations, the relative difference between O_3 concentrations in rural and urban areas should be larger than in regions dominated by type B situations. This hypothesis was tested selecting an arbitrary threshold of 20% difference between rural and urban stations (Urban/Rural Ox ratio). In order to quantify this difference, the ratio between simultaneous daily Ox concentrations in rural and urban sites was calculated, selecting for this purpose the urban site with the lowest daily Ox concentration and the rural site with the highest daily Ox concentration, for each day and for each region. Each day was then classified as follows (Figure 2.9):

- ratio Urban/Rural=0.8-1.0: O_3 concentrations between both types of stations were considered sufficiently similar to discard the combination of the two mechanisms taking place during type A situations (decreased urban concentrations and increased rural concentrations), and therefore the situation was classified as type B.
- ratio Urban/Rural <0.8: O_3 concentrations between both types of stations were considered sufficiently different (>20% difference), implying that probably two mechanisms are combined (decreased urban concentrations and increased rural concentrations), and therefore the situation was classified as type A.
- The remaining dates were classified as “Missing data”, due to the absence of either O_3 or NO_2 data (and thus the inability to calculate the Ox concentrations).

Type A situation

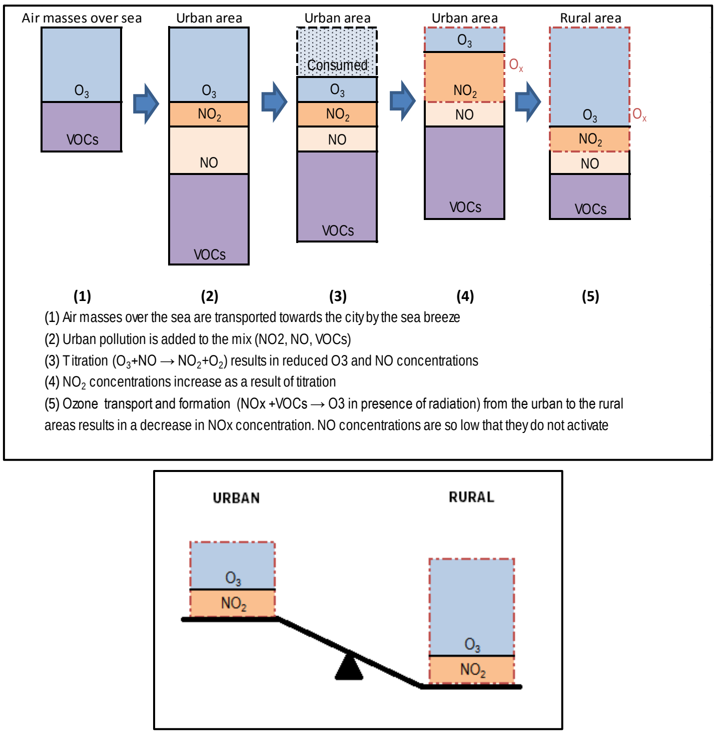

Type B situation

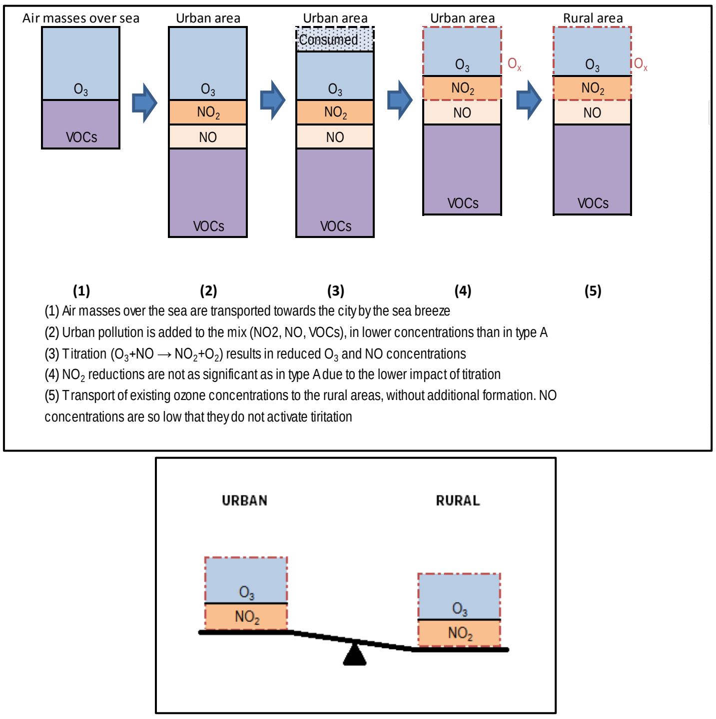

Figure 2.9. **O_3 and urban pollutants (NO, NO_2, VOC) variability during type A and B O_3 situations. Differences between O_3 formation and consumption in urban and rural areas.**

O_3 concentrations for each day between 2011-2015 were classified following this methodology, with the results shown in Figure 2.10. Results evidence that, even though both types of situations occur in both regions, the local/regional O_3 formation episodes (type A) are more present in the Western Mediterranean (e.g., Valencia) whereas the regional/long-range O_3 transport episodes (type B) are more prevalent in the East (Brindisi/Taranto). This trend seems to be consistent over the study period, with only an inverse trend (prevalence of type B situations) being detected in 2013 in Valencia. As stated above, these results would have implications from the point of view of mitigation strategies to reduce O_3 impacts: whereas in the case of type A episodes (and thus, in the Western Mediterranean) mitigation strategies should be directed towards reductions in precursor gas emissions (NOx, VOCs) in the nearby urban areas, in the case of type B episodes (mainly in the Eastern Mediterranean) local measures targeted at urban emissions would have a lower impact on O_3 concentrations due to their larger-scale transport and origin. In the latter cases, O_3 forecasts and behavioural measures (e.g., alerts for the population to remain indoors) may be considered as more effective strategies. Regional-scale measures targeted at reducing background concentrations would also be effective in these cases. Also, with regard to local-scale contributions of precursors, assessments should take into account whether the source areas may be more VOC or NOx driven, in view of the mitigation strategies to be designed. Given that both types of situations are detected in the Eastern and Western regions, a combination of measures (emissions reductions, coupled with forecasts and behavioural changes) taking into consideration the relative frequency of each type of situation would constitute the most optimal approach.

It should be noted that this approach is strongly dependent on the urban and rural stations selected (their location with respect to the main emission sources, pollutant concentrations and distance between them), given that the analysis is based on the relative difference in Ox concentrations between the stations. Therefore, further analyses should be carried out in other cities in order to test the robustness of this methodology. The arbitrary threshold selected (in this case, 20%) could need to be different for other cities.

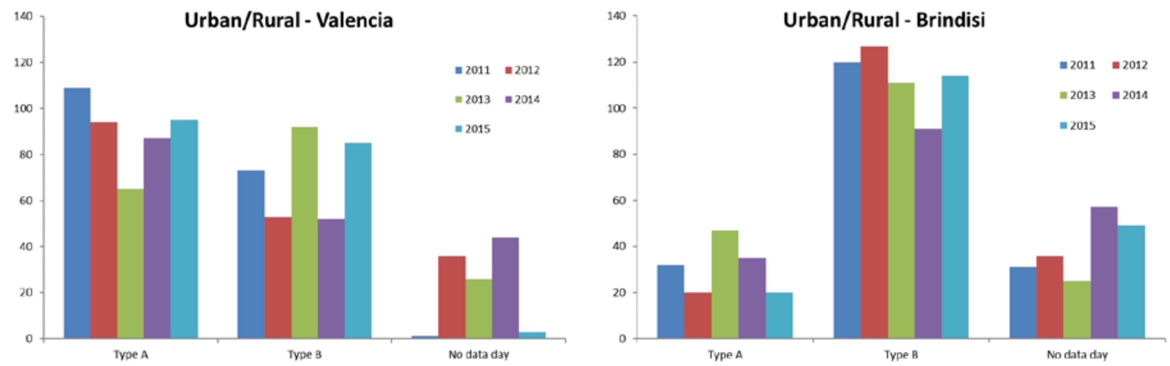

Figure 2.10. Number of days/year recording type A and B O_3 situations between 2011 and 2015 in the Valencia and Brindisi/Taranto regions, based on the Ox methodology described above.

2.6. Summary and conclusions from the time-series analysis

The main conclusions of the time-series analysis may be summarised as follows:

- Time series of O_3 concentrations were assessed for the period 2011-2015 for six major urban agglomerations across the Mediterranean basin: Valencia and Barcelona (Spain), Marseille (France), Rome and Brindisi/Taranto (Italy), and Athens (Greece).

- As already described in the literature, understanding O_3 concentrations and trends is especially complex when compared to other atmospheric pollutants given the variety of metrics available, each of which highlights a different aspect of O_3 pollution (baseline concentrations, episodes, hourly trends, etc.).
- Because O_3 pollution has a strong spatial component (with precursor emissions being generated in regions which are not frequently impacted by O_3 episodes), the selection of stations to monitor O_3 pollution is a key issue. The availability of stations under similar types (rural/suburban/urban) and located along paths where O_3 concentrations are formed and transported, is essential for comparison of O_3 impacts and exposure in different geographical regions.
- Based on the results from the present analysis, an increasing gradient in O_3 concentrations was frequently observed from urban to rural stations across the Mediterranean basin. This gradient evidenced the mechanism whereby O_3 precursors are emitted in urban areas and O_3 concentrations are formed, through transport and solar radiation, during transport from the urban to the rural areas by means of sea breeze circulations. As described in section 1, vertical transport of O_3 from high altitude atmospheric layers is an additional factor especially in the Western Mediterranean basin. This kind of situation is prevalent in the Western Mediterranean regions. In addition to this trend, suburban stations especially in the Eastern Mediterranean registered high O_3 concentrations when assessing the number of exceedances of the 120 $\mu g/m^3$ threshold or the maximum 1-hour concentrations.
- In addition to this mechanism, a second one was described in the literature: meso-scale or long-range transport of O_3 concentrations under anticyclonic conditions, with lower influence of sea breeze circulations and without vertical fumigation. This mechanism was also observed in the course of the present analysis, and was seen to present a higher frequency in the Eastern than in the Western Mediterranean regions.
- These results have implications from the point of view of mitigation strategies to reduce O_3 impacts: whereas in the case of episodes dominated by local/regional transport between urban and rural areas (and thus, in the Western Mediterranean, where those episodes are more frequent) mitigation strategies should be directed towards reductions in precursor gas emissions in urban areas, in the case of episodes dominated by regional and long range transport (mainly in the Eastern Mediterranean) local measures targeted at urban emissions would have a lower impact on O_3 concentrations due to their larger-scale transport and origin. In the latter cases, O_3 forecasts and behavioural measures (e.g., alerts for the population to remain indoors) together with regional-scale measures targeted at reducing background concentrations may be considered as more effective strategies. However, given that both types of episodes are detected in the Eastern and Western regions, a combination of measures (emissions reductions, coupled with forecasts and behavioural changes) taking into consideration the relative frequency of each type of episode would constitute the most optimal approach.

After assessing the trends and mechanisms behind O_3 episodes in Southern Europe, the following section reviews short- and long-term mitigation strategies available in the literature and their effectiveness. Based on a modelling approach, a specific O_3 episode was modelled for the Barcelona (NE Spain) region and different emission reduction scenarios were tested.

3. Assessment of mitigation strategies

To reduce pollution in general, and O_3 in particular, the European legislation proposes a double axis strategy associating durable and short-term control of anthropogenic emissions. The permanent measures implemented at the European scale consist in reducing pollutant emissions either by a progressive implementation of new technologies, reducing energetic consumption or by substituting identified pollutants by less harmful products. At local or regional levels, additional permanent measures can be implemented such as increasing public transport offer or acting for energy performance of buildings. At the local scale, in addition to these permanent measures, short-term action plans can be implemented to rapidly respond to severe pollution episodes and limit their impact. Concerning O_3 episodes, recommended short term measures mainly consist in reducing road traffic emissions (speed limitation, alternate or differentiated traffic, local driving bans), but also industrial emission through the recommendation for industrial restriction or suspension of some activities (EU, 2008).

Because of the complexity of O_3 production and destruction (non-linear phenomenon) it is difficult to evaluate the efficiency of mitigation measures. It requires good understanding of the atmospheric dynamics, as well as of the regional and local O_3 production system and of complex meteorological situations (e.g., where sea and land breeze circulations lead to the build-up of O_3 and to the exceedance of regulatory thresholds). For these reasons, fine-scale regional modelling is required to represent both meteorological regional patterns and complex photochemistry. Modelling O_3 episodes also allows testing different scenarios and their impact on photochemistry and O_3 levels. While most studies in the literature focus on the assessment of the effectiveness of long-term measures, only a few studies have been conducted on the efficiency of short term measures on O_3 levels. The present section aims to fill this gap taking as example a field campaign undertaken in the Barcelona area in summer 2015. In addition to modelling this episode, several emission reduction scenarios were tested aiming to answer to the following questions:

- In the Mediterranean region, do short-term measures have a real impact on O_3 peak values? Can O_3 hourly information threshold exceedances be significantly reduced through the implementation of short-term measures, or are structural measures required?
- Can numerical tools help stakeholders to take the decision to initiate short-term measures to avoid O_3 threshold exceedances? If so, how many days in advance should these measures be implemented, in case of episodic measures?

3.1. O_3 abatement strategies and their effectiveness in reducing O_3 concentrations

3.1.1. Long-term O_3 abatement strategies

Because of its secondary nature and long atmospheric lifetime (~2-3 weeks), O_3 long-term trends are the result of a hemispheric background and the balance of formation and destruction from precursor emissions at local and regional scales. Thus, policy measures to reduce its concentration should target emission reductions of its precursors (NO_2 and VOCs) and be efficient at local/regional scales, but also coordinated at a continental level, and even generally at a global scale.

The existing legislation includes different levels of action. Short-term O_3 episodes, described in the section below, can be addressed by local measures applied at city or regional scales. According to European legislation they have to be applied when there is a risk that the O_3 alert threshold will be exceeded. At pan-European scale, on the other hand, long-term and background O_3 reductions are addressed for instance through the application of the Convention on Long-range Transboundary Air Pollution (LRTAP), initiated in 1979. This convention aims to limit and, as far as possible, gradually reduce and prevent air pollution including long-range transboundary air pollution. Under LRTAP Convention, the 1999 Gothenburg Protocol was signed with the objective to abate O_3 ground levels

together with acidification and eutrophication. This protocol, revised in 2012, set national emission reduction commitments for SO_2, NO_x, VOC, NH_3 and $PM_{2.5}$. The European National Emission Ceiling Directive originally enforced in 2001 and revised in 2016 transposed for 2020 the reduction commitments agreed by the EU and its Member States under the Gothenburg Protocol, and fixed even more ambitious reduction commitments for 2030.

Important emission reductions of these O_3 precursors were achieved in Europe during the past 20 years. According to the European Environment Agency (EEA, 2017b), reductions by 40% of NO_x and VOC emissions were achieved in Europe in 2016 compared to 2000 levels. Much of the reduction is a combined result of end-of-pipe abatement measures and structural changes in the energy, industry and transport sectors. Depending on the pollutant, dominating factors may change. As an example, Rafaj et al. (2014) estimated that dedicated end-of-pipe abatement measures played a dominant role in the reduction of NO_x emissions (see Figure 3.1). This can be mainly attributed to pollution control measures affecting petrol-fuelled cars, e.g., with catalytic converters.

These reductions in emissions result in a reduction in the measured concentrations. NO_2 concentrations in Europe were reduced by around 20-24% from the period 2000-2014 (EEA, 2016), less than NO_x emissions, probably due to an increase in the NO_2/NO_x emission ratio from diesel cars. For VOCs, long time series of measurements are available only for the less reactive pollutants: benzene and toluene. They both show a reduction of concentration by about 70% reflecting mainly reduction in traffic emissions. Colette et al., (2016) point out that a positive trend in concentrations of VOCs with a longer lifetime (ethane or propane) was found in different European sites without providing an explanation for such trends. However, a general decrease in VOCs concentrations over Europe is measured and expected from emission reductions.

In combination with short-term measures for O_3, which are known to be less effective (see next section), structural measures (permanent reductions of VOCs and NOx) should be suggested in order to tackle this issue in an effective and long-term, sustainable manner. Examples of sectors and measures to abate O_3 precursors are:

- Industry and power generation: de-NOx technologies have been proved to be effective, but are only mandatory in a number of Member States.
- Traffic: reduction of NOx emissions with EURO6c vehicles, successful congestion charge experiences (e.g., Stockholm, Milano), or improvement of urban freight distribution.

Despite important reductions in European NO_x and VOCs emissions and concentrations, O_3 trends are not that conclusive. Over Europe, EEA (2016) shows different behaviours depending on the O_3 metrics assessed and on the location of the station. Measured O_3 trends were analysed at different stations (rural, urban and traffic) for six different O_3 metrics used in the calculation of quality objectives or target values, for human health or vegetation. For all stations types, metrics calculated from summer times values with a focus on the higher concentrations showed a negative trend (AOT40 and the maximum daily 8-hour average). This confirms the results by Collette et al (2016), which estimated a 10% reduction in maximum O_3 concentrations in Europe between 1990 and 2012. However, these trends are not as important as for O_3 precursors. EEA (2016) shows that for other metrics, the trend depends on the typology of the station. For rural sites, located far from traffic emission sources, all metrics show a negative trend, more pronounced for the metrics based on higher concentrations. For traffic stations the trend is positive with higher values in 2014 than in 2000 for all indicators except AOT40 and the maximum daily 8-hour average. The behaviour at urban and suburban stations falls between that of traffic and rural situations. This paradoxical situation is explained by different trends in the phenomena that lead to final O_3 concentrations:

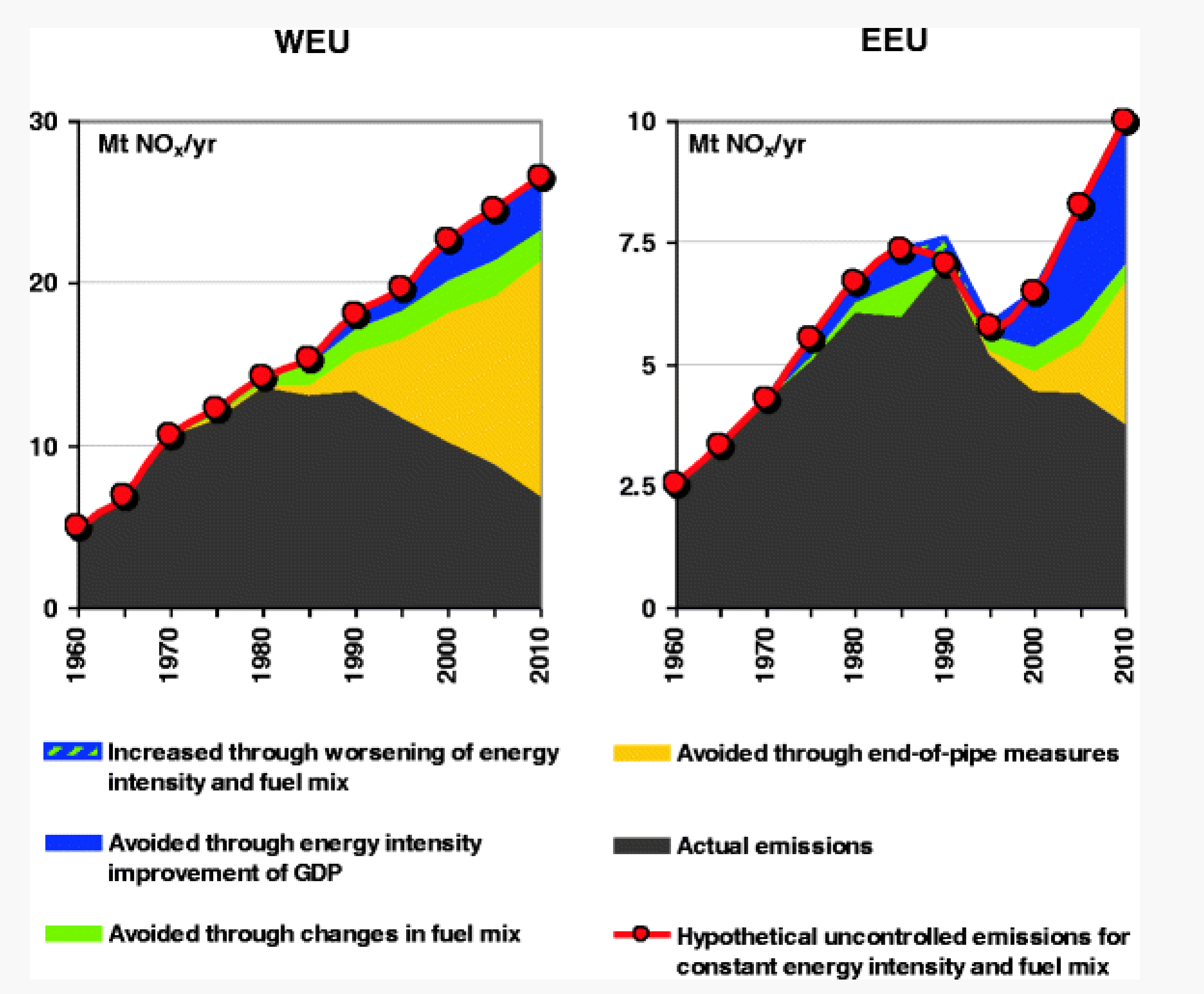

Figure 3.1. Determinants of reductions in NOx emissions in western Europe (WEU) and Eastern Europe (EEU) between 1960 and 2010. Extract from Rafaj et al. (2014).

1) The photochemical production of O_3 is decreasing in Europe due to reduction in precursors concentrations
2) The hemispheric background O_3 is increasing due to increase in VOCs and NO_x emissions from Asia
3) Close to traffic, the destruction of O_3 by titration (reaction with NO) is decreasing due to NO_x decrease.

At rural sites, where the titration is not acting, the reduction in O_3 photochemical production is more efficient than hemispheric increase leading to reduction of both mean and maximum O_3 concentrations. At traffic stations, the increase of O_3 concentrations due to reduction of titration effect is more important than the decrease in photochemical production, except for peak O_3 concentrations.

This suggests that managing NO_2 concentrations (via NO_x emissions) may have a detrimental effect on mean and background O_3 concentrations in urban areas where large populations are exposed, especially in NO_x-driven regions. This issue was highlighted in Chapter 1 (Chang et al., 2016). It suggests that NO_x emission control in traffic/urban areas needs to be counterbalanced by sufficient VOCs emission control to ensure mean O_3 decreases. However, due to the variety of VOCs sources (both anthropogenic and natural), controlling VOCs concentrations has been proven to be a complex

task. Overall, the issues of non-compliance with the O_3 target values among European Member States remains. The long-term objectives for O_3 cannot be met without additional action worldwide and an integrated approach. As an example, the last LRTAP Scientific Assessment Report (Maas and Grennfelt, 2016) emphasises the need for an integrated approach on air quality and climate mitigation measures that goes beyond the current domain of the LRTAP Convention and includes major emitters in South and Southeast Asia. The report points out in particular measures targeting methane that would be beneficial both for climate change and also for O_3 reduction.

3.1.2. Short-term measures to abate emissions of precursors during O_3 peak episodes

A list of short-term measures implemented in local short-term action plans which target atmospheric pollutants including O_3 is presented in Table 3.1. This list is not exhaustive but gives an idea of current short-term measures and of the associated emission reduction estimations in different studies. As evidenced by Table 3.1, some of these measures target O_3 episodes through precursors emissions reductions (Lasry et al., 2007, and Interreg III ASPA report). Other measures are dedicated to reduction in NOx and particle concentrations and may have an indirect impact on O_3 concentrations.

The main reductions in O_3 precursors´ emissions are often obtained for measures targeting road traffic emissions. Large reductions are estimated for driving ban scenarios with NO_x reductions up to 20% of total NO_x emissions over the domain and up to 15% reduction of total VOCs emissions. Impact of speed limit measures on emissions depends strongly on the initial speed and on the speed reduction. Ranges of emission reductions are gathered in the report (Ademe, 2014). It was found that for high speed roads (> 80 $km.h^{-1}$), speed reductions generally lead to reduction in traffic emissions, up to 20% for NO_x and 11% for VOCs emissions. In the city, the reduction from 50 km/h to 30 km/h shows highly variable or even contradictory results, from -10% to +30% depending on pollutants and studies. Several factors interact including obstacle along the road (speed bumps, etc.), user behaviours and the configuration of the tracks (Ademe report, 2014).

Measures for other sectors can also significantly reduce VOCs emissions, with industrial processes and residential sources being two of the three main VOC emission sources. These measures could be reductions of VOC emissions (by 20 to 50%) for the largest industrial sources, or the prohibition of use of VOCs-containing paints. Of course, the impact of a specific measure on total emission of an area depends on the country, and on the region. For example, very large reductions in total emissions over Beijing during the Olympics in 2008 were estimated by Wang et al. (2010): 47%, 55% and 57% for NOx, PM_{10} and NMVOCs, respectively. These strong reductions are associated with ambitious short-term measures targeting road traffic (around 50% emission reduction for the whole sector), industry (30 to 50% sector emission reduction) but also prohibition construction works (90% sector emission reduction, i.e. -35% of the total emissions of PM_{10}). These measures should have less impact in European cities (different fleet in circulation, end-pipe emission reductions already implemented, etc.). According to the different estimates found in the literature, 30% reductions of total NO_x and VOCs emissions in a specific region could be seen as a maximum but feasible reduction associated with short-term measures implemented in this region. For example, this order of magnitude is explored in the CAMS short term green scenarios forecasting system[2]. As stated above, the measures found in the literature target atmospheric pollutants including O_3 precursors, but they do not have a direct focus on O_3 episodes. In addition, the reduction in emissions of specific precursors does not cause a proportional reduction of ambient O_3 concentrations.

[2] http://policy.atmosphere.copernicus.eu/GreenScenarios.html

Table 3.1. List of short-term emergency measures. The pollutants targeted by the measures are indicated together with the estimated changes in emissions and concentrations (if they are evaluated), and their references. NMVOC: non-methane VOCs.

Short-term measure	Pollutants targeted	Change in emissions (if estimated)	Reductions in O_3 concs. (if estimated)	Region	Reference
Industrial sector					
Stabilization of activities and postponement of degassing for the largest industrial sites	O_3	VOC: -10%		France (Marseille region)	Lasry et al. (2007)
Progressing closure of the installations (in case of extremely severe O_3 concentration)	O_3	VOC, NOx, SO_2: -20%		France (Marseille region)	Lasry et al. (2007)
50% reduction in VOCs emission from the larger industrial site (NMVOC emission > 60 tons): individual action per site to reach this level.	O_3	VOC: -50% for the larger individual industrial sites	In the plume: -1% (daily max. hourly concentrations)	France (Alsace)	Interreg III report – ASPA (ASPA-06072104-ID)
Road traffic sector					
Speed limitation for high speed roads	PM_{10}	NOx: 20% to +6%; VOC: +11% to -11%; PM_{10}: -20% to +2%; CO: -8% to -25% (% of road traffic emission)		Europe	Ademe report (2014)

Speed limitation for urban roads (< 70 km/h)	PM_{10}	NOx: -40% to +30% ; VOC: +5% to +97%;PM: -33% to +8% ; CO: -45% to +86% (% of road traffic emission)		Europe	Ademe report (2014)
Alternate license plate circulation (alternate driving bans)	O_3	Impact on total emissions from the city (all sectors): NOx: -14%, VOC:-16% , PM_{10}: -14%, CO: -48%	In the plume: -3.5 % (daily max. hourly concentrations)	France (Alsace)	Interreg III report – ASPA (ASPA-06072104-ID)
Alternate license plate circulation (alternate driving bans) **Restriction on road traffic transit**	NOx, PM_{10}, CO, O_3	Impact on total emissions from the city (all sectors): PM_{10}: -15% ; NOx: -20%		France (Paris)	Airparif press pack (2014)
Restriction on heavy goods vehicles traffic transit	O_3	Impact on total emissions from the city (all sectors): NOx: -8%, VOC:-2%, PM_{10}: -5%, CO: -10%	In the plume: -1.2 % (daily max. hourly concentrations)	France (Alsace)	Interreg III report – ASPA (ASPA-06072104-ID)
Residential sector					
Prohibition of painting activity and motor machines	O_3	VOC: -3% over the region, -11% in agglomerations		France (Alsace)	Interreg III report – ASPA (ASPA-06072104-ID)

In the 1990's, the impact of speed limits, partial driving bans or industrial emission restrictions were studied in the Netherlands and Germany (Smeets and Beck, 1999; Bruckmann and Wichmann-Fiebig, 1997). They all concluded to a small efficiency of these short-term measures on O_3 concentrations. A study of short-term measures taken during an O_3 episode in Belgium (CELINE report, 2007) even showed that reduction of traffic emission is counterproductive on O_3 concentration (increase in mean O_3 concentration, AOT60[3] and MDA8). This is because the O_3 regime in Germany, Belgium and the Netherlands is mainly a VOCs limited regime (i.e., NOx-driven; Sillman, 1999; Chang et al., 2016): dominated by large NOx emissions and low OH (low amount of sunlight). For such types of regimes, reduction in NO_x may lead to O_3 increases. As discussed in the previous section (section 2.5), an effective design of mitigation strategies must take into account whether the source and receptor regions are VOCs- or NOx-driven (Chang et al., 2016). In the case of Germany, Belgium and the Netherlands, these regions are in addition largely influenced by transboundary pollution, reducing the potential impact of local measures.

The dynamics of O_3 episodes in the Mediterranean region differs substantially. Lasry et al. (2007) focused on South of France, where meteorological conditions are more favourable for local O_3 production. They evaluated the impact of several measures included in the short-term action plan implemented in the region (speed limitation, limitation of industrial activity, prohibition of private individual activities such as painting or exterior motor machines use…). They evaluated different level of ambition for emissions restriction, different geographical areas concerned by these restrictions, and also different time periods for the application of the measures. They conclude that with severe restrictions of activities, a maximum decrease of 10 $\mu g/m^3$ can be obtained in the region surrounding the plume (located tens of kilometres downwind from the large city centre), while the decrease was limited to 2 to 4 $\mu g/m^3$ in its periphery. They also demonstrate that action plans after 14:00 UTC are inefficient in reducing O_3 on the same day because pollutants that participate in the formation of the O_3 plume are those released before 14:00 UTC. These results are also applicable in other Southern European regions such as NE Spain, where as shown in Figure 1.3 (chapter 1) O_3 impacts are registered >70 km up the valley at 20h whereas precursor emissions are generated in the Barcelona region in the early hours of the day. However, they demonstrate the importance of reducing emissions at least one night before the episode in the case of sea breeze events because pollutants accumulate during the night over the sea and vertically re-circulate within the domain during the following day (e.g., Millán et al., 2002).

3.2. Case study: a high O_3 episode in the Barcelona Metropolitan Area

This subsection is dedicated to the study of a high O_3 concentration episode recorded in the Barcelona area (Spain) originally documented in Querol et al. (2017). This episode is used to perform a new assessment of the efficiency of local and short-term emission reduction measures to mitigate O_3 pollution.

3.2.1. Summer 2015 O_3 episode in the Barcelona area

O_3 pollution episodes registered during summer 2015 in the Catalonia region (NE Spain) and more specifically in the northern region of the Barcelona metropolitan area (BMA), were described by Querol et al. (2017).

[3] AOT60: Accumulated Ozone exposure above a Threshold of 60 ppb (120 $\mu g/m^3$)

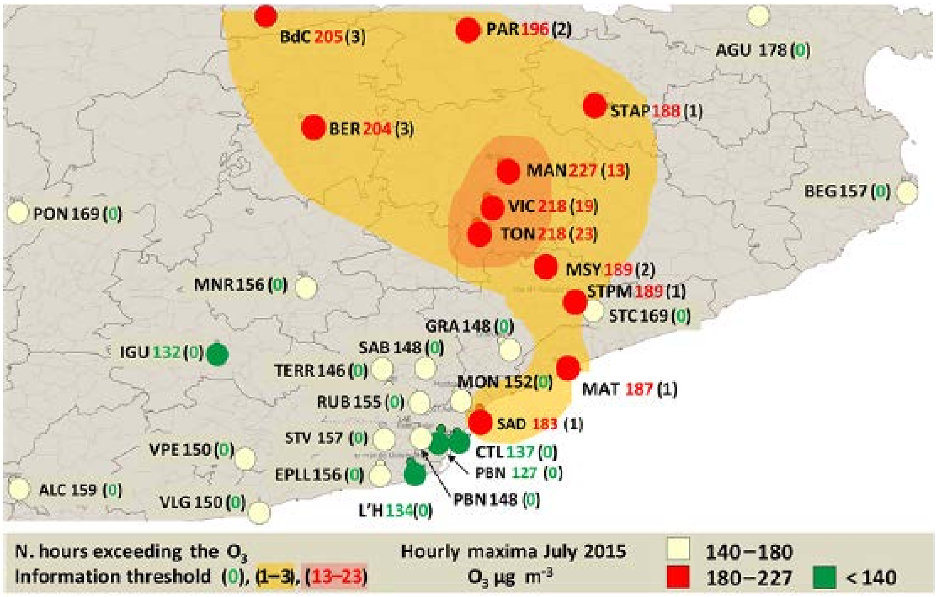

Figure 3.2. Hourly O_3 maxima (real-time O_3 data) and number of hours exceeding 180 µg/m^3 in the vicinity of Barcelona in July 2015 (shaded areas indicate two different degrees of exceedances, 1–3 and 13–23 h). Source: Querol et al. (2017).

These episodes are illustrated in Figure 3.2 with O_3 daily maximum 1-hour concentrations and exceedances of the information threshold (hourly concentration > 180 µg/m^3) for July 2015. O_3 sites located in Barcelona city centre (for example PBN or CTL stations) did not show exceedances. The first exceedances were observed several kilometres away from this centre to its northeast (SAD, MAT, etc.). Maxima were reached, 60 km to the north, in the Vic plains and valleys of the northern region of the BMA (MAN, VIC, TON), an area typically recording the highest O_3 episodes in Spain.

O_3 episodes in Spain and specifically in the Barcelona region, are of two types, previously described by Querol et al. (2017) for this area (see subsection 1.1.1):

- Type A: characterised by major local/regional O_3 recirculation and including fumigation of O_3 from high atmospheric layers where air masses are transported towards the sea. These O_3 concentrations are superimposed on the typical regional/long-range O_3 transport mechanisms. The episodes produced in this way are characterised by major exceedances of the O_3 information threshold. Spatially, this type of episodes affects mainly rural areas downwind of major urban agglomerations, possibly within 100-200 km (Millán et al., 2002; Gangoiti et al., 2006; Querol et al., 2017).
- Type B: characterised by larger-scale, regionally transported O_3 contributions governed by the arrival of aged air masses (in the case of the Western Mediterranean, from the East/Northeast). Transport from the coastal urban agglomerations (e.g., Barcelona) to inland or vertical recirculation of air masses are not determining factors during this type of O_3 episode. The spatial impact of this kind of episode, when compared to the previous one, is generally much larger.

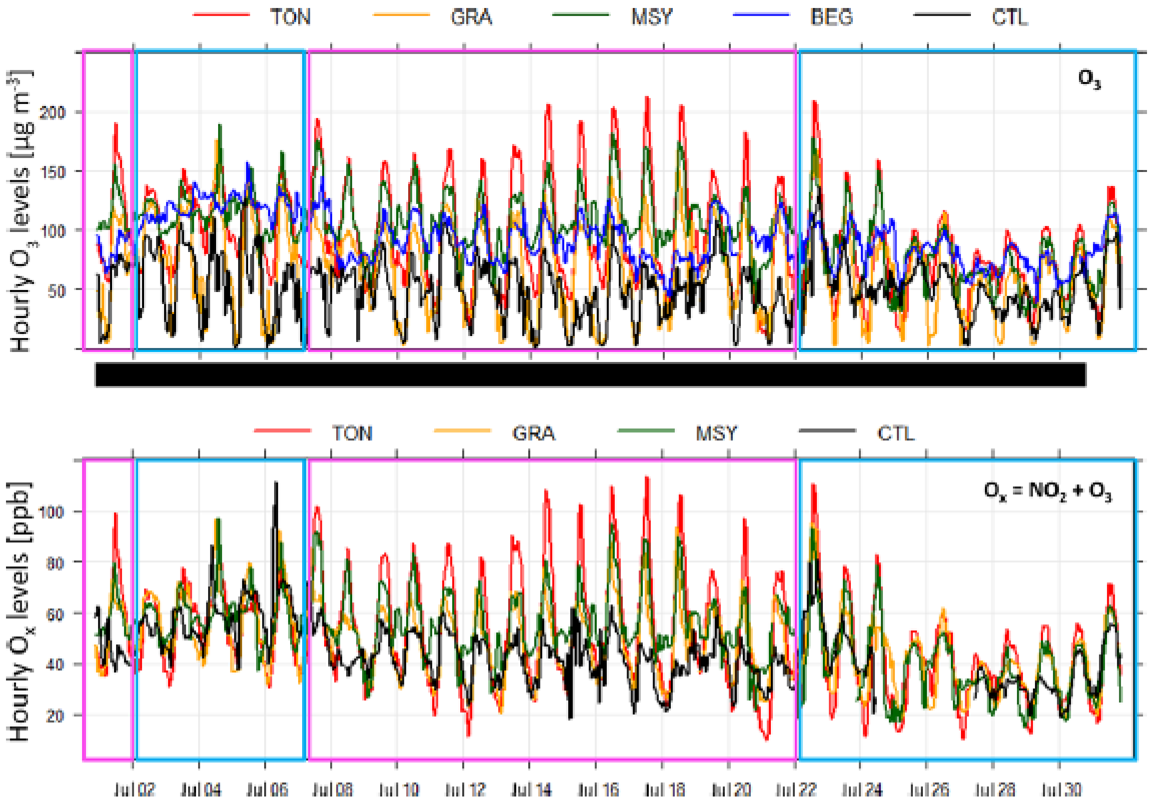

Figure 3.3. **O_3 and Ox (O_3+NO_2) hourly concentrations recorded at the coastal (BEG, blue, at this site only O_3 is available due to the lack of NO_2 measurements), an urban background site of Barcelona (CTL, black), an urban site in the northern periphery of Barcelona metropolitan area (GRA, orange), the intermediate inland rural site of MSY (720 m a.s.l., green), and the inner Vic Plain site (TON, red) during July 2015. Pink and blue squares mark the A and B episodes, respectively. Source: Querol et al., (2017).**

The two types of episodes are illustrated in Figure 3.3 (Querol et al., 2017). Time periods highlighted in pink represent type A episodes with increasing O_3 concentrations but also increasing O_x levels (see section 2.5) from urban stations to rural stations of the valley, with maxima observed in the VIC valley (7 – 21 July). Blue squares represent type B episodes with elevated O_3 peaks for inland stations but more intense at the south and east to the Vic valley (MSY, GRA), and also high O_3 at BEG, a coastal station. The uniform O_x levels for all these different stations, meteorology and the high O_3 concentrations at a costal site suggest import by the easterlies of old polluted plumes (e.g., from continental Italy, Sardinia and Corsica for July 2 - 7, 2015).

3.2.2. Modelling: set-up and results for the reference case

The chemistry transport model CHIMERE (Mailler et al., 2017) was used to simulate the impact of short-term measures on O_3 concentrations taking as example the case study documented by Querol et al. (2017), corresponding to the whole month of July 2015. It was chosen to not analyse systematically all O_3 metrics classically used in calculation of O_3 standards, but to focus on O_3 peaks

(daily maximum 1-hour O_3 concentration) and mean values. The CHIMERE model has been in development for more than fifteen years and is intended to be a modular framework available for community use. CHIMERE simulates transport, transformation and deposition of several dozens of pollutants. It is commonly used to evaluate air pollution policies for the French authorities and at the European level (Bessagnet et al., 2014; PREPA 2016[4]) and also for air quality operational forecast (PREV'AIR, CAMS) (Marécal et al., 2015). External forcing required to perform a simulation consists of meteorological fields, primary pollutant emissions, and chemical boundary conditions. Using these input data, CHIMERE calculates and provides air pollutant concentration fields with an hourly resolution.

For the reference simulation, concentrations were calculated over Spain with a 5 km horizontal resolution, from 16 June to 31 July 2015 (see Figure 3.6 below). This period allows a 15-days model spin-up period before covering the period described in Querol et al. (2017) (stabilise the model from arbitrary initial conditions to conditions representative of the period). It should be noted, however, that Salvador et al. (1999) demonstrated that vertical re-circulations cannot be captured adequately with spatial resolutions coarser than 2x2 km, in this study area. Meteorological conditions were extracted from the IFS[5] model that includes re-analysed meteorological data, and therefore integrate observations in the model. The meteorological fields were available at a 15 km resolution. Emissions over Spain were provided by the Spanish Ministry of the Environment and Agriculture at a 10 km resolution. Emissions over Europe were extracted from the EMEP emission inventory at 50 km resolution re-spatialised using various proxies such as land-use data, large point source databases, etc. Biogenic emissions were calculated online by the MEGAN model. Boundary conditions were obtained through a European simulation at 15 km resolution, using the same meteorology and emissions data than the 5 km simulation. For the reference simulation, all inputs data were interpolated to the 5km grid resolution used for Spain.

[4] «Aide à la décision pour l'élaboration du PREPA», «Evaluation Ex-ante du PREPA», French Ministry of Environment:
http://www.developpement-durable.gouv.fr/sites/default/files/06-1_PREPA_Synth%C3%A8se_-_aide_a_la_decision_pour_l_elaboration_du_PREPA.pdf,
http://www.developpement-durable.gouv.fr/sites/default/files/Evaluation_ex_ante_du_PREPA[1].pdf

[5] Integrated Forecast System from the European meteorological center ECMWF

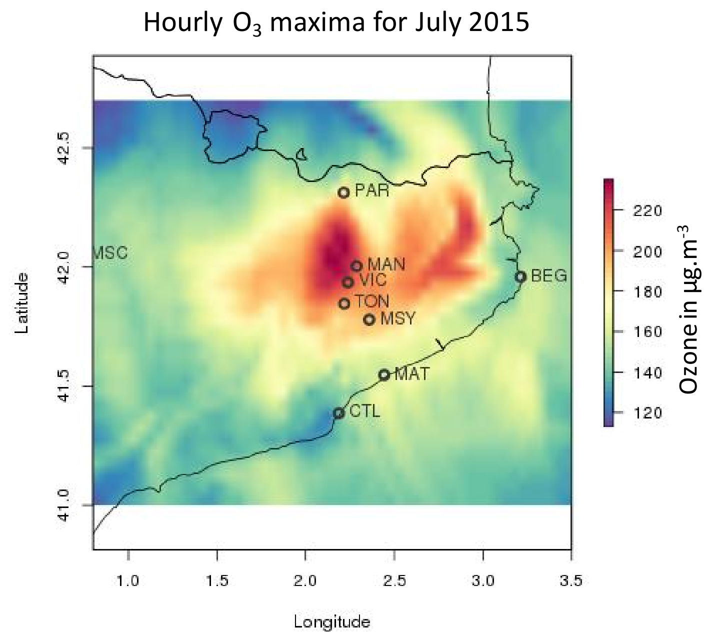

Figure 3.4. O_3 maximum 1-hour concentration reached in each grid over the entire month of July 2015, simulated in the reference simulation.

Figure 3.4 represents the composite hourly O_3 maxima simulated over the whole month of July; this map is referred to as composite because the maximum represented at various locations might have occurred on different days (i.e. the concentrations shown are the maxima registered in a month, which may have been recorded on different days for different locations). It can be directly compared with Figure 3.2 (extracted from Querol et al., 2017) that represents a schematic of the hourly O_3 maxima based on measured concentrations. The O_3 maximum zone observed over the Vic valley (MAN, VIC and TON stations) was well represented by the model, as well as the gradient of O_3 from low values in Barcelona to maxima in the Vic valley, and the decrease in O_3 maximum further north. The extent of the high O_3 region up to the PAR station, close to the Pyrenees was also well simulated. These fluctuations result from O_3 formation in the Barcelona plume as well as the influence of the boundary layer height, which is much higher in this region than in coastal areas and thus the fumigation from high reserve strata in the Vic plain is much more intense than in the coast. By contrast, the observed extent of the high O_3 region up to the coast (SAD station close to Barcelona city or even MAT station) was not seen by the model. Relatively low O_3 maxima in Barcelona (CTL and PBN stations) were well simulated. Low O_3 concentrations in Barcelona were due to O_3 titration by NO. O_3 was produced downwind of the Barcelona plume when NO values were low enough to change from a destruction regime typical of very high NO_x plumes, to a production regime initiated by moderate NO_x and also the presence of VOCs in the plume. The second pattern simulated by the model with maximum concentration to the east of the first plume was not represented in Querol et al. (2017). This does not mean that this pattern did not occur, simply that the data were not available for validation at the time of this study.

The correspondence between measured and simulated O_3 concentrations was further explored by providing their temporal variation in Figure 3.5 at four stations: MAN in the Vic valley, close to the maximum O_3 in the plume, MSY, located at higher altitude in between the Vic valley and Barcelona, CTL, located in Barcelona city and BEG a coastal station on the east coast of Catalonia.

Observed hourly O_3 concentrations were well simulated at the MAN station. Mean, maximum and minimum values were well represented by the model. The same features were simulated for the other stations located in the Vic valley (VIC and TON) with correlations over 75% and normalised RMSE and normalised bias under 20% for the 3 stations (MDA8 statistics). O_3 peaks were also well

simulated at MSY station but night time simulated O_3 concentrations were too low compared to observations, possibly in relation with the high altitude of the MSY station which is frequently influenced during night by high O_3 reserve strata which are injected at the MSY altitude. It is probable that the model is unable to reproduce these reserve strata with the 5x5 km resolution used. In BEG, a coastal station located at the east of the region, the correlation was generally good (69 %) with a normalised RMSE around 11% and a small bias. From 3 to 7 July, observations showed an increase from mean values around 100 µg/m^3 to around 130 µg/m^3 with peaks at 160 µg/m^3 and high night-time values, typical of an import of polluted air masses originated from other regions or country that have accumulated O_3 over the sea. This increase is partially reproduced by the model, but underestimated. Results at the CTL station were less satisfactory for O_3 maxima that were overestimated by the model. Overestimation of O_3 concentrations by the model are frequent in urban stations. This is mainly due to the spatial resolution of such models (here 5 km) that smooth over one grid cell the high NO_x plumes observed close to the main city roads. By this effect, the titration of O_3 by high NO plume is reduced and O_3 levels higher in the model. Results at the MAT station (not shown) were not as good as in the Vic valley.

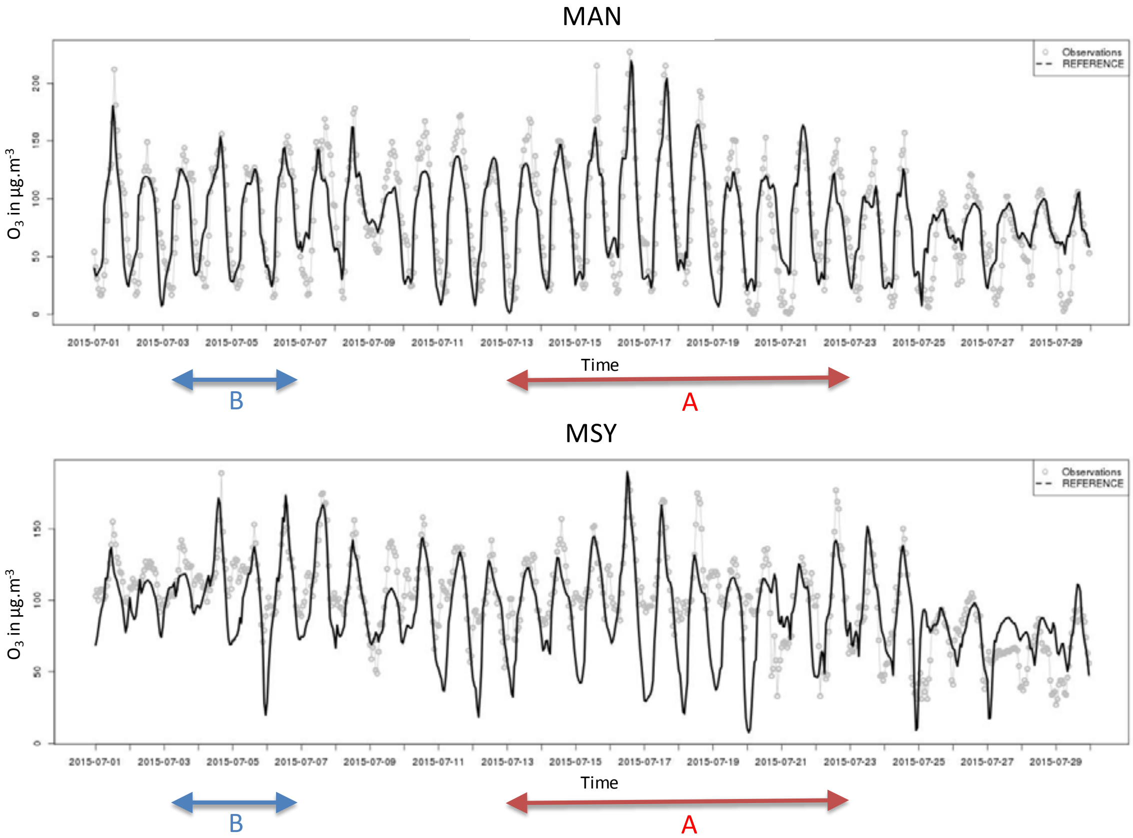

Figure 3.5. **Observed and simulated hourly O_3 concentrations (µg/m^3) at the stations MAN, MSY, BEG and CTL. The selected episodes are represented by the blue (episode B) and red (episode A) arrows.**

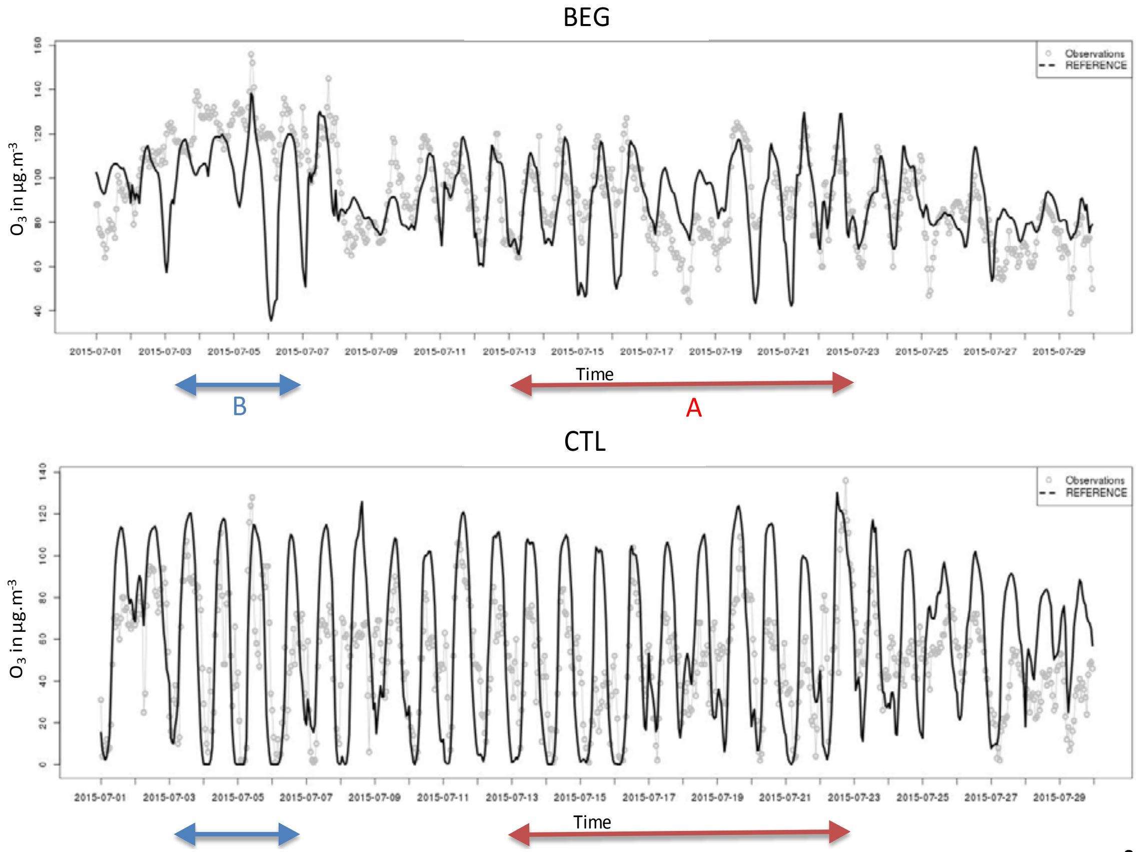

Figure 3.5. Continued. Observed and simulated hourly O_3 concentrations (µg/m^3) at the stations MAN, MSY, BEG and CTL. The selected episodes are represented by the blue (episode B) and red (episode A) arrows.

Based on the analysis above, the comparison between modelling and observed O_3 concentrations at measurement stations gave confidence on the capacity of the model to reproduce the O_3 episode recorded during July 2015 in the Barcelona region and described by Querol et al. (2017).

3.3. Assessment of the efficiency of short-term measures

3.3.1. Description of scenarios

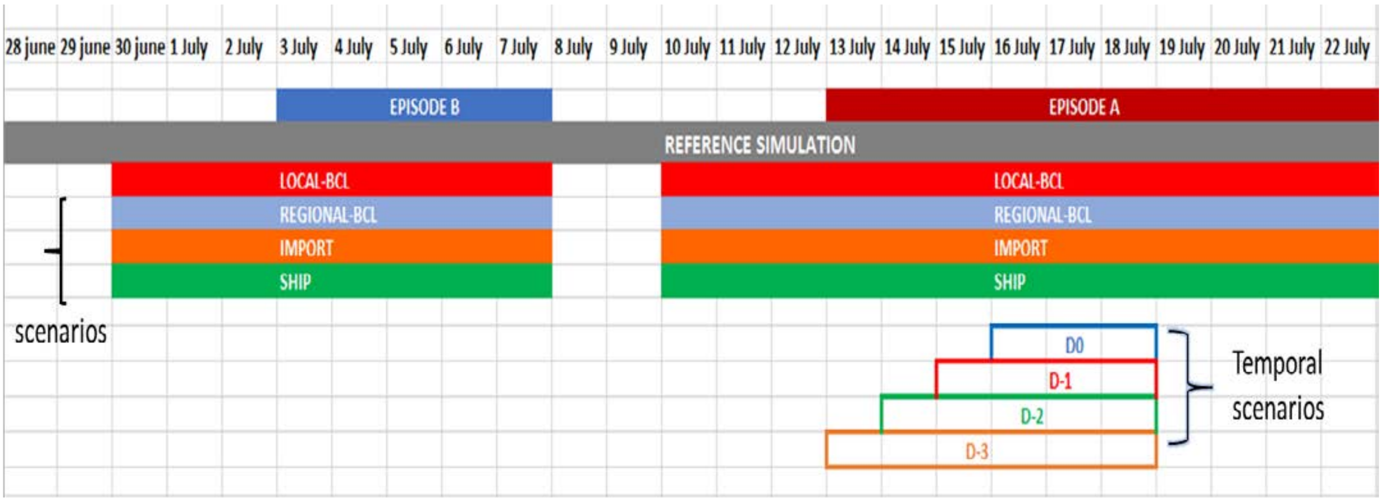

Figure 3.6. Temporal schemas of the O_3 episodes (Episode A and Episode B), the reference simulation (June 16 – July 31) and the scenarios simulations (LOCAL-BCL, REGIONAL-BCL, IMPORT and SHIP). Temporal scenarios focusing on the 16-18 July (strongest O_3 episode) are also represented.

When air quality forecasts anticipate an exceedance of O_3 alert thresholds authorities may implement short-term measures to decrease O_3 precursor emissions (EU, 2008). The objective of this chapter is to assess the efficiency of such short-term measures in reducing O_3 concentrations and avoiding O_3 alert threshold exceedances. Different scenarios of emission reduction of O_3 precursors were tested, and their impact on O_3 concentrations and peaks estimated. The two periods selected to test those measures were 3-7 July 2015 for the so-called episode type B, and 13-22 July 2015 for episode type A (see blue and red arrows in Figure 3.5 and Figure 3.6). These correspond to episodes identified in Querol et al. (2017), with Type B dominated by long-range transport pollution and Type A by local/regional pollution. For the 2 periods, scenario simulations with emission reductions were initiated 3 days before the beginning of the episode. This simulates that authorities would implement measures 3 days before the beginning of the O_3 episode. The impact of anticipating emission reductions was further tested.

Based on the literature and on the specific characteristics of the two selected episodes, four different emission reduction scenarios were investigated for NO_x and VOCs:

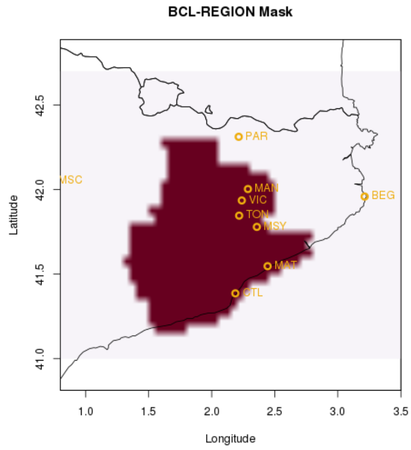

Figure 3.7. Area of the Barcelona region over which emissions are reduced in the REGIONAL-BCL scenario.

- LOCAL-BCL scenario: 30% reduction on NO_x and VOCs emissions was applied on all anthropogenic sources only in the Barcelona urban area.
- REGIONAL-BCL scenario: 30% reduction on NO_x and VOCs gridded anthropogenic emissions was applied in the Barcelona urban area as well as over inland domain (Figure 3.7) up to the Vic valley (see Figures 3.2 and 3.4). It should be noted that over this regional domain, NO_x and VOCs emission from Barcelona city represent respectively 34% and 24% of the total emissions.
- IMPORT scenario: 30% reduction on NO_x and VOCs was applied on anthropogenic emission from European countries except Spain, and except maritime areas.
- SHIP scenario: 30% reduction on NO_x and VOCs emissions from maritime traffic emissions only.

The objective of these scenarios was to evaluate the impact of emission reductions from different geographic zones. Two scenarios tested the impact of applying measures only in the large city or to extend those measures to the region around (LOCAL-BCL vs REGIONAL-BCL). The IMPORT scenario evaluated impact of reducing emissions from other European countries. It should be seen as an evaluation of the import of O_3 and its precursors to the region. Finally, the SHIP scenario evaluated the short-term impact of reducing emissions over the sea (shipping emissions).

The 30% reduction in gridded emissions used in the study can be seen as a maximum but feasible reduction to be reached with short-term measures, as described in subsection 3.1.2. In practice, it is probable that this 30% reduction of total emissions would be reached mainly by reducing the traffic sectors for the LOCAL-BCL scenario and by acting on both traffic and industrial sectors for the REGIONAL-BCL. Therefore, we can conclude on the optimum spatial scale for mitigation measures, but we can also point out a few activity sectors such as urban sources and shipping.

Subsequently, the impact of the implementation schedule of the short-term emissions reductions was analysed. For the 4 scenarios described above, reductions were applied from 3 days before the beginning of the period under study (see Figure 3.6). Focusing on the 16-18 July 2015 period (showing the highest O_3 concentrations) the impact of anticipating (or not) the emission reduction was analysed in various scenarios (referred to as TEMPORAL scenarios). In each scenario a 30% reduction was applied over Barcelona and its region with different starting dates for the emission reductions: applied on the same day (D0), one day before (D-1), two days before (D-2) or three days before (D-3), and then maintained for the whole episode (see Figure 3.6 for temporal representation of these scenarios).

3.3.2. Effectiveness of local/regional/international measures

O_3 concentrations simulated with the different emission reduction scenarios are represented over periods A and B.

Figure 3.8 shows, for the 4 scenarios, the average of differences in daily peak O_3 maps (obtain at each grid point with 1) calculation of the hourly difference between reference and scenario 2) calculation of the daily maximum of this hourly difference, and 3) averaging this daily maximum over the period). Negative values indicate that mean O_3 peak over the period were reduced compared to the reference simulation. The main impact was observed for the REGIONAL-BCL scenario, where 30% emission reductions were applied not only to the Barcelona city but also to the entire region. The largest reductions were simulated in the Vic valley (see results at MAN station, Figure 3.9), about 40-50 km from Barcelona, where the largest O_3 peak have been observed and simulated (see Figure 3.2). The LOCAL-BCL scenario for which reductions were applied only to Barcelona city showed much lower reduction of O_3 in the Vic valley. For these two scenarios, increases of O_3 peaks were found locally within Barcelona. These O_3 increases are due to O_3 titration by NO and are further explained in the following paragraph. The two remaining scenarios (IMPORT and SHIP) did not show any increase of O_3 peaks in Barcelona and the reductions that can be attributed to either of those scenarios were limited.

Hourly observed and simulated O_3 time-series at the MAN station in the Vic valley were represented for both the reference simulation and the different scenarios in Figure 3.9. The largest impact of the REGIONAL-BCL scenario (blue line) compared to the other scenarios appear clearly in the figure. We also notice that O_3 reduction was highest during the day, due to O_3 production reduction (less NO_x), but increases in O_3 concentration during the night were also simulated. This is due to night-time O_3 loss ($NO_2+O_3 \rightarrow NO_3 + O_2$) which is less effective due to decrease in NO_2 concentration (Monks et al., 2015; Pusede et al., 2015; among others). This explains why daily O_3 maxima were much more impacted by such a scenario than O_3 mean values (which average day and night concentrations). Concerning O_3 impacts on health or vegetation, the main focus is on high O_3 concentrations, or on accumulated concentrations over a specific threshold (70 µg/m^3 for the lowest) as opposed to average concentrations. Therefore, increased night-time low concentrations are not considered relevant from a health and ecosystem point of view. For this reason, analyses of episodes focus on daily maximum O_3 values throughout this work.

Episode type A

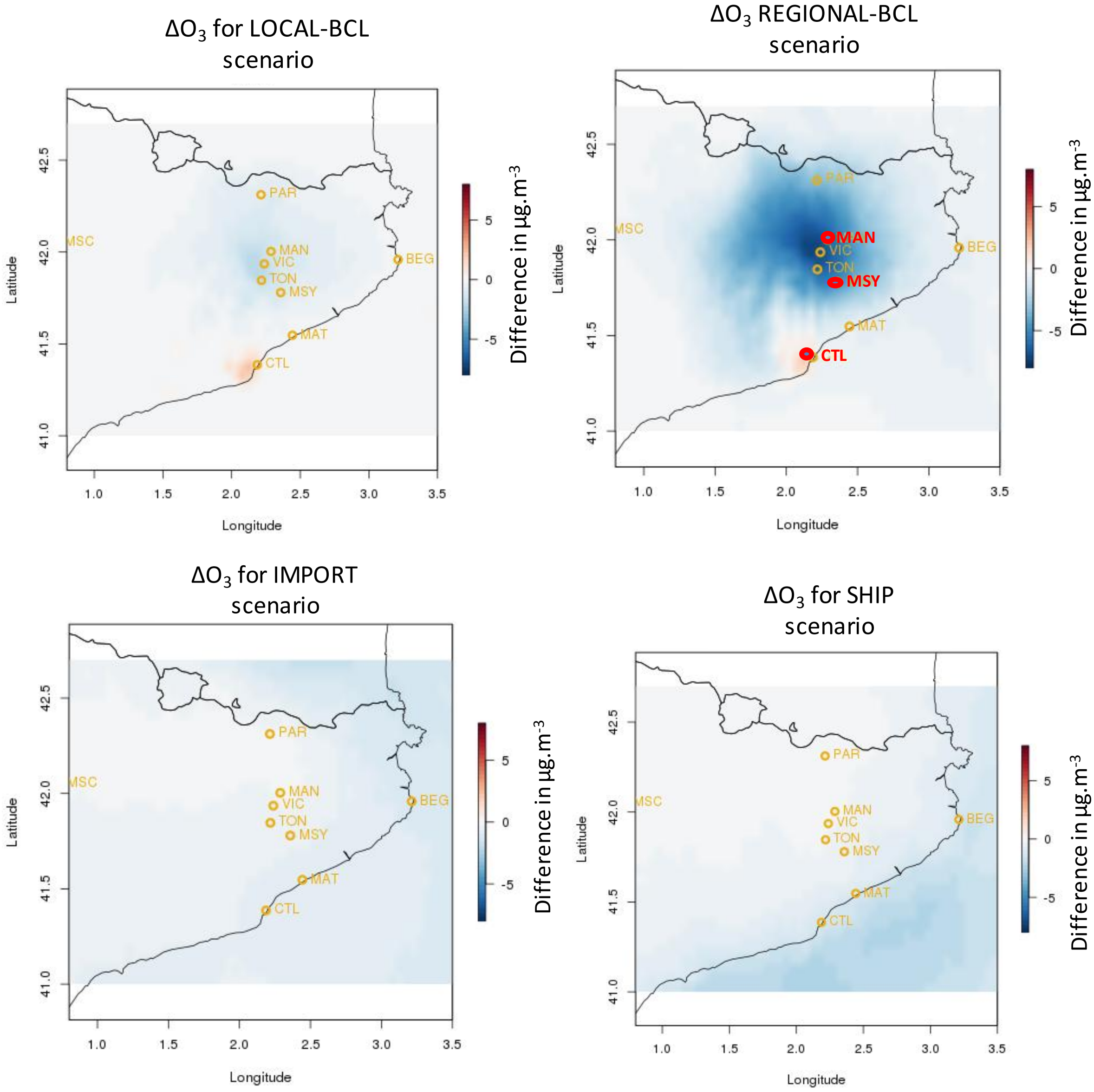

Figure 3.8. **For the episode type A (July 13-22, 2015) dominated by local O_3 formation: average reduction, over July 13-22 of the daily maximum hourly concentration (in µg/m^3) from the LOCAL-BCL scenario (top left), REGIONAL-BCL (top right), IMPORT (bottom left) and SHIP scenario (bottom right), compared to the reference simulation (without emission reduction).**

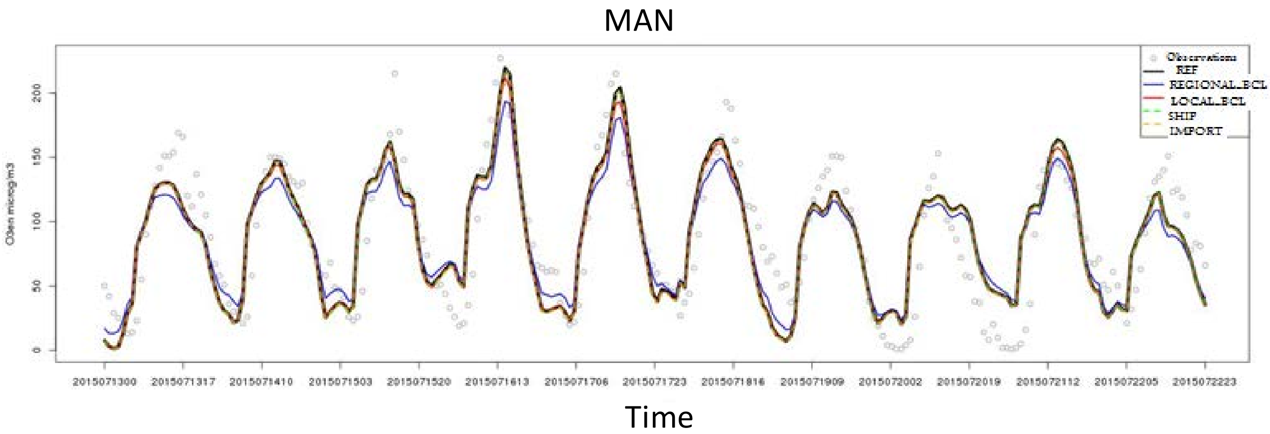

Figure 3.9. Hourly O_3 concentrations observed (dots) and simulated (full lines) at the MAN station from 13-22 July 2015 (episode type A dominated by local O_3 formation). The reference simulation is represented as black line; blue line for REGIONAL-BCL scenario, red line for LOCAL-BCL scenario, dotted green line for SHIP scenario, dotted yellow line for IMPORT scenario.

O_3 concentrations were further analysed for 3 specific stations: CTL (located in Barcelona and typical of urban stations in a highly polluted city), MSY (720 m a.s.l. of altitude, 42 km from Barcelona in a NE direction) and MAN (498 m a.s.l., 65 km from Barcelona in a NNE direction). These stations are highlighted in red in the top-right map in Figure 3.8.

Figure 3.10 shows for the 3 stations (CTL, MSY and MAN) histograms representing the impact of each scenario on maximum hourly-concentrations throughout the period. Simulated daily maximum O_3 concentrations are also represented (dotted line). For each day, the impact of a scenario was calculated as the daily maximum of the (hourly-O_3 with the scenario) – (hourly-O_3 in the reference simulation). Negative values indicate a decrease in O_3 due to the scenario emission reduction. The sole impact of the region (noted as REGION scenario in the figure) is isolated from the following subtraction: daily maximum of the (hourly-O_3 in the REGIONAL-BCL scenario) – (hourly-O_3 in the LOCAL-BCL scenario). It represents the O_3 reductions that can be attributed to emissions reductions in the region surrounding Barcelona but no reduction in Barcelona, considering that the impact of reduction in Barcelona and in the surrounding region are linear and can be added, which constitutes a strong approximation.

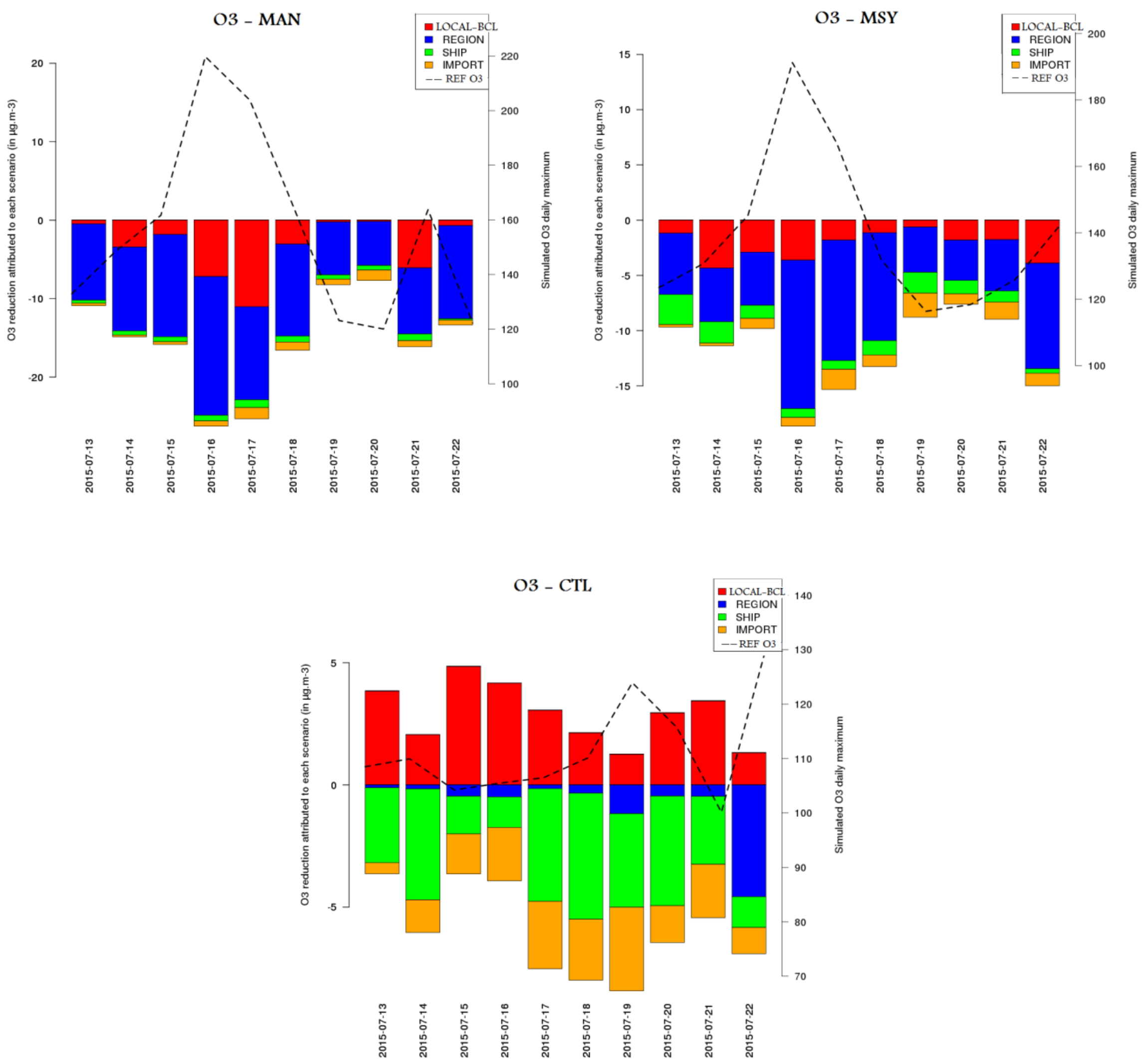

Figure 3.10. Episode A: simulated daily maximum hourly O_3 concentrations (black dotted line and right axis) and reductions due to each scenario (left axis, in µg/m^3). For a given scenario X, reduction is calculated as (Scenario X-REF).

At the MAN station, and during the whole episode A period, the scenario LOCAL-BCL+REGION (red + blue) had a large impact on O_3 peak concentrations. For the two days exceeding the information threshold of 180 µg/m^3 (16-17 July), the emission reduction of 30% in those regions led to a reduction of 25 and 23 µg/m^3 at MAN station. For July 17, where O_3 concentrations of 203 µg/m^3 were simulated, this reduction would have allowed to avoid information threshold exceedance. The influence of Barcelona emissions on O_3 concentrations at the MAN station (65 km north of the city) varied greatly from day to day. For example, for July 17, the impact was almost equal to those of the surrounding region but for July 13, 19, 20 or 22, this influence was almost null. Generally, O_3 peaks corresponded to days where Barcelona emission impact was not negligible evidencing that direct transport of pollutant from Barcelona is contributing decisively to the high O_3 episodes, even if it did not show up in the map of average impact of that scenario over the whole period in Figure 3.8, top left. The impacts of both the ship emissions and the “imported” emissions were negligible throughout the entire episode. Nevertheless, in other type A situations (Pay et al., 2014; Valverde et al., 2016; Querol et al., 2017) authors observed O_3 concentrations close to 150 µg/m^3 at high altitude (2.5 km a.s.l.) which may suggest regional (external) contributions which would thus be non-negligible.

At the MSY station, located at higher altitude, O_3 concentrations (simulated and observed) were lower than further north west (at lower altitude) but the information threshold was exceeded the 16th of July. For this day, the 30% reduction in BCL+REGION emissions also allowed to bring O_3 concentrations below the threshold.

The behaviour simulated at the CTL station located in Barcelona city was very different. LOCAL-BCL reductions led to an increase in O_3 due to a slowdown of titration when NO_x is reduced in Barcelona. In contrast, emission reductions from REGION, SHIP and IMPORT scenarios led to a decrease of O_3 peaks in the city. O_3 produced outside the city and transported to the city (from surrounding areas, surrounding countries or over the sea due to ship emissions) was reduced. Depending on the day, decrease in O_3 maxima due to the reduction in ship emissions (up to -6 µg/m^3) could be larger than increases due to Barcelona emissions reductions.

To evaluate the general impact on exceedances of the O_3 information threshold during the episode type A, we can estimate pseudo observations by subtracting modelled O_3 contributions for each scenario from the observed O_3 hourly concentrations. 53 exceedances were measured at the 9 stations studied in this work. The modelled effect of the LOCAL-BCL+REGION scenario on O_3 reduced exceedances to 26 (decrease by 50 %). Reductions in the Barcelona city area only reduced exceedances to 45 (decrease of 15%). IMPORT and SHIP scenarios alone did not impact the number of exceedances of the information threshold. Local modelling studies of other A episodes have reported different results with regard to the regional O_3 contributions (Pay et al., 2014; Valverde et el., 2015).

In conclusion, for the episode A period, the scenario where emissions are reduced by -30% over Barcelona and its region had a strong impact on O_3 peak concentrations, with maximum reductions of 25 µg/m^3 on the most polluted day. The number of exceedances observed of the O_3 information threshold would be reduced by 50% with this scenario. Reducing emission in the city alone is much less efficient, according to these results. In addition, the magnitude of these reductions should be evaluated in the framework of the maximum O_3 concentrations reached in the region: even if concentrations are reduced by 25 µg/m^3, peaks of 200 µg/m^3 may still be registered, and probably the 120 µg/m^3 8-hr limit may be exceeded. Therefore, caution should be exercised when interpreting these O_3 reductions.

Figures 3.11 and 3.12 show that, for the type B episode, the maximum impact on daily O_3 peak was also simulated for the REGIONAL- BCL scenario. For this episode the largest differences were not located in the Vic valley, as for the episode type A, but further east. However, we could not validate this pattern as the data for the stations between the Vic valley and the coast was unavailable when the modelling was carried out. To further analyse the simulations results we focused on 4 stations: in addition to CTL, MSY and MAN, simulations at the coastal site of BEG were also included.

Episode type B

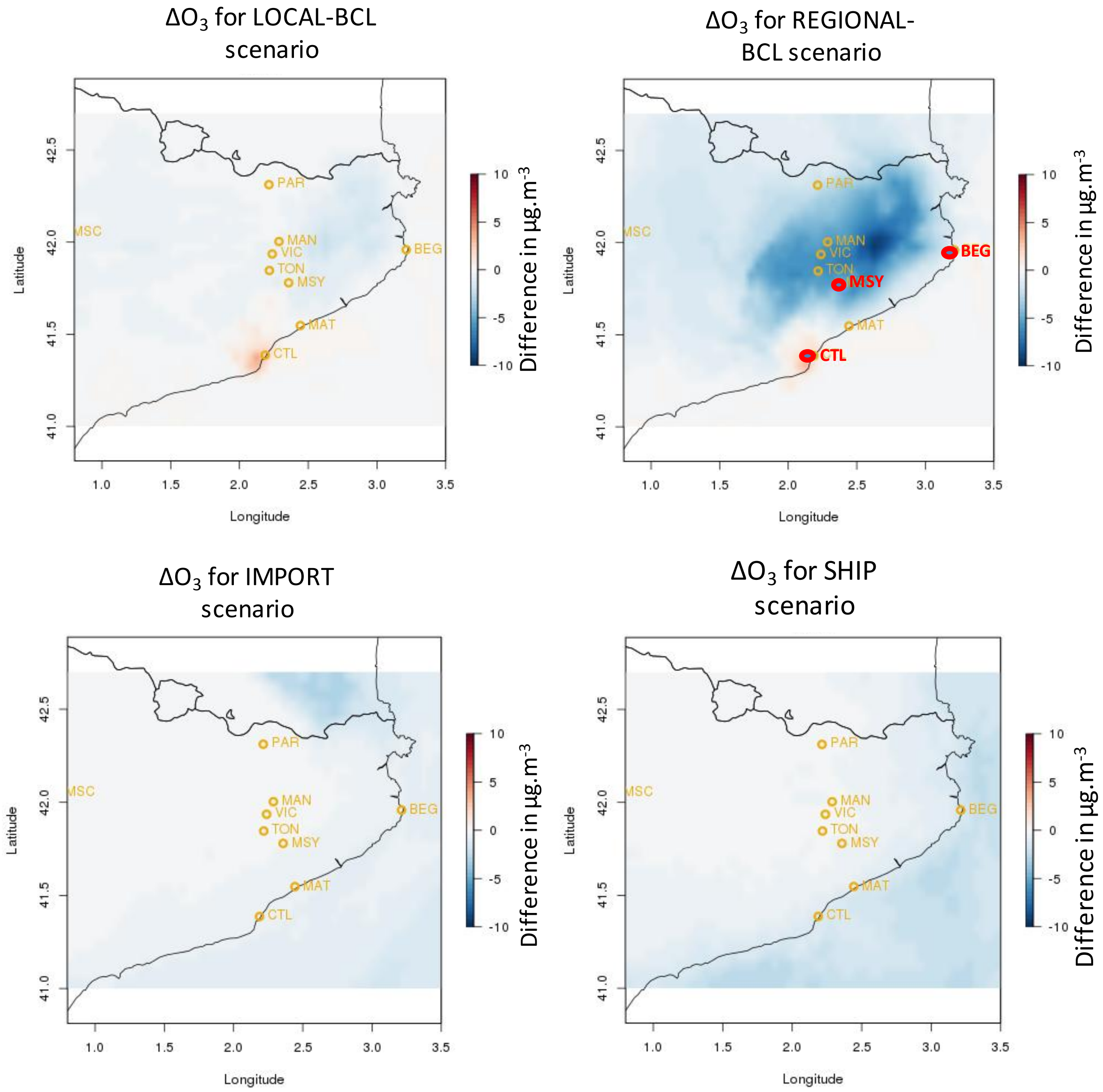

Figure 3.11. Type B period (July 3-7, 2015): average over July 3-7, 2015 of the daily maximum hourly concentration (in µg/m^3) from the LOCAL-BCL scenario (top left), REGIONAL- BCL (top right), IMPORT (bottom left) and SHIP scenario (bottom right), compared to the reference simulation (without emission reduction).

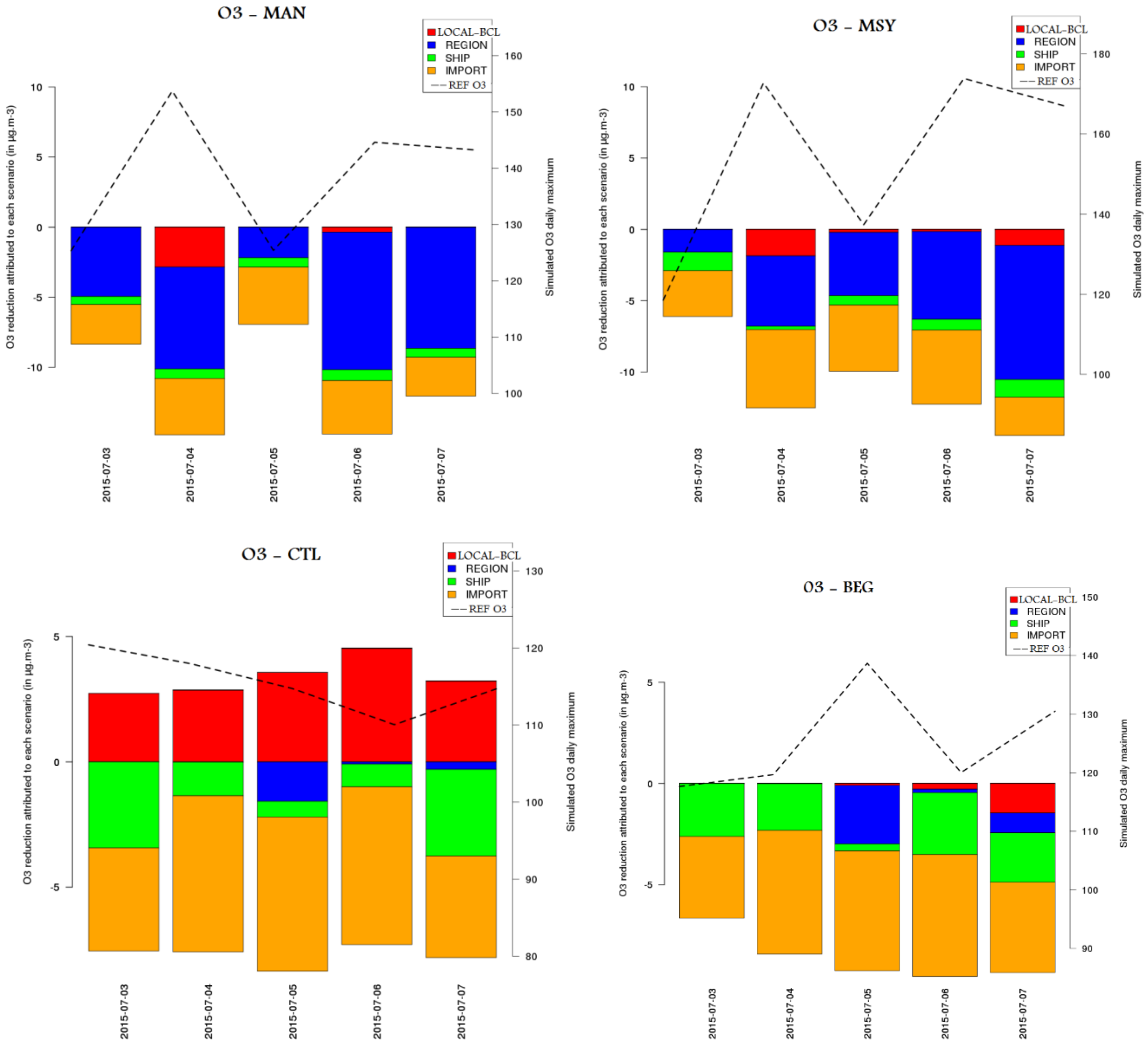

Figure 3.12. Episode B: simulated daily maximum hourly O_3 concentrations (black dotted line and right axis) and reductions due to each scenario (left axis, in µg/m^3). For a given scenario X, reduction is calculated as (Scenario X -REF).

As in the type A episode, local emission reductions increased O_3 concentrations within Barcelona city (CTL). The lower impact of ship emission reductions at this station suggests that import of O_3 produced from ship emissions to the city was less important during episode B. These results coincide with those from the time series analysis in section 2, where transport of O_3 and its precursors during type B episodes was seen to have a larger spatial scale. On the contrary, the import of O_3 from European countries to BCL was much more important during this period. This import of O_3 can be seen even more clearly at the BEG coastal site, with a maximum reduction of -7 µg/m^3 due to the 30% emission reductions in other European countries. Moreover, the comparison of observed and simulated O_3 concentrations at the BEG station (see time series in Figure 3.5) suggests that import of O_3 from the west Mediterranean was underestimated and that impact of scenario IMPORT could be even more important. At the MSY (station showing the highest O_3 levels during episode type B) the impact of the IMPORT scenario is almost equivalent to that of LOCAL-BCL+REGION scenario. For example, on July 4 2015, the information threshold was exceeded with observations and even if the model did not succeed in reproducing that exceedance, it showed a peak and estimated the reduction attributed to the IMPORT scenario to -6 µg/m^3 for that day. At the MAN station the impact of imported O_3 was slightly reduced (maximum of -4 µg/m^3) and the impact of transport from LOCAL-BCL+REGION was more important.

As in the episode type A, pseudo observations were constructed by subtracting O_3 contributions for each scenario from the observed O_3 hourly concentrations. During the episode type B, 4 exceedances were observed over the 9 stations. Under the LOCAL-BCL+REGION scenario, exceedances were again reduced by 50% but here the IMPORT contribution scenario allowed to suppress one more exceedance. The other scenarios alone (LOCAL-BCL and SHIP) did not have any direct impact on exceedances.

In conclusion, for the episode type B, we confirmed that the impact of local and regional emission reductions is less important due to a larger contribution of imported polluted air masses. However, the highest hourly O_3 concentrations can still be reduced by 10 $\mu g/m^3$ by means of regional-scale measures for the most polluted days. Once more, it is essential to assess the effectiveness of these reductions by comparison to peak O_3 concentrations potentially reached (e.g., 180 $\mu g/m^3$).

3.3.3. Temporal tests: effect of anticipating short term measures

The purpose of this section is to analyse the impact of anticipating emission reductions to mitigate O_3 peaks, i.e., to anticipate the implementation of mitigation strategies in order to prevent O_3 pollution episodes. The analysis focused on the period July 16-18, 2015, that showed the highest O_3 peaks over a large region in July 2015. Emission reductions were applied to Barcelona and its region (LOCAL-BCL+REGION scenario) to maximize the impact, as this was seen in the previous section to be the most effective scenario. Four temporal scenarios were tested:

- D0: emission reductions (-30% over LOCAL-BCL+REGION) were applied only during the peaks (i.e. from July 16 to 18, 2015)
- D-1, D-2 and D-3 (corresponding to the scenario presented in the previous section): emission reductions were initiated respectively one day before (and therefore applied for the period of July 15-18), two days before (July 14-18) and three days before (July 13-18). The duration of the emission reductions was therefore 1 day longer in each case.

O_3 concentrations for the 4 scenarios were analysed more specifically at 3 stations: CTL, MSY and MAN. Results are shown in Figure 3.13.

The O_3 concentrations simulated with the 4 scenarios are represented by 4 lines with different colours in Figure 3.13. At the urban station CTL, there was almost no difference between the scenarios. For this urban station with strong O_3 titration processes, O_3 concentration is directly linked with local NOx concentrations and did not show any time-lag effects.

At the MSY station, a clear difference was simulated between D0 (blue line) and the other scenarios (D1, D-2, and D-3) only for the first day (July 16, 2015). Reducing emissions on the same day (D0) reduced O_3 peak on July 16 by 5 $\mu g/m^3$, which was not enough to meet the O_3 information threshold. Anticipating emission reductions at least one day before (D-1 scenario), decreased O_3 peak concentrations by 18 $\mu g/m^3$, i.e. an additional reduction of 13 $\mu g/m^3$ compared to D0. This decrease allows reaching a level below the information threshold on July 16. There was no real added value to anticipate emission reduction 2 or 3 days before (D-1, D-2 and D-3 were equivalent). Likewise, after one day of simulation, there was no more difference between D-1 and D0 scenario: differences did not last after one day.

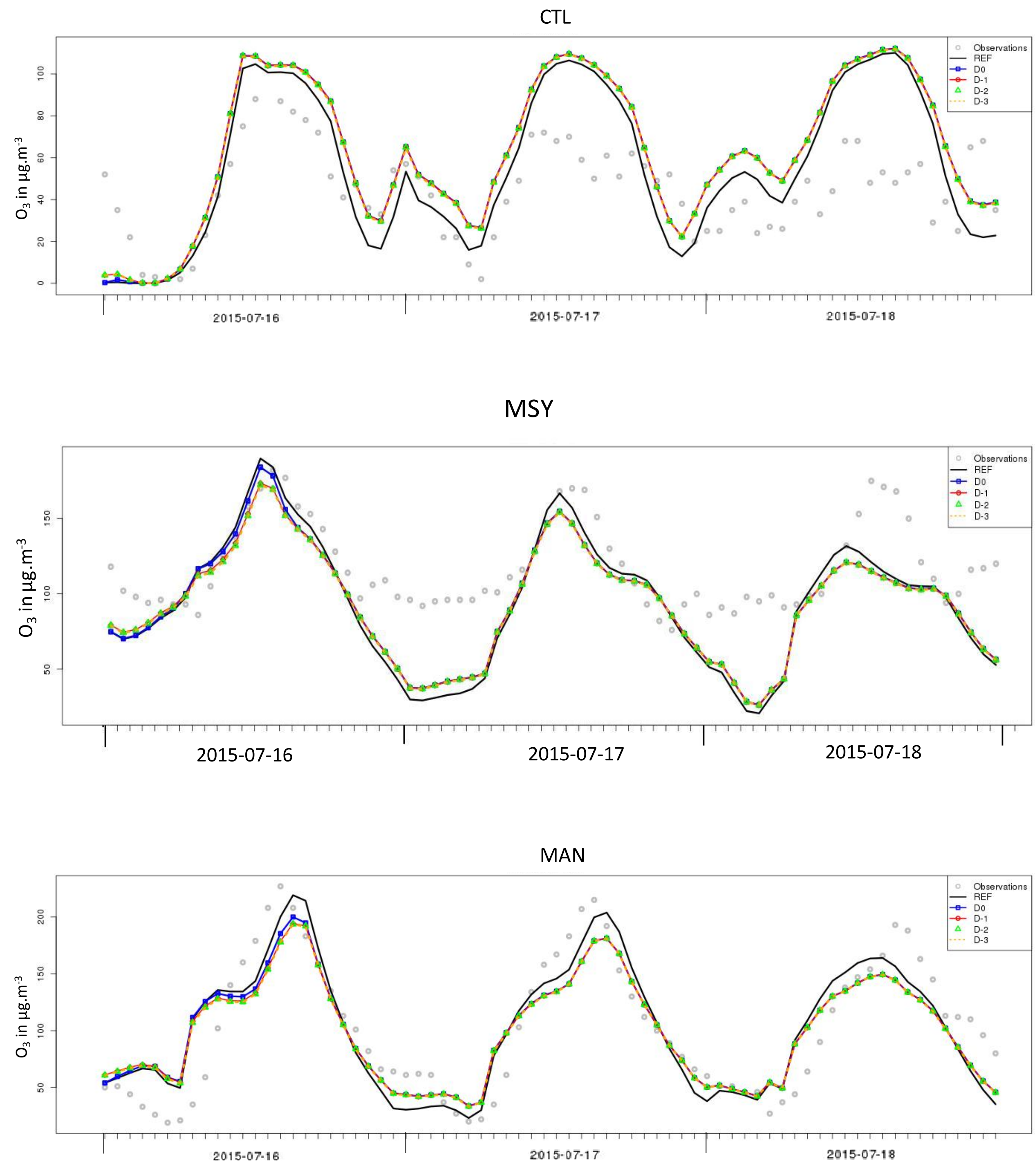

Figure 3.13. Observed (dots) and simulated (lines) hourly O_3 concentrations from July 16-18, 2015. The reference simulation is represented as black lines, D0 scenario as blue lines, D-1 as dots red lines, D-2 as triangles and D-3 as dashed orange lines.

At the MAN station, differences existed between D0 and D-1 on July 16 but they were small. Indeed, the map of the differences between D0 and D-1 over the period July 16-18 (Figure 3.14) shows that the main differences were located to the east of the Vic valley, with higher altitudes. This could reflect the night-time contribution from O_3 reserve strata, which is only detected at higher altitudes (Querol et al., 2017) and not in the lower valley areas (e.g., stations VIC, MAN). Because these O_3

rich layers (located around 1500-2000 m) are formed from accumulation of O_3 and precursors over several days (at least two days in our simulation), anticipating emission reduction may have an impact on the highest altitudes. At lower altitudes where direct surface transport (transport over one single day) is more important, anticipating emission reductions was less useful.

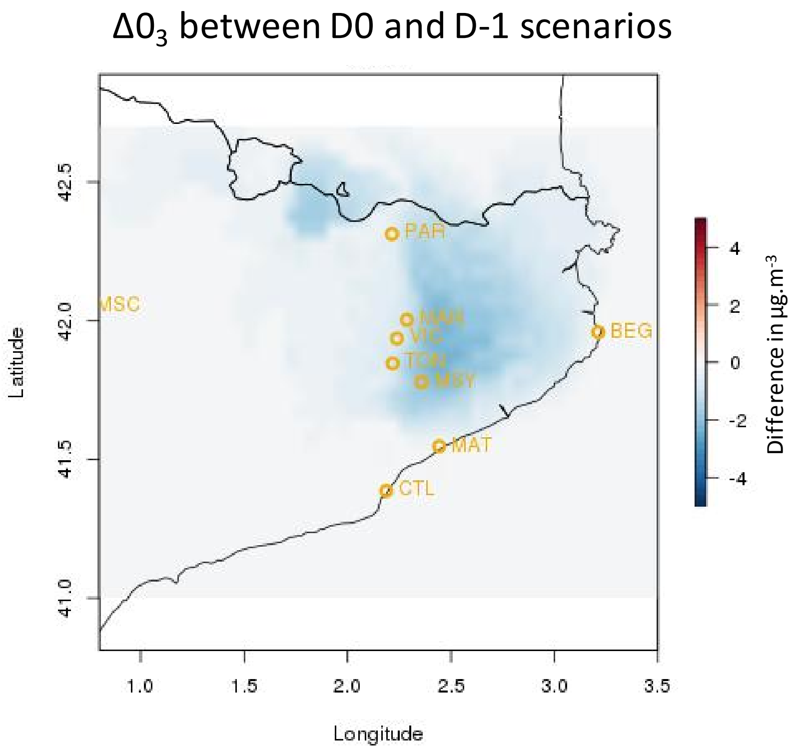

Figure 3.14. Mean differences in O_3 peaks between D0 and D-1 temporal scenarios (July 16-18, 2015).

Results of the simulation suggest that for type A episode, with impact of local/regional O_3 production but also O_3 downward fumigation, anticipating emission reductions one day ahead of the episode has a certain impact, allowing to avoid more exceedances than when reductions are applied on the day of the event. Further anticipation of 2 or 3 days ahead does did not yield any additional benefit.

3.4. Conclusions from the Barcelona-region case study

The O_3 pollution episodes described in Querol et al. (2017; corresponding to July 2015) were reproduced with the CHIMERE chemistry-transport model. Using numerical simulations allows testing different scenarios of emission reduction and analysing their impact on O_3 peaks. In particular, the purpose of this analysis was to test the efficiency of local and short-term mitigation measures. Model results showed that local and regional reductions of 30% of NOx and VOCs anthropogenic emissions may allow to significantly reduce exceedances (-50% for the two types of episodes, A and B). Reduction in the city of Barcelona itself was much less efficient than reductions associating Barcelona and its surroundings, and may even generate O_3 increases locally due to the slowdown of the titration effect. However, this should not have impact on exceedances, as they were recorded further inland, away from the main NO_x sources. Scenario tests also showed that local increases in O_3 peaks levels in the city may be compensated by a reduction in shipping emissions in the vicinity of the Barcelona area.

Two types of episodes were reproduced:

- Type A characterised by 1) direct local/regional transport of polluted air masses over one single day, and 2) vertical recirculation of polluted air masses over several days and accumulation in high altitude O_3 rich layers that can reach the ground by downward fumigation. For this type, emissions reductions in Barcelona and its region were efficient with maximum O_3 concentration reductions of 25 µg/m^3 on the most polluted day. The exceedances observed were reduced by 50% (from 53 to 26) compared to 15% when only Barcelona emissions were reduced. Thus, reducing emission in the city alone is much less efficient, according to these results. For the "Barcelona and its region" case, the benefit of anticipating or not emission reductions was evaluated. At low altitude, dominated by direct surface transport of polluted air masses, the model did not simulate any added value from anticipating reductions: emission reduction on the same day had the same impact as anticipation. Conversely, at higher altitude where contributions from O_3 reserve atmospheric strata may result in night-time O_3 peaks, anticipation could be effective even if only over a 1-day period (afterwards there is no difference among scenarios with one, two or three days on anticipation). The magnitude of these reductions (-25 µg/m^3) should be evaluated in relation to the maximum O_3 concentrations reached in the region, which may be as high as 200 µg/m^3.

- Type B episodes are characterised by a stronger influence of O_3 polluted air masses imported from other regions or countries. In these cases, the impact of local and regional emission reductions was less important due to a larger contribution of imported polluted air masses. The maximum O_3 concentration reduction was 10 µg/m^3 (which is lower than for type A episodes) by means of regional-scale measures for the most polluted days, with the scenario reducing emission in Barcelona and its region. However, these reductions are enough to reduce observed exceedances from 4 to 2. One more exceedance was also suppressed with the scenario that reduced emissions outside the domain. Once more, it is essential to assess the effectiveness of these reductions by comparison to peak O_3 concentrations potentially reached (e.g., 180 µg/m^3).

4. General conclusions and take-home messages

The present report aimed to review ozone (O_3) concentrations, spatial trends and potential mitigation strategies in Southern Europe. The specific complexity of O_3 formation in the Mediterranean basin, especially linked to vertical transport, as well as assessment methodologies tailored to this environmentally sensitive region, are in need of continued research. The ultimate goal of this research should be the design and implementation of effective mitigation plans and programs for this air pollutant in the region.

With the aim to partially fill this research gap, time series of O_3 concentrations were assessed in six regions across the Mediterranean basin (Valencia and Barcelona, Spain; Marseille, France; Rome and Brindisi/Taranto, Italy; Athens, Greece) for the period 2011-2015. The main conclusions extracted were:

- An increasing gradient in O_3 concentrations was frequently observed from urban to rural stations across the Mediterranean basin. This gradient evidenced the mechanism whereby O_3 precursors are emitted in urban areas and O_3 concentrations are formed, through transport and solar radiation, during transport from the urban to the rural areas by means of sea breeze circulations. Vertical transport of O_3 from high altitude atmospheric layers is an additional factor, especially in the Western Mediterranean basin.
- A second mechanism was observed in agreement with the literature: meso-scale or long-range transport of O_3 concentrations under anticyclonic conditions, with lower influence of sea breeze circulations and without vertical fumigation.
- These two mechanisms have implications from the point of view of mitigation strategies to reduce O_3 impacts: whereas in the case of episodes dominated by local/regional transport between urban and rural areas mitigation strategies should be directed towards reductions in precursor gas emissions in urban areas, in the case of episodes dominated by regional and long range transport local measures targeted at urban emissions would have a lower impact on O_3 concentrations. In the latter cases, O_3 forecasts and behavioural measures (e.g., alerts for the population to remain indoors) together with regional-scale measures targeted at reducing background concentrations would be more effective strategies. A combination of measures taking into consideration the relative frequency of each type of episode would constitute the most optimal approach.

Finally, the O_3 pollution episodes described in Querol et al. (2017) were reproduced with the CHIMERE chemistry-transport model in order to test potential mitigation scenarios. This analysis suggested that short-term measures for emission reduction have the potential to effectively reduce O_3 hourly threshold exceedances for photochemical pollution episodes dominated by local production. Conversely, in cases of strong import of polluted air masses the efficiency of short-term measures is limited, and large-scale spatial and temporal structural measures are the only solution. For short-term measures to be effective, they should be applied at regional and local scale (reductions in the city itself are not sufficient in most cases) and be restrictive enough (here, a 30% reduction is applied to anthropogenic NO_x and VOCs emissions). Anticipating emission reduction by one day may help to avoid some more O_3 threshold exceedances in some cases, while larger anticipation (2 days before) does not seem to bring any improvement, according to these results. The order of magnitude of the O_3 concentration reductions modelled should always be placed in context with regard to the maximum daily O_3 concentrations reached in a given area, in order to assess the actual effectiveness of mitigation strategies to reduce population exposure to O_3 pollution.

The reductions applied to NO_x and VOCs emissions were ambitious but seem achievable when compared with previous estimations of short-term measures (see section 3.1.2). As shown in Table 3.1, targeting large industrial installation and speed limits for urban roads have the potential to

achieve emission reductions >30%, whereas other measures such as alternate driving license plates, restrictions on heavy goods vehicle transit, or speed limitation for high speed roads do not seem to have the potential to achieve such reductions, according to the literature. The specific short-term measures to reach these reductions levels should be analysed on a case by case basis depending on the area where they have to be implemented. In addition, as stated above structural measures should also be implemented to tackle this issue in an effective and long-term, sustainable manner. Examples of such measures are de-NOx technologies in the industrial and power generation sectors, and emission standards (e.g., EURO6c), congestion charge or the improvement of urban freight distribution, with regard to traffic.

Forecasting systems that predict O_3 concentrations with at least a 2-day horizon (to simulate both cases with direct transport of polluted air masses and cases impacted by accumulated O_3 layers), together with emission reduction scenarios, can be useful tools to estimate the contribution of local/regional sources *vs.* imported sources. Such forecasting systems should offer a detailed enough spatial resolution: this is a key aspect. The 5-km resolution used in this work allows reproducing local/regional transport in an area where orography can play an important role, while previous studies (Salvador et al., 1999) evidence that a 2x2 km resolution is necessary to reproduce vertical air mass re-circulation in this study area. Additionally, forecasting tools such as described in Annex 2 can help to identify the specific sectors which should be targeted. Ideally, this kind of modelling approaches would include (a) reproducing the recirculation cells and complex meteorological patterns (e.g., fumigation processes and plume transport); (b) geographically resolved and accurate emission inventories of O_3 precursors; and (c) the ability to reproduce the origin of high altitude O_3 strata of external origin. (e.g., ACP special issue Atmospheric Chemistry and Climate Model Intercomparison Project, ACCMIP https://www.atmos-chem-phys.net/special_issue296.html; FAIRMODE, Thunis et al., 2015; and the Monitoring Atmospheric Composition & Climate (MACC)). Because of the complex phenomenology of O_3 episodes across the Mediterranean basin mitigation strategies policies should follow different approached to those applied in Central Europe.

References

ADEME (2014) Impacts des limitations de vitesse sur la qualité de l'air, le climat, l'énergie et le bruit, June 2014.

Akritidis D., Pozzer A., Zanis P., Tyrlis E., Škerlak B., Sprenger M., Lelieveld J., 2016. On the role of tropopause folds in summertime tropospheric ozone over the eastern Mediterranean and the Middle East. Atmos. Chem. Phys. 16, 14025–14039.

Asaf, D., Peleg, M., Alsawair, J., Soleiman, A., Matveev, V., Tas, E., Gertler, A., Luria, M., 2011. Trans-boundary transport of O_3 from the Eastern Mediterranean Coast. Atmos. Environ. 45, 5595–5601. doi: http://dx.doi.org/10.1016/j.atmosenv.2011.04.045

Astitha, M., Kallos, G., Katsafados, P., 2008. Air pollution modeling in the Mediterranean Region: Analysis and forecasting of episodes. Atmos. Res. 89, 358–364. doi: http://dx.doi.org/10.1016/j.atmosres.2008.03.006

Barros N., Borrego C., Toll I., Soriano C., Jiménez P., Baldasano J.M., 2003. Urban Photochemical Pollution in the Iberian Peninsula: Lisbon and Barcelona Airsheds. J. Air & Waste Manage. Assoc. 53:347–359.

Bessagnet, B. et al. (2014) Can further mitigation of ammonia emissions reduce exceedances of particulate matter air quality standards? Environmental Science & Policy, 44, 149-163.

Bruckmann, P., Wichmann-Fiebig, M. (1997). The efficiency of short-term actions to abate summer smog: results from field studies and model calculations. EUROTRAC Newsletter 19, 2–9

Buffard, F., Odent, P: Scénario PRIMEQUAL – Sensibilité des émissions aux vitesses de circulation

CELINE report (2007), Simulation de l'impact de mesures à court terme prises sur le trafic lors de l'épisode d'O_3 du 1 au 13 août 2003. Cellule interrégionale de l'environnement (CELINE), Belgique.

Carapiperis L. N. and Katsoulis B. D. (1977) Contribution to the study of sea-breezes in Athens area during winter. Bull. Hellenic Met. Soc. 2, 1-18 (in Greek).

Castell N., Mantilla E., and Millán M.M., 2008. Analysis of tropospheric O_3 concentration on a Western Mediterranean site: Castellon (Spain). Environmental Monitoring and Assessment, 136, 3-11.

Castell N., Tellez L., and Mantilla E., 2012. Daily, seasonal and monthly variations in O_3 levels recorded at the Turia river basin in Valencia (Eastern Spain). Environmental Science and Pollution Research, 19, 3461-3480.

Chang C-Y, E. Faust, X. Hou, P. Lee, H.C. Kim, B.C. Hedquist, K-J Liao (2016) Investigating ambient ozone formation regimes in neighboring cities of shale plays in the Northeast United States using photochemical modeling and satellite retrievals. Atmospheric Environment 142, 152-170.15:27 05/03/2018.

Chevalier A., Gheusi F., Delmas R., Ordóñez C., Sarrat C., et al., 2007. Influence of altitude on ozone levels and variability in the lower troposphere: a ground-based study for Western Europe over the period 2001-2004. Atmos. Chem. Phys. 7, 4311-4326.

Colette, A., Aas, W., Banin, L., Braban, C. F., Ferm, M., González Ortiz, A.., Ilyin, I., Mar, K. A., Pandolfi, M., Putaud, J.-P., Shatalov, V., Solberg, S., Spindler, G., Tarasova, O., Vana, M., Adani, M., Almodovar, P., Berton, E., Bessagnet, B., Bohlin-Nizzetto, P., Boruvkova, J., Breivik, K., Briganti, G., Cappelletti, A., Cuvelier, K., Derwent, R., D'Isidoro, M., Fagerli, H., Funk, C., Vivanco, M. G., Haeuber, R., Hueglin, C., Jenkins, S., Kerr, J., de Leeuw, F., Lynch, J., Manders, A., Mircea, M., Pay, M. T., Pritula, D., Querol, X., Raffort, V., Reiss, I., Roustan, Y., Sauvage, S., Scavo, K., Simpson, D., Smith, R. I., Tang, Y. S., Theobald, M., Tørseth, K., Tsyro, S., van Pul, A., Vidic, S., Wallasch, M., Wind, P. (2016): Air pollution trends in the EMEP region between 1990 and 2012. Joint Report of the EMEP Task Force on Measurements and Modelling (TFMM), Chemical Co-ordinating Centre (CCC), Meteorological Synthesizing Centre-East (MSC-E), Meteorological Synthesizing Centre-West (MSC-W)., (EMEP/CCC-Report 1/2016), Kjeller: Norwegian Institute for Air Research.

Cristofanelli, P., Bonasoni, P., 2009. Background O_3 in the southern Europe and Mediterranean area: Influence of the transport processes. Environ. Pollut. 157, 1399–1406. doi: http://dx.doi.org/10.1016/j.envpol.2008.09.017

De Leeuw F., JetskeVan Rheineck Leyssius H., Builtjes P. (1990) Calculation of long term averaged ground level ozone concentrations. Atmospheric Environment. Part A. General Topics, Volume 24, Issue 1, 1990, Pages 185-193.

Dieguez, J. J., Millán, M., Padilla, L., and Palau, J. L.: Estudio y evaluación de la contaminación atmosférica por ozono troposférico en España, CEAM Report for the Ministry of Agriculture, Food and Environment, INF FIN/O3/2009, 372 pp., available at: http://origin.magrama.gob.es/es/calidad-y-evaluacion-ambiental/temas/atmosfera-y-calidad-del-aire/8_A_Informe_final_ozono-ceam_Julio_2009_tcm7-438818.pdf

Doherty, R. M., Wild, O., Shindell, D. T., Zeng, G., Collins, W. J., MacKenzie, I. A., Fiore, A. M., Stevenson, D. S. Dentener, F. J., Schultz, M. G., Hess, P., Derwent, R. G., and Keating, T. J. (2013) Impacts of climate change on surface O_3 and intercontinental O_3 pollution: A multi-model study, J. Geophys. Res., 118, 3744–3763.

Doval M., Castell N., Téllez L., and Mantilla E., 2012.The use of experimental data and their uncertainty for assessing O_3 photochemistry in the Eastern Iberian Peninsula. Chemosphere, 89, 796-804.

EEA, 2015. Air Quality in Europe — 2015 report. Copenhagen.

EEA, 2016. Air Quality in Europe — 2016 report. Copenhagen.

EEA, 2017a, Global and European temperature, Core Set Indicator 012 (https://www.eea.europa.eu/data-and-maps/indicators/global-and-european-temperature-4/assessment).

EEA, 2017b, European Union emission inventory report 1990–2015 under the UNECE Convention on Long-range Transboundary Air Pollution (LRTAP), EEA Report n°9/2017

Escudero M., Lozano A., Hierro J., del Valle J., and Mantilla E., 2014. Urban influence on increasing O_3 concentrations in a characteristic Mediterranean agglomeration. Atmospheric Environment, 99, 322-332.

EU, 2008, Directive 2008/50/EC of the European Parliament and of the Council of 21 May 2008 on ambient air quality and cleaner air for Europe (OJ L 152, 11.6.2008, p. 1–44).

Eurostat (2014). http://ec.europa.eu/eurostat

Gangoiti G., Millán M.M., Salvador R., and Mantilla E., 2001.Long-range transport and re-circulation of pollutants in the western Mediterranean during the project Regional Cycles of Air Pollution in the West-Central Mediterranean Area. Atmospheric Environment, 35, 6267-6276.

Gerasopoulos E., G. Kouvarakis, M. Vrekoussis, M. Kanakidou, N. Mihalopoulos (2005) O_3 variability in the marine boundary layer of the eastern Mediterranean based on 7-year observations. J. Geophys. Res., 110, D15309, doi:10.1029/2005JD005991.

Gerasopoulos, E., Kouvarakis, G., Vrekoussis, M., Donoussis, C., Mihalopoulos, N., Kanakidou, M., 2006. Photochemical O_3 production in the Eastern Mediterranean. Atmos. Environ. 40, 3057–3069. doi: http://dx.doi.org/10.1016/j.atmosenv.2005.12.061

Gerasopoulos E., E. Koulouri, N. Kalivitis, G. Kouvarakis, S. Saarikoski, T. Makela, R. Hillamo, N. Mihalopoulos (2007) Size-segregated mass distributions of aerosols over Eastern Mediterranean: seasonal variability and comparison with AERONET columnar size-distributions. Atmos. Chem. Phys., 7, pp. 2551-2561.

Gerasopoulos E., V. Amiridis, S. Kazadzis, P. Kokkalis, K. Eleftheratos, M.O. Andreae, T.W. Andreae, H. El-Askary, C.S. Zerefos (2011) Three-year ground based measurements of aerosol optical depth over the Eastern Mediterranean: the urban environment of Athens. Atmos. Chem. Phys., 11 (2011), pp. 2145–2159.

Gonçalves M., Jiménez-Guerrero P. and Baldasano J.M. 2009. Contribution of atmospheric processes affecting the dynamics of air pollution in South-Western Europe during a typical summertime photochemical episode. Atmos. Chem. Phys., 9, 849-864.

Hogan, C.M. (2011) Aegean Sea. Eds. P.Saundry & C.J.Cleveland. Encyclopedia of Earth. National Council for Science and the Environment. Washington DC.

IPCC - Climate Change 2013: The Physical Science Basis. Contribution of Working Group I to the Fifth Assessment Report of the Intergovernmental Panel on Climate Change (2013) T.F. Stocker, D. Qin, G.-K. Plattner, M. Tignor, S.K. Allen, J. Boschung, A. Nauels, Y. Xia, V. Bex, P.M. Midgley (Eds.) Cambridge University Press, Cambridge, United Kingdom and New York, NY, USA (2013) http://dx.doi.org/10.1017/CBO9781107415324 1535 pp

Kalabokas P.D., Viras, L.G., Bartzis, J.G., Repapis, C.C., 2000. Mediterranean rural ozone characteristics around the urban area of Athens. Atmos. Environ. 34, 5199–5208.
Kalabokas, P.D., Mihalopoulos, N., Ellul, R., Kleanthous, S., Repapis, C.C., 2008. An investigation of the meteorological and photochemical factors influencing the background rural and marine surface O_3 levels in the Central and Eastern Mediterranean. Atmos. Environ. 42, 7894–7906. doi: http://dx.doi.org/10.1016/j.atmosenv.2008.07.009
Kalabokas, P.D., Cammas, J.P., Thouret, V., Volz-Thomas, A., Boulanger, D., Repapis, C.C., 2013. Examination of the atmospheric conditions associated with high and low summer ozone levels in the lower troposphere over the eastern Mediterranean. Atmos. Chem. Phys. 13, 10339–10352.
Kalabokas, P.D., Thouret, V., Cammas, J.P., Volz-Thomas, A., Boulanger, D., and Repapis, C.C., 2015. The geographical distribution of meteorological parameters associated with high and low summer ozone levels in the lower troposphere and the boundary layer over the Eastern Mediterranean (Cairo case). Tellus B, 67, 27853.
Kalabokas P.D., Hjorth J., Foret G., Dufour G., Eremenko M., Siour G., Cuesta J., Beekmann M., 2017. An investigation on the origin of regional springtime ozone episodes in the western Mediterranean. Atmos. Chem. Phys. 17, 3905–3928.
Kalabokas P.D., Repapis C.C., 2004. A climatological study of rural surface ozone in central Greece. Atmos. Chem. Phys., 4, 1139–1147.
Kallos G., Kassomenos P. and Pielke R. (1993) Synoptic and mesoscale circulations associated with air pollution episodes in Athens, Greece. Bound. Layer. Met. 62, 163-184.
Kallos G., M. Astitha, P. Katsafados, C. Spyrou (2007) Long-range transport of anthropogenically and naturally produced particulate matter in the Mediterranean and North Atlantic: current state of knowledge. J Appl Meteorol Climatol, 46 (8) (2007), pp. 1230–1251
Kallos G., Solomos S., Kushta J., Mitsakou C., Spyrou C., Bartsotas N., Kalogeri C. (2014) Natural and anthropogenic aerosols in the Eastern Mediterranean and Middle East: possible impacts. Sci Total Environ.;488-489:389-97.
Kanakidou M., N. Mihalopoulos, T. Kindap, U. Im, M. Vrekoussis, E. Gerasopoulos, E. Dermitzaki, A. Unal, M. Koçak, K. Markakis, D. Melas, G. Kouvarakis, A.F. Youssef, A. Richter, N. Hatzianastassiou, A. Hilboll, F. Ebojie, F. Wittrock, C. von Savigny, J.P. Burrows, A. Ladstaetter-Weissenmayer, H. Moubasher (2011) Megacities as hot spots of air pollution in the East Mediterranean. Atmos. Environ., 45 (2011), pp. 1223–1235
Kassomenos, P., Kotroni, V., Kallos, G., 1995. Analysis of climatological and air quality observations from Greater Athens Area. Atmos. Environ. 29, 3671–3688. doi: http://dx.doi.org/10.1016/1352-2310(94)00358-R
Kley, D. and Geiss, H.: Tropospheric O_3 at elevated sites and precursor emissions in the United States and Europe, Atmos. Environ., 8, 149–158, 1994.
Kourtidis K., Zerefos C., Rapsomanikis S., Simeonov V., Balis D., Perros P. E., Thomson A. M., Witte J., Calpini B., Sharobiem W. M., Papayiannis A., Mihalopoulos N., Drakou R., 2002. Regional levels of ozone in the troposphere over eastern Mediterranean. J. Geophys. Res., 107, 8140, doi:10.1029/2000JD000140.
Lasry, F., Coll, I., Fayet, S., Havre, M., & Vautard, R. (2007). Short-term measures for the control of O_3 peaks: expertise from CTM simulations. Journal of atmospheric chemistry, 57(2), 107-134.
Lazaridis M., Eleftheriadis K., Smolik J., Colbeck I., Kallos G., Drossinos Y., Zdimal V., Vecera Z., Mihalopoulos N., Mikuska P., Bryant C., Housiadas C., Spyridaki A., Astitha M., Havrane V. (2006) Dynamics of fine particles and photo-oxidants in the Eastern Mediterranean (SUB-AERO). Atmospheric Environment 40 (2006) 6214-6228.
Lefohn A.S., Wernli H., Shadwick D., Oltmans S.J., Shapiro M., 2012. Quantifying the frequency of stratospheric-tropospheric transport affecting enhanced surface ozone concentrations at high- and low-elevation monitoring sites in the United States. Atmos. Environ. 62, 646-656.
Lelieveld J., H. Berresheim, S. Borrmann, P.J. Crutzen, F.J. Dentener, H. Fischer, J. Feichter, P.J. Flatau, J. Heland, R. Holzinger, R. Korrmann, M.G. Lawrence, Z. Levin, K.M. Markowicz, N. Mihalopoulos, A. Minikin, V. Ramanathan, M. De Reus, G.J. Roelofs, H. a Scheeren, J. Sciare, H. Schlager, M. Schultz, P. Siegmund, B. Steil, E.G. Stephanou, P. Stier, M. Traub, C. Warneke, J. Williams, H. Ziereis (2002) Global air pollution crossroads over the Mediterranean. Science, 298 (2002), pp. 794–799

Liakakou E., B. Bonsang, J. Williams, N. Kalivitis, M. Kanakidou, N. Mihalopoulos (2009) C2–C8 NMHCs over the Eastern Mediterranean: seasonal variation and impact on regional oxidation chemistry. Atmos. Environ., 43 (2009), pp. 5611–5621

Lin, M., Horowitz, L. W., Payton, R., Fiore, A. M., and Tonnesen, G.: US surface O_3 trends and extremes from 1980 to 2014: quantifying the roles of rising Asian emissions, domestic controls, wildfires, and climate, Atmos. Chem. Phys., 17, 2943-2970, doi:10.5194/acp-17-2943-2017, 2017.

Maas, R., P. Grennfelt (eds), 2016. Towards Cleaner Air. Scientific Assessment Report 2016. EMEP Steering Body and Working Group on Effects of the Convention on Long-Range Transboundary Air Pollution.

Mailler, S., Menut, L., Khvorostyanov, D., Valari, M., Couvidat, F., Siour, G., ... & Colette, A. CHIMERE-2016: From urban to hemispheric chemistry-transport modeling

Mantilla E., Millán M.M., Sanz M.J., Salvador R., and Carratalá A., 1997. Influence of mesometeorological processes on the evolution of O_3 levels registered in the Valencian Community. In: I Technical workshop on O_3 pollution in southern Europe. Valencia.

Marécal, V., Peuch, V. H., Andersson, C., Andersson, S., Arteta, J., Beekmann, M., Benedictow, A., Bergstrom, R., Bessagnet, B., Cansado, A., Chéroux, F., Colette, A., Coman, A., Curier, R. L., Denier van der Gon, H. A. C., Drouin, A., Elbern, H., Emili, E., Engelen, R. J., Eskes, H. J., Foret, G., Friese, E., Gauss, M., Giannaros, C., Guth, J., Joly, M., Jaumouilla, E., Josse, B., Kadygrov, N., Kaiser, J. W., Krajsek, K., Kuenen, J., Kumar, U., Liora, N., Lopez, E., Malherbe, L., Martinez, I., Melas, D., Meleux, F., Menut, L., Moinat, P., Morales, T., Parmentier, J., Piacentini, A., Plu, M., Poupkou, A., Queguiner, S., Robertson, L., Rouil, L., Schaap, M., Segers, A., Sofiev, M., Tarasson, L., Thomas, M., Timmermans, R., Valdebenito, A., van Velthoven, P., van Versendaal, R., Vira, J., and Ung, A. (2015): A regional air quality forecasting system over Europe: the MACC-II daily ensemble production, Geosci. Model Dev., 8, 2777-2813.

Mészáros, E., 1999. Fundamentals of Atmospheric Aerosol Chemistry. Akadémiai Kiado, Budapest.

Millán M.M., Artiñano B., Alonso L., Navazo M., Castro M., 1991. The effect of meso-scale flows on regional and long-range atmospheric transport in the Western Mediterranean area. Atmospheric Environment 25A, 5/6, 949-963.

Millán M.M., Salvador R., Mantilla E., Artiñano B., 1996. Meteorology and photochemical air pollution in southern Europe: experimental results from EC research projects. Atmospheric Environment, 30, 1909-1924.

Millán M.M., Salvador R., Mantilla E., and Kallos G., 1997.Photooxidant dynamics in the Mediterranean basin in summer: Results from European research projects. Journal of Geophysical Research 102, 8811-8823.

Millán M.M. and Sanz M. J., 1999. O_3 in Mountainous regions and in Southern Europe. In: Ad hoc Working group on O_3 Directive and Reduction Strategy Development, (eds.). O_3 Position Paper.145-150. European Commission, Brussels.

Millán M.M., Mantilla E., Salvador R., Carratalá A., Sanz M.J., Alonso L., Gangoiti G., and Navazo M., 2000. O_3 Cycles in the Western Mediterranean Basin: Interpretation of Monitoring Data in Complex Coastal Terrain. Journal of Applied Meteorology, 39: 487-508.

Millán, M. M. (Ed.): O_3 Dynamics in the Mediterranean Basin: A collection of scientific papers resulting from the MECAPIP, RECAPMA and SECAP Projects, European Commission (DG RTD I.2) Air Pollution Research Report 78, available from CEAM, Valencia, Spain, 287 pp., 2002.

Millán M.M., Sanz M.J., Salvador R., and Mantilla E., 2002. Atmospheric dynamics and O_3 cycles related to nitrogen deposition in the western Mediterranean. Environmental Pollution, 118, 167-186.

Millán M., M. Estrela, M. Sanz (2005) Climatic feedbacks and desertification: the Mediterranean model. J. Clim., 18 (2005), pp. 684–701

Monks, P.S., Archibald A.T., Colette A., Cooper O., Coyle M., Derwent R., Fowler D., Granier C., Law K.S., Mills G.E., Stevenson D.S., Tarasova O., Thouret V., von Schneidemesser E., Sommariva R., Wild O., and Williams M.L., 2015. Tropospheric O_3 and its precursors from the urban to the global scale from air quality to short-lived climate forcer. Atmos. Chem. Phys., 15, 8889-8973.

Myriokefalitakis, S., Daskalakis, N., Fanourgakis, G.S., Voulgarakis, A., Krol, M.C., Aan de Brugh, J.M.J., Kanakidou, M., 2016. O_3 and carbon monoxide budgets over the Eastern Mediterranean. Sci. Total Environ. 563–564, 40–52. doi: http://dx.doi.org/10.1016/j.scitotenv.2016.04.061

Nali C., C. Pucciariello, G. Lorenzini (2002) Mapping O_3 critical levels for vegetation in Central Italy. Water, Air and Soil Pollution, 141 (2002), pp. 337–347

Otero, N., Sillmann, J., Schnell, J.L., Rust, H.W., Butler, T., 2016. Synoptic and meteorological drivers of extreme O_3 concentrations over Europe. Environ. Res. Lett. 11, 24005. doi:10.1088/1748-9326/11/2/024005

Paoletti E. (2006) Impact of O_3 on Mediterranean forests: A review. Environmental Pollution, 144 (2006), pp. 463–474

Parrish D.D., Law K.S., Staehelin J., Derwent R., Cooper O.R., et al., 2012. Long-term changes in lower tropospheric baseline ozone concentrations at northern mid-latitudes. Atmosph. Chem. Phys. 12, 11485-11504.

Pay M.T., Guevara M., Baldasano J.M. (2014) Air quality modelling of fugitive dust emissions caused by agricultural activities using two different chemical transport models. 13th Annual CMAS Conference, October 27-29, 2014 Chapel Hill, NC.

Peleg, M., Luria, M., Sharf, G., Vanger, A., Kallos, G., Kotroni, V., Lagouvardos, K., Varinou, M., 1997. Observational evidence of an O_3 episode over the Greater Athens Area. Atmos. Environ. 31, 3969–3983. doi: http://dx.doi.org/10.1016/S1352-2310(97)00251-3

Pilinis, C., Kassomenos, P., Kallos, G., 1993. Modeling of photochemical pollution in Athens, Greece. Application of the RAMS-CALGRID modeling system. Atmos. Environ. Part B. Urban Atmos. 27, 353–370. doi: http://dx.doi.org/10.1016/0957-1272(93)90014-W

Poupkou, A., Symeonidis, P., Lisaridis, I., Melas, D., Ziomas, I., Yay, O.D., Balis, D., 2008. Effects of anthropogenic emission sources on maximum O_3 concentrations over Greece. Atmos. Res. 89, 374–381. doi: http://dx.doi.org/10.1016/j.atmosres.2008.03.009

Pusede, S.E., Steiner, A.L., Cohen, R.C., 2015. Temperature and recent trends in the chemistry of continental surface O_3. Chem. Rev. 115, 3898–3918.

Querol X., Alastuey A., Orio A., Pallares M., Reina F., Dieguez JJ., Mantilla E., Escudero M., Alonso L., Gangoiti G., Millán M. 2016. On the origin of the highest O_3 episodes in Spain. Science of the Total Environment, 572, 379-389.

Querol, X., Gangoiti, G., Mantilla, E., Alastuey, A., Minguillón, M.C., Amato, F., Reche, C., Viana, M., Moreno, T., Karanasiou, A., Rivas, I., Pérez, N., Ripoll, A., Brines, M., Ealo, M., Pandolfi, M., Lee, H.K., Eun, H.R., Park, Y.H., Escudero, M., Beddows, D., Harrison, R.M., Bertrand, A., Marchand, N., Lyasota, A., Codina, B., Olid, M., Udina, M., Jiménez-Esteve, B., Jiménez-Esteve, B.B., Alonso, L., Millán, M., Ahn, K.H., 2017. Phenomenology of high-O_3 episodes in NE Spain. Atmos. Chem. Phys. 17, 2817–2838. doi:10.5194/acp-17-2817-2017.

Querol, X., Alastuey, A., Gangoiti, G., Perez, N., Lee, H. K., Eun, H. R., Park, Y., Mantilla, E., Escudero, M., Titos, G., Alonso, L., Temime-Roussel, B., Marchand, N., Moreta, J. R., Revuelta, M. A., Salvador, P., Artíñano, B., García dos Santos, S., Anguas, M., Notario, A., Saiz-Lopez, A., Harrison, R. M., and Ahn, K.-H.: Phenomenology of summer ozone episodes over the Madrid Metropolitan Area, central Spain (2018) Atmos. Chem. Phys. Discuss., https://doi.org/10.5194/acp-2017-1014, in review, 2017.

Rafaj P., M. Amann, J. Siri, H. Wuester (2014) Changes in European greenhouse gas and air pollutant emissions 1960–2010: decomposition of determining factors, Climatic Change, Volume 124, Issue 3, pp 477–504.

Richards, N.A.D., Arnold, S.R., Chipperfield, M.P., Miles, G., Rap, A., Siddans, R., Monks, S.A., Hollaway, M.J., 2013. The Mediterranean summertime O_3 maximum: global emission sensitivities and radiative impacts. Atmos. Chem. Phys. 13, 2331–2345. doi:10.5194/acp-13-2331-2013.

Sahu, L.K., Saxena, P., 2015. High time and mass resolved PTR-TOF-MS measurements of VOCs at an urban site of India during winter: role of anthropogenic, biomass burning, biogenic and photochemical sources. Atmos. Res. 164, 84–94.

Sahu, L.K., Yadav, R., Pal, D., 2016. Source identification of VOCs at an urban site of western India: effect of marathon events and anthropogenic emissions. J. Geophys. Res. Atmos. 121. http://dx.doi.org/10.1002/2015JD024454.

Salvador R., Millán M.M., and Calbo J., 1999.Horizontal Grid Size Selection and its influence on Mesoscale Model Simulations. Journal of Applied Meteorology, 38, 1311-1329.

Scebba F., F. Canaccini, A. Castagna, J. Bender, H.-J. Weigel, A. Ranieri (2006) Physiological and biochemical stress responses in grassland species are influenced by both early-season O_3 exposure and interspecific competition. Environmental Pollution, 142 (2006), pp. 540–548

Sciare J., K. Oikonomou, O. Favez, E. Liakakou, Z. Markaki, H. Cachier, N. Mihalopoulos (2008) Long-term measurements of carbonaceous aerosols in the Eastern Mediterranean: evidence of long-range transport of biomass burning. Atmos. Chem. Phys., 8 (2008), pp. 5551–5563

Sicard P., Anav A., De Marco A., Paoletti E., 2017. Projected global tropospheric ozone impacts on vegetation under different emission and climate scenarios. Atmos. Chem. Phys. 17, 12177–12196.

Sillman S. (1999) The relation between ozone, NOx and hydrocarbons in urban and polluted rural environments, Atmos. Environ., 33, pp. 1821-1845.

Smeets CJJP., Beck, JP. (2001). Effects of Short-term abatement measures on peak O_3 concentrations during summer smog episodes in the Netherlands. Rep 725501004/2001, RIVM, Bilthoven.

Stein A.F., Mantilla E., and Millán M.M., 2005. Using measured and modelled indicators to assess O_3-NOx-VOC sensitivity in a western Mediterranean coastal environment. Atmospheric Environment, 39: 7167-7180.

Thunis P., Cuvelier C. (2000) Impact of biogenic emissions on O_3 formation in the Mediterranean area – a BEMA modelling study, Atmospheric Environment, 34 pp. 467–481.

Thunis P., Pisonia E., Degraeuwe B., Kranenburg R., Schaap M., Clappier S., 2015. Dynamic evaluation of air quality models over European regions. Atmos. Environ. 111, 185-194.

Thunis P., Degraeuwe B., Pisoni E., Meleux F., Clappier A. (2017) Analyzing the efficiency of short-term air quality plans in European cities, using the CHIMERE air quality model, Air Quality, Atmosphere & Health, Volume 10, Issue 2, pp 235–248.

Toll, I., Baldasano, J.M., 2000.Modeling of photochemical air pollution in the Barcelona area with highly disaggregated anthropogenic and biogenic emissions. Atmos. Environ.34, 3069–3084.

UNECE, 2010.Hemispheric transport of air pollution 2010. Part A: O_3 and particulate matter. Air pollution studies, 17. UNECE, LRTAP, Task Force on Hemispheric Transport of Pollutants HTAP 2010: Part A. O_3 and particulate Matter, 278 pp, ECE/EB.AIR/100, ISBN 978-92-1-117043-6

Valverde V., Pay M.T., Baldasano J.M., 2016. O_3 attributed to Madrid and Barcelona on-road transport emissions: Characterization of plume dynamics over the Iberian Peninsula. Science of the Total Environment 543, 670–682.

van Loon M., R. Vautard, M. Schaap, et al. (2007) Evaluation of long-term O_3 simulations from seven regional air quality models and their ensemble. Atmos. Environ., 41 (10) (2007), pp. 2083–2097

Varinou, M., Kallos, G., Tsiligiridis, G., Sistla, G., 1999. The role of anthropogenic and biogenic emissions on tropospheric O_3 formation over greece. Phys. Chem. Earth, Part C Solar, Terr. Planet. Sci. 24, 507–513. doi: http://dx.doi.org/10.1016/S1464-1917(99)00081-1

Wang, S., Zhao, M., Xing, J., Wu, Y., Zhou, Y., Lei, Y., He, K., Fu, L. and Hao, J. (2010) Quantifying the Air Pollutants Emission Reduction during the 2008 Olympic Games in Beijing, Environmental Science & Technology 44 (7), 2490-2496.

Whalley, L., Stone, D., Heard, D., 2014. New insights into the tropospheric oxidation of isoprene: combining field measurements, laboratory studies, chemical modelling and quantum theory. In: McNeill, V.F., Ariya, P.A. (Eds.), Atmospheric and Aerosol Chemistry Topics in Current Chemistry. Springer, Berlin Heidelberg, pp. 55–96.

WHO, 2006a, *Air Quality Guidelines: Global update 2005. Particulate matter, ozone, nitrogen dioxide and sulphur dioxide*, World Health Organization, Regional Office for Europe, Copenhagen.

WHO, 2008. Health risks of O_3 from long-range transboundary air pollution. WHO Regional Office for Europe Scherfigsvej 8 DK-2100 Copenhagen Ø, Denmark.

World Bank; Institute for Health Metrics and Evaluation. 2016. The Cost of Air Pollution: Strengthening the Economic Case for Action. World Bank, Washington, DC. © World Bank. https://openknowledge.worldbank.org/handle/10986/25013 License: CC BY 3.0 IGO.

Zanis P., Hadjinicolaou P., Pozzer A., Tyrlis E., Dafka, S., Mihalopoulos N., Lelieveld J., 2014. Summertime free-tropospheric ozone pool over the eastern Mediterranean/Middle East, Atmos. Chem. Phys. 14, 115–132.

Annex 1. O_3 statistics per station

Table A.1 **O_3 concentrations in the Valencia region (maximum 1-hr concentration, number of 8-hr means exceeding 120 µg/m^3, percentile 93.15, percentile 99 and average concentration), averaged for each station for the years 2011-2015. U: urban. SU: suburban. R: rural.**

	València (Spain)						
	Station	**Code**	**Max conc.**	**8H mean >120**	**93.15 perc.**	**99 perc.**	**Average**
R	ES0012R	1	154.4	168	129	139	95
	ES1670A	7	156.6	192	124	134	80
	ES1671A	8	183.2	94	129	141	80
	ES2001A	19	150.2	113	114	124	79
	ES2018A	20	148.5	24	124	135	75
SU	ES1617A	4	135.8	147	110	121	60
	ES1691A	9	153.6	165	118	131	70
	ES1709A	10	151.8	156	123	134	72
	ES1711A	11	154.2	74	127	138	85
	ES1826A	12	138.2	57	111	122	68
	ES1886A	14	147.8	4	110	121	66
	ES1911A	15	158.8	16	129	139	73
	ES2019A	21	165	16	131	143	73
U	ES1181A	2	139.8	52	110	121	64
	ES1239A	3	136.6	21	100	113	56
	ES1619A	5	144.8	17	105	118	59
	ES1625A	6	145.8	13	117	129	71
	ES1885A	13	142.6	14	113	124	70
	ES1912A	16	123.4	8	97	107	60
	ES1926A	17	132.6	7	103	114	60
	ES1970A	18	127.6	0	101	112	59

Table A.2 O_3 concentrations in the Barcelona region (maximum 1-hr concentration, number of 8-hr means exceeding 120 µg/m^3, percentile 93.15, percentile 99 and average concentration), averaged for each station for the years 2011-2015. U: urban. SU: suburban. R: rural.

	Barcelona						
	Station	**Code**	**Max conc.**	**8H mean >120**	**93.15 perc.**	**99 perc.**	**Average**
	ES1778A	22	181.4	272	135	149	87
	ES1851A	23	197.2	211	132	148	78
R	ES1923A	25	191.2	260	139	156	73
	ES1840A	70	208.8	275	137	157	63
SU	ES1874A	69	209.6	336	143	163	66
	ES1856A	24	152.8	37	111	126	66
U	ES1904A	71	148.6	40	110	123	66

Table A.3 O_3 concentrations in the Marseille region (maximum 1-hr concentration, number of 8-hr means exceeding 120 µg/m^3, percentile 93.15, percentile 99 and average concentration), averaged for each station for the years 2011-2015. U: urban. SU: suburban. R: rural.

	Marseille						
	Station	**Code**	**Max conc.**	**8H mean >120**	**93.15 perc.**	**99 perc.**	**Average**
	FR02023	27	181.3	166	133	146	74
	FR03027	35	200.3	381	150	169	99
	FR03086	37	202.8	242	139	154	74
	FR08204	38	181.4	186	137	149	79
	FR08209	40	190.9	218	142	153	81
R	FR24038	26	204.6	168	144	160	96
	FR03037	30	189.7	178	134	154	67
	FR03048	32	222.0	237	143	163	73
	FR03067	33	188.1	274	142	160	81
SU	FR03088	36	195.9	181	140	152	76
	FR03029	28	224.8	174	136	157	70
	FR03032	29	187.3	152	135	156	71
	FR03043	31	188.1	66	121	138	67
	FR03080	34	181.8	145	130	144	73
U	FR24018	39	215.1	267	141	159	80

Table A.4 **O_3 concentrations in the Rome region (maximum 1-hr concentration, number of 8-hr means exceeding 120 µg/m^3, percentile 93.15, percentile 99 and average concentration), averaged for each station for the years 2011-2015. U: urban. SU: suburban. R: rural.**

	Rome						
	Station	Code	Max conc.	8H mean >120	93.15 perc.	99 perc.	Average
R	IT0952A	60	177.8	86	121	139	67
SU	IT2012A	68	179.8	96	127	144	72
	IT0869A	59	162.0	50	117	132	67
	IT0953A	61	189.0	147	132	150	59
	IT0956A	62	192.8	144	130	149	61
	IT0957A	63	196.8	129	130	149	59
	IT1176A	64	193.0	172	132	152	65
	IT1835A	65	183.6	61	119	140	56
	IT1836A	66	170.0	52	115	129	52
U	IT1906A	67	158.8	11	110	122	55

Table A.5 **O_3 concentrations in the Brindisi/Taranto region (maximum 1-hr concentration, number of 8-hr means exceeding 120 µg/m^3, percentile 93.15, percentile 99 and average concentration), averaged for each station for the years 2011-2015. U: urban. SU: suburban. R: rural.**

	Brindisi/taranto						
	Station	Code	Max conc.	8H mean >120	93.15 perc.	99 perc.	Average
	IT2149A	46	163.8	273	134	144	85
R	IT1665A	42	157.7	81	133	141	90
	IT2139A	45	175.1	262	135	146	87
	IT1953A	43	170.5	239	135	146	89
SU	IT1679A	44	153.0	13	114	132	75
U	IT1614A	41	171.2	215	132	147	84

Table A.6 **O_3 concentrations in the Athens region (maximum 1-hr concentration, number of 8-hr means exceeding 120 μg/m^3, percentile 93.15, percentile 99 and average concentration), averaged for each station for the years 2011-2015. U: urban. SU: suburban.**

	Athens						
	Station	**Code**	**Max conc.**	**8H mean >120**	**93.15 perc.**	**99 perc.**	**Average**
	GR0027A	49	214.6	226	138	157	88
	GR0029A	51	185.6	95	123	146	67
	GR0035A	55	233.8	269	142	163	84
	GR0037A	56	256.2	383	144	178	103
	GR0039A	57	211.8	340	139	165	96
SU	GR0120A	58	157.8	196	122	135	87
	GR0002A	47	153.6	12	100	119	49
	GR0022A	48	203.6	161	132	151	82
	GR0028A	50	209.6	191	135	159	84
	GR0030A	52	155.8	3	95	109	46
	GR0031A	53	206	262	139	161	85
U	GR0032A	54	115.2	0	82	98	32

Annex 2. Example of forecasting tools existing at European level (Copernicus policy support products)

The Barcelona case study shows that ambitious short-term measures can significantly reduce O_3 peak concentrations and exceedances of the O_3 information threshold. The study assumed a 30% reduction in NO_x and NMVOCs emissions without targeting any specific emission sectors. Models such as the Barcelona Supercomputing Centre (BSC) CALIOPE model (www.bsc.es/caliope/es) and the Copernicus Atmospheric Monitoring Service policy support website (http://policy.atmosphere.copernicus.eu/) can help to identify the specific sectors which should be targeted. As an example, the Copernicus policy support tool consists in model scenarios at the European level (see Figure A1), produced every day. The impact of emission reduction scenarios over all Europe is estimated based on Chemistry Transport simulations with the CHIMERE model performed with different scenarios of emissions reductions (road traffic, industrial activities, agricultural sectors, NEC emissions, etc.) and compared with a baseline simulation. The impacts are calculated for daily peak for the day 0, D+1 and D+2. Figure A1 is an example of such products for the period analysed in the modelling case study in section 3. It shows daily O_3 peaks simulated by the model for July 15, 2015, as well as differences in O_3 peak levels simulated by a 30% reduction in emissions due to transport and due to industrial activities over Europe. These scenarios can help to identify which sector is mainly responsible at European level for O_3 peaks. However, it should be highlighted that due to the scale of the model (25x25 km) this scenario would be somewhat comparable to the IMPORT scenario discussed in section 3. In the present case it appears that at the European scale it could be mainly road transport and, to a lesser extent, industrial activity that contribute to the O_3 peak of July 15, 2015. It is also the case in the Barcelona area, although it should be stressed that the CAMS scenario target road transport emissions for Europe as a whole, and not only urban emissions from a given city (Barcelona in this case). The spatial scale used in Figure A1 (25 km) is not applicable for a city-scale case study such as the July 2015 episode in the Barcelona region, and it can’t be validated.

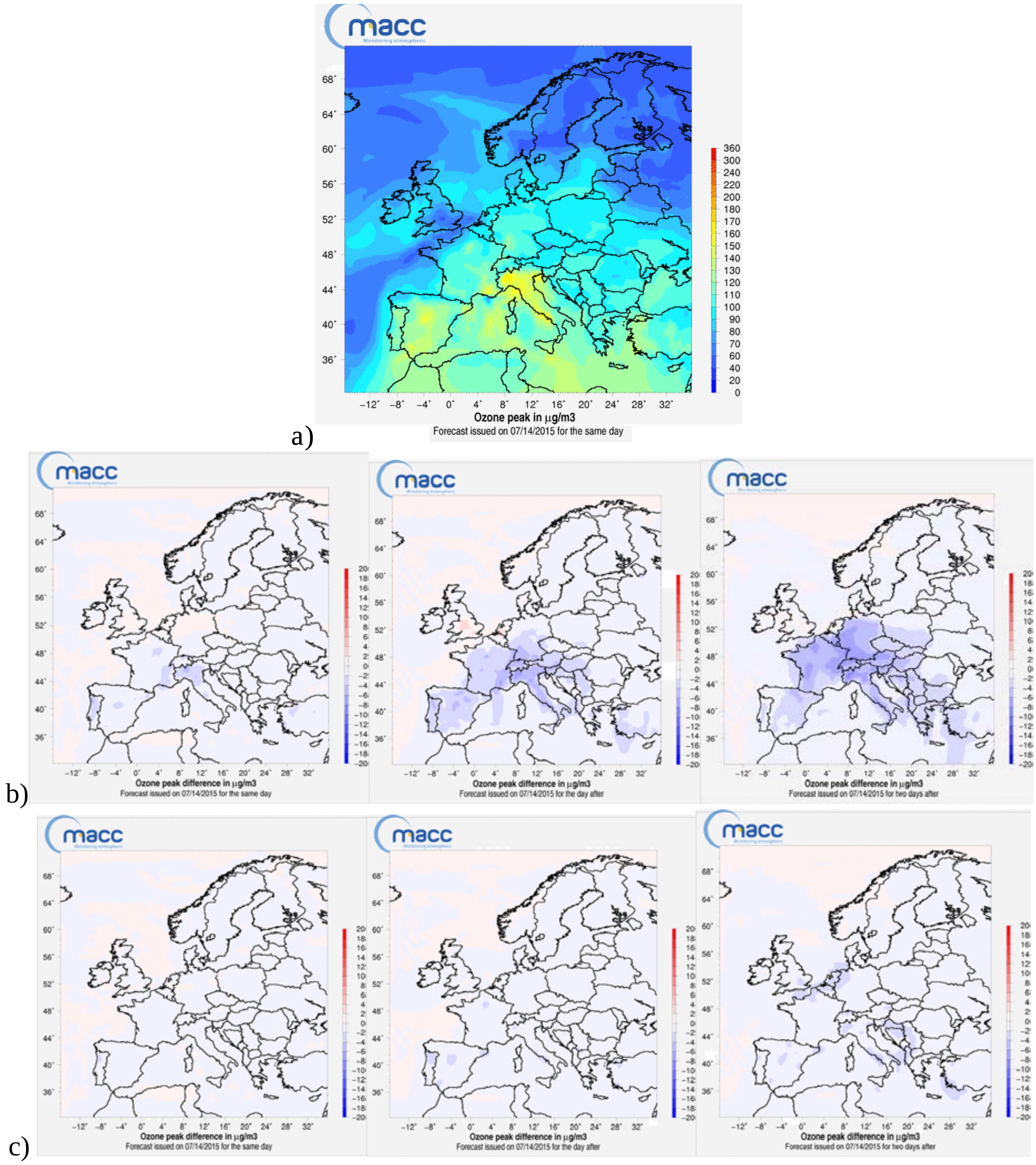

Figure A1: Example of scenario simulations for July 15, 2015 with the Copernicus Atmospheric Monitoring Service policy support tool. a) O_3 peaks in µg/m^3 for the reference simulation (15/07/2015); b) impact (difference in O_3 peak in µg/m^3) of a 30% reduction in traffic emissions over Europe. Impact is evaluated for July 15, 2015 and the 2 following days; c) same as (b) for a 30% reduction in industrial emissions over Europe.